NUREG/CR-3722
EGG-2305

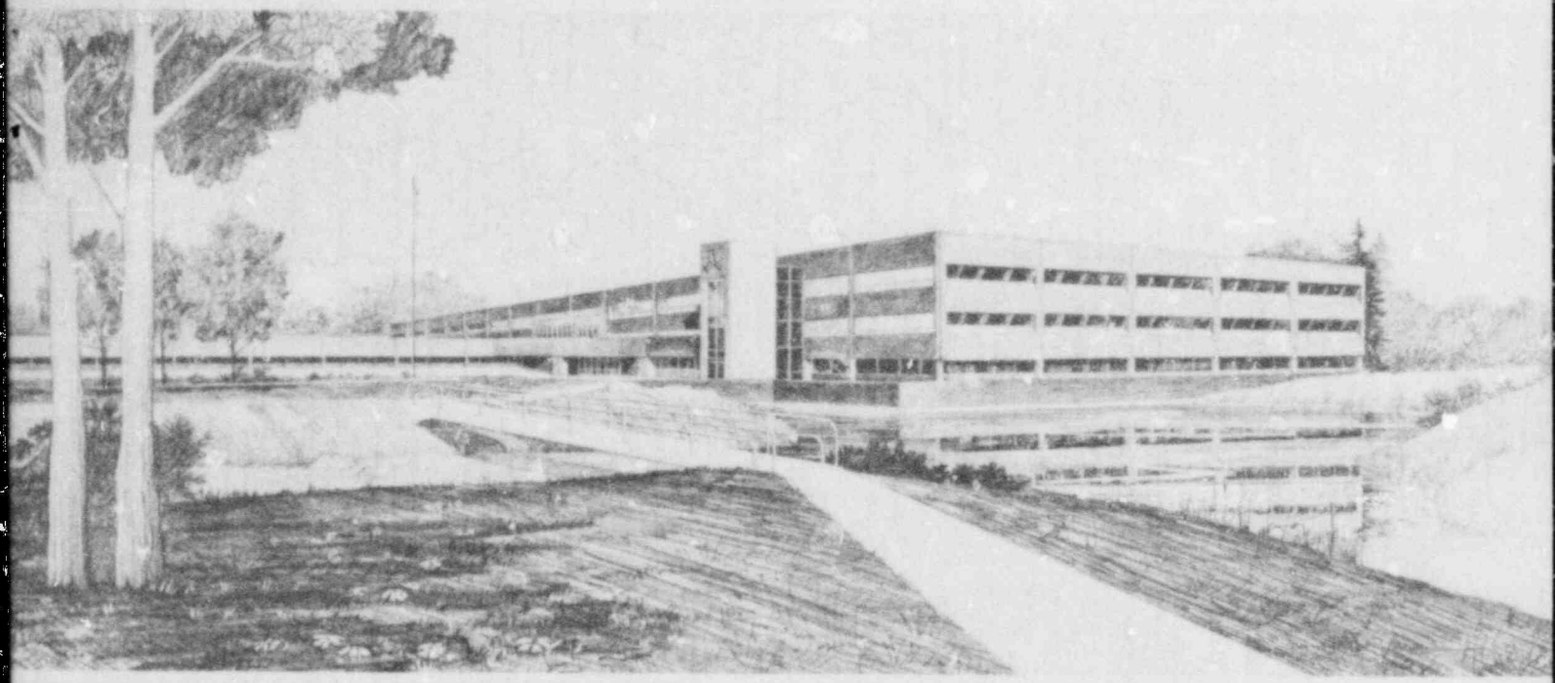

Idaho National Engineering Laboratory
Operated by the U.S. Department of Energy

Damping Test Results for Straight Sections of 3-inch and 8-inch Unpressurized Pipes

Arthur G. Ware
Gary L. Thinnes

April 1984

Prepared for the
U.S. Nuclear Regulatory Commission
Under DOE Contract No. DE-AC07-76IDO1570

EG&G Idaho

Available from

GPO Sales Program
Division of Technical Information and Document Control
U.S. Nuclear Regulatory Commission
Washington, D.C. 20555

and

National Technical Information Service
Springfield, Virginia 22161

NUREG/CR-3722
EGG-2305
Distribution Category: RM

DAMPING TEST RESULTS FOR STRAIGHT SECTIONS OF 3-INCH AND 8-INCH UNPRESSURIZED PIPES

Arthur G. Ware
Gary L. Thinnes

Published April 1984

EG&G Idaho, Inc.
Idaho Falls, Idaho 83415

Prepared for the
U.S. Nuclear Regulatory Commission
Washington, D.C. 20555
Under DOE Contract No. DE-AC07-76IDO1570
FIN No. A6216

ABSTRACT

EG&G Idaho is assisting the Nuclear Regulatory Commission and the Pressure Vessel Research Committee in supporting a final position on revised damping values for structural analyses of nuclear piping systems. As part of this program, a series of vibrational tests on unpressurized 3-in. and 8-in. Schedule 40 carbon steel piping was conducted to determine the changes in structural damping due to various parametric effects. The 33-ft straight sections of piping were supported at the ends. Additionally, intermediate supports comprising spring, rod, and constant-force hangers, as well as a sway brace and snubbers, were used. Excitation was provided by low-force-level hammer impacts, a hydraulic shaker, and a 50-ton overhead crane for snapback testing. Data was recorded using acceleration, strain, and displacement time histories. This report presents test results showing the effect of stress level and type of supports on structural damping in piping.

SUMMARY

At present, studies are under way to determine whether an increase in the allowable damping values used in dynamic structural analyses of nuclear power plant piping systems is justified. The Welding Research Council's Pressure Vessel Research Committee (PVRC) recently developed revised interim pipe damping recommendations which have been approved for ad hoc use by the Nuclear Regulatory Commission. Increasing the allowable damping could lead to safer, more reliable, and less costly piping systems. A prevailing view is that conservative values for seismic design has led to overly stiff piping with excessive numbers of supports ill-suited to resisting thermal transients.

To assess the damping induced in piping at various levels of excitation and with a range of typical piping supports, a series of vibration tests on unpressurized 3-in. and 8-in. Schedule 40 pipe was conducted at the Idaho National Engineering Laboratory (INEL). One objective of these tests is to support the final position of the PVRC.

A majority of the previous tests used to establish damping values have been conducted on actual power plant piping systems or on laboratory models of these systems. These systems were fairly complicated and the many variables tended to mask the influence of any single parameter on the damping in the system. Therefore, in the initial phase of testing at the INEL, a very simple system was selected in order to be able to vary one parameter at a time. The configuration chosen was a straight section of pipe, supported at both ends, with one or more typical piping supports along its length. Using results and insights gained from the testing, more and more complicated geometries could be used to increase understanding of damping in a building block manner.

The system was excited by impact hammer, shaker, and snapback methods. Data was recorded on the EG&G modal analyzer from strain gauge, accelerometer, and linear variable differential transformer displacement probe instruments. Typical piping supports used in the tests were a sway brace, a rod hanger, spring hangers, a constant-force hanger, and snubbers.

The constant-force hangers produced the highest damping of all the supports tested. The spring hangers and sway brace contributed little to the damping except at very low vibration levels. Higher damping was induced by supports with gaps, such as snubbers and rod hangers with loose connections.

For linear systems, time-domain and frequency-domain calculations produced similar results. To improve confidence, use of several excitation and calculational methods on the same configuration is recommended. Displacement, acceleration, and strain measurements provided similar damping results.

At higher levels of response, in the operating basis earthquake and safe shutdown earthquake ranges, damping increased with response level. Damping for the 8-in. pipe at these levels was considerably greater than for the 3-in. pipe. Modal damping is dependent on the position of the support with relation to the mode shape. Modes that exercise energy dissipating supports have higher damping than modes where supports are located near nodal points. There was no apparent trend to indicate that damping at frequencies of 33-50 Hz (above the seismic range) were different from damping values in the 20-33 Hz range.

Future tests planned for 1984 will involve a more complicated two- or three-dimensional piping system. Tests at high strain levels will be emphasized, and data at frequencies above 33 Hz will be recorded to assess the effect of damping at higher frequencies.

ACKNOWLEDGMENTS

Assistance in planning and testing was provided by many people. We wish to acknowledge our technical monitor, John O'Brien of the U.S. Nuclear Regulatory Commission, for his encouragement, helpful suggestions with the test planning, and funding. Guy Arlotto, Bill Anderson, and Jim Richardson of the USNRC also showed interest in these tests and provided many beneficial insights. Bob Taylor of the Tennessee Valley Authority assisted us by reviewing and commenting on the test plan.

Design of the test fixture and snapback apparatus was the work of Bob Blandford, Bob Peel, and Bob Guenzler of EG&G Idaho. Vince Gorman set up the shaker and data acquisition equipment and Jim Arendts recorded most of the 3-in. pipe test data. Carl Larsen of South Dakota School of Mines and Technology worked as a summer student and was very helpful in the equipment setup and initial stages of testing.

The EG&G Idaho staff at ARA-III provided invaluable technical services in testing, suggestions, and equipment modifications. Our thanks go to Gil Thorsen and Rolf Strahm who worked together with us on supervisory and scheduling matters; to Craig Christensen for electrical troubleshooting and initial testing setup; to Bud Stephens for strain gauge mounting and hookup; and to Bill Stoddard, Bill Siegal, Eric Yarger, and Jim Wayslow for equipment modification, test assistance and setup, and the many details, both large and small, needed to complete the testing.

CONTENTS

DAMPING TEST RESULTS FOR STRAIGHT SECTIONS OF 3-INCH AND 8-INCH UNPRESSURIZED PIPES

INTRODUCTION

One of the parameters that a structural analyst routinely uses in the dynamic seismic analysis of nuclear power plant piping systems is the structural damping. The damping values are prescribed, according to the pipe size and the earthquake level, in Regulatory Guide (RG) 1.61[1] issued by the U.S. Atomic Energy Commission, predecessor of the present U.S. Nuclear Regulatory Commission (NRC). At the time of issue of RG 1.61 (1973), the Atomic Energy Commission had gathered the best available experimental data on piping system damping values, and the opinions of the leading experts in the field, to establish a set of values that would be easy for an analyst to use and that would be conservative. These values (1 to 3% of critical damping) are generally conservative in that piping system motions are overpredicted so that the resulting calculated stresses are high enough to ensure the system is adequately supported for seismic motions.

Since the issue of RG 1.61, nuclear power plant piping has been designed as relatively stiff systems, employing many seismic supports, to keep the combined stresses due to earthquakes plus other loads below allowable values. These stiff systems are unduly restrained from thermal growth, leading to a greater susceptibility to thermal cracking of the pipe wall due to fatigue. In addition, many systems are supported by snubbers that resist sudden high acceleration seismic motions, but that allow slow thermal movements without resistance. These snubbers are costly to purchase and install. They sometimes lock when no sudden movements are occurring or do not lock at the high acceleration levels and they sometimes leak fluid (hydraulic snubbers). Consequently the NRC requires inspection and maintenance programs in the Standard Review Plan,[2] resulting in increased cost and worker radiation exposure. Thus, considerable benefit would be gained by reducing the number of seismic supports used in piping systems.

It has been widely recognized that piping systems have a great deal of design margin, and are generally overdesigned. This is due to a combination of factors: seismic analysis methods, seismic design allowables, standard industry practices, and low damping values. In order to improve piping design, the Welding Research Council's Pressure Vessel Research Committee (PVRC) Technical Committee on Piping Systems has appointed various task groups to look into the problem of piping system overdesign. The NRC has been an active participant in this venture along with nuclear steam supply system vendors, architect/engineers, the national laboratories, and electric utilities. This program's goal is to recommend changes, where warranted, to make stress analysis more accurate, and to allow safer, more reliable, and less costly piping systems.

One part of the program was to examine damping values and determine the possibility of revising the present guidelines to reflect current best-estimate values. The NRC has contracted with EG&G Idaho, Inc., at the Idaho National Engineering Laboratory (INEL) to study structural damping in nuclear power plant piping systems and provide data to support the final PVRC position. This program began in FY-81 and has proceeded in phases. In the first phase, a literature survey of existing piping system damping data was conducted. The results, as well as some of the data previously unpublished in this country, were published in References 3 and 4. From this study, it was concluded that there was a good deal of data to support higher allowable damping values, particularly for certain sets of parameters. In the second phase, the parameters that seemed to have the greatest influence on damping were identified and a test program was proposed to generate more damping data and investigate these parameters. Results of this portion of the program were published in References 5 and 6. At the same time, a limited analytical investigation was conducted to determine whether an increase of the allowable damping value from the present 2% of critical damping to a value of 5% of critical damping would indeed reduce the number of required seismic supports for typical piping systems. The results in Reference 7 demonstrated that at least for a few typical systems, increasing the allowed damping would permit removal of supports while still meeting stress criteria.

In the third phase, the initial test sequence proposed in the second phase was carried out. A majority of the previous tests used to establish damping values have been conducted on actual power plant piping systems or on laboratory models of these systems. These systems were fairly complicated and many variables were present, which could tend to mask the nature of the damping in the system. Therefore, in the initial phase of testing at the INEL, a very simple system was selected in order to be able to vary one parameter at a time. The configuration chosen was a straight section of pipe, supported at both ends, with one or more typical piping supports along its length. Using results and insights gained from this testing, more and more complicated geometries could be used to increase understanding of damping in a building block manner. This report details the results of these initial tests. A brief description of plans for future work is discussed in the final section, Future Work.

BACKGROUND

This section presents the current NRC regulations for the damping to be used in structural dynamic analyses of nuclear power plant piping systems, and a summary discussion of damping itself.

Present Guidelines

RG 1.61[1] states the current NRC position on damping values to be used in the dynamic structural analysis of nuclear power plant piping. These are listed in Table 1 and are derived from recommendations given by Newmark, Blume, and Kapur.[8] Note that the only two parameters considered are pipe size and design level of earthquake, whereas in Reference 5, several other parameters are considered important: frequency, insulation, supports, and excitation level. Further discussion on the basis for the RG 1.61 values is found in Reference 5. The guide also allows damping values other than those in Table 1 to be used if these values can be justified to the NRC for the particular piping system. Because using alternate values would, in most cases, be difficult to justify with existing test data, most of the newest generation of nuclear power plants have their piping systems designed with the damping values of Table 1.

Table 1. Damping values from Regulatory Guide 1.61 (percent of critical damping)

Pipe Size	OBE or 1/2 SSE	SSE
Large Diameter (>12 in.)	2	3
Small Diameter (≤12 in.)	1	2

Damping

Damping is a measure of energy dissipation of a material or system under cyclic motion. References 5, 9, and 10 give a more detailed discussion on the subject.

In RG 1.61, the damping referred to is based on an equivalent viscous damping for the entire system. All the complicated mechanisms that represent energy losses are lumped together.

For a single degree-of-freedom system, the critical damping of the system (C_c) is as a function of the circular frequency ω and the system mass M, and is defined as

$$C_c = 2\,M\omega \ .$$

This term, as related to the amount of energy loss, would allow a linear oscillator to return to its original position, without cycling, in the minimum time.

It is often convenient to express damping as the ratio

$$\zeta = \frac{C}{C_c} = \frac{C}{2\,M\omega} \ .$$

When expressed as a fraction, ζ is called the fraction of critical damping; when expressed as percent, ζ is called percent of critical damping.

The true damping characteristics of structural systems are very complex and difficult to determine. In fact, purely nonlinear systems cannot be characterized at all by parameters such as natural frequency and percent of critical damping, but only by response histories. However, it is common practice to express the damping of real systems in terms of ζ. This is reasonable if the system is only slightly nonlinear. In such cases, a linear dynamic system analysis is commonly performed, with the nonlinearities approximated by a larger value of damping. Although this method is mathematically computationally convenient, it does not necessarily represent the best combination of realistic experimental data and state-of-the-art analytical techniques.

Another type of damping commonly encountered is Coulomb damping, which results from the sliding of two dry surfaces. The damping force is equal to the product of the normal force and the coefficient of friction and changes in direction with each half cycle. This type of damping results in much more complicated mathematical relations for the prediction of piping motions, and thus is not commonly used. However, as will be demonstrated later in this report, Coulomb damping is frequently observed in testing. As derived in Reference 10, the decay in amplitude per cycle with Coulomb friction is a constant. While for viscous damping the percentage of

each cycle's amplitude to that of the previous cycle is constant, resulting in a decaying exponential curve for free vibration, the free decay for Coulomb damping is a straight line. This is demonstrated in Figure 1. Mathematically, the relationship of successive cycles is

$$\underbrace{\frac{x_n}{x_{n+1}} = k_v}_{\text{viscous damping}} \qquad \underbrace{x_n - x_{n+1} = k_c}_{\text{Coulomb damping}},$$

where x is the displacement of the oscillator. When the displacement x is less than the Coulomb constant k_c, motion will cease. The effect on the apparent viscous damping when Coulomb damping is present is demonstrated in Figure 2. The apparent viscous damping becomes very high at low amplitudes for Coulomb damping. For the last cycle, the apparent damping is infinite since motion ceases when $x < k_c$.

Experimental Measurement Techniques

A number of techniques have been developed to estimate damping from experimental data. The simplest and most commonly used are the logarithmic-decrement and half-power methods.[4] In the logarithmic-decrement method, which uses the time domain of structural response, the ratios of the amplitude of vibration x_n at any time and

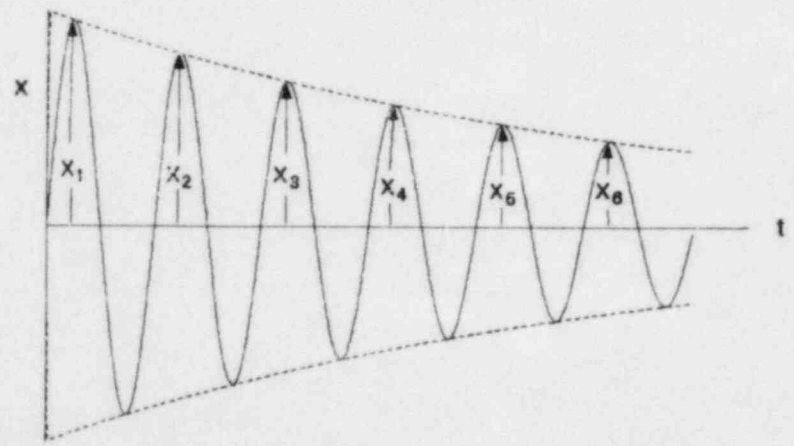

a. Free vibration with viscous damping

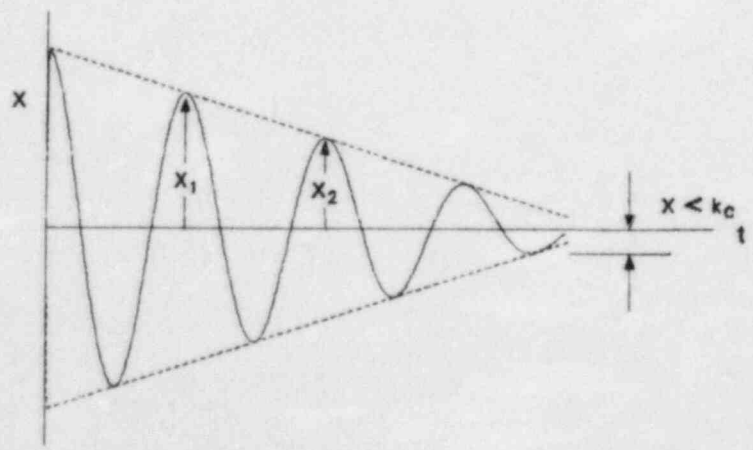

b. Free vibration with Coulomb damping

Figure 1. Free vibration traces.

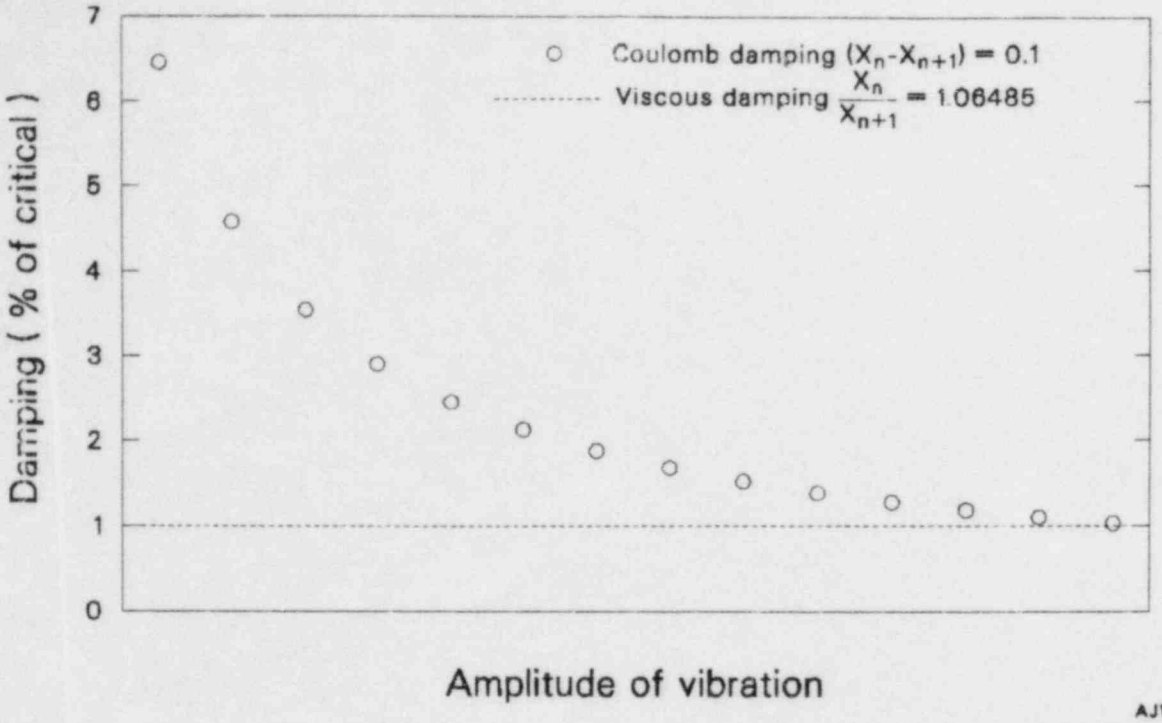

Figure 2. Comparison of Coulomb and constant-force damping curves.

the amplitude after m cycles x_{n+m} are used to form the logarithmic decrement, δ_m,

$$\delta_m = \frac{1}{m} \ln \frac{x_n}{x_{n+m}} .$$

It can be shown that

$$\zeta = \frac{\delta_m}{2\pi \frac{\omega}{\omega_d}} \sim \frac{\delta_m}{2\pi} = \frac{1}{2\pi m} \ln \frac{x_n}{x_{n+m}}$$

where ω and ω_d are the undamped and damped natural frequencies, respectively. If the damping is less than 20%, the approximate form that neglects the change in frequency due to damping is sufficiently accurate (the error in calculating ζ is less than 2%). The method is generally used with snapback testing, in which the structure is displaced, released, and allowed to vibrate freely. Typical time-displacement histories suitable for use with this technique are shown in Figure 1. Note that, with this time-domain calculation, only one mode should be represented. Thus, either the vibration of the structure should be confined to a single mode or digital filtering of the data is required. Consequently, usually only the lowest few modes of vibration can be evaluated by the method.

The half-power method uses a plot of response amplitude as a function of frequency to determine damping. The damping ratio is approximately equal to

$$\zeta = \frac{f_2 - f_1}{f_2 + f_1}$$

where f_1 and f_2 are the frequencies where the response amplitude is 0.707 times the peak amplitude (see Figure 3). This method is generally applicable to tests in which the excitation is sufficient to generate a frequency response curve, such as with shaker tests. The method can also be used with snapback tests by transforming the time histories to the frequency domain. However, sometimes poor frequency resolution, especially at low frequencies, and nonlinearities, can present obstacles to obtaining good results.

More complicated procedures have been developed, using the frequency response function

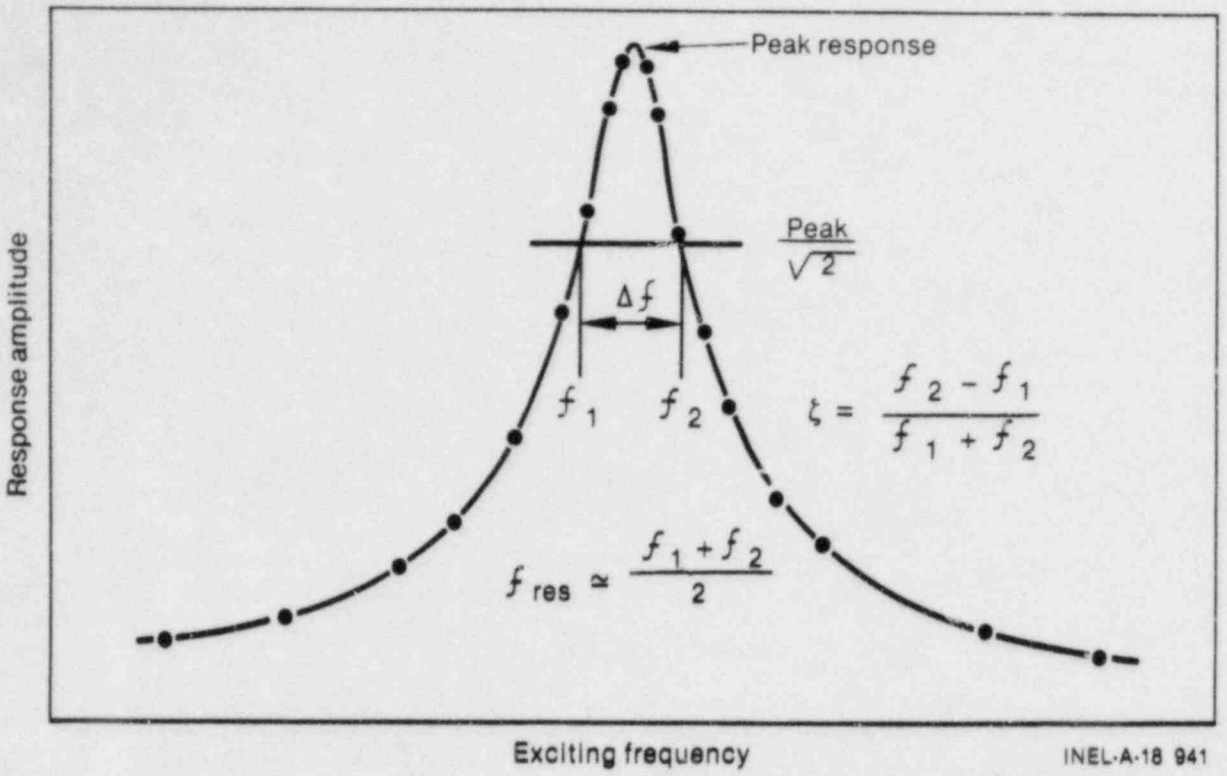

Figure 3. Half-power method computation.

of the input and output forces. A discussion and literature survey of these additional methods are contained in Reference 11. One type of curve fitting method that was used by EG&G Idaho to evaluate some of the damping data in this report is called the complex exponential method. This method obtains the inverse Fourier transform of the frequency response function to give the impulse response in the time domain. This response form, which can be written as the sum of complex exponential functions, is approximated by an interactive polynomial curve fitting procedure. The roots of this polynomial yield the natural frequencies and modal damping of the measured response. Details of the theory of modal analysis can be found in Reference 12.

TEST PROGRAM

A test plan was developed to understand the physical nature of damping and to expand the data base of recorded damping values. For this initial series of tests, a simple system consisting of a straight piping segment, supported at the ends, was chosen. Various types of intermediate supports could be added to investigate the effect of the following on piping system damping:

1. Pipe size
2. Excitation magnitude
3. Excitation type or source
4. Response frequency
5. Individual piping supports
6. Support installation (boundary conditions)
7. Damping calculation methods.

The experience gained from this simple system will be used to develop future tests of more complicated systems.

Test Facility and Equipment

A suitable location for conducting pipe damping experiments was found at the Auxiliary Reactor Area-III (ARA-III) at the INEL. This facility was originally the site of a gas-cooled test reactor. After the reactor was decommissioned, the site has been used for various physical and material tests. A high bay in Building 608 at ARA-III provided space and services for the pipe damping tests.

The overall test fixture consisted of a section of pipe approximately 33-ft in length supported at the ends, an overhead beam from which to hang pipe supports, the pipe supports themselves, and floor mounts on which to attach the hydraulic shaker. Figure 4 shows the overall arrangement.

The overhead support was a large, wide-flange beam with vertical column supports at each end and intermediate supports at angles. The design was stiff so that there would be only a very small deflection under pipe support loads. The stiffness gave a high natural frequency well above the maximum 33-Hz range for seismic loads. Impedance testing measurements of the structure gave a minimum natural frequency of 88 Hz. At points along the length of the beam corresponding to the midpoint, quarter point, and third point locations of the pipe, holes were drilled to which plates could be bolted. These plates were the end fittings for the various pipe supports. Figure 5 shows how the plate fitted to the overhead beam to support a sway brace.

Pipes for the tests were SA-106 Grade B carbon steel, each slightly longer than 33 ft. Two sizes of Schedule 40 pipe were tested: 3-in. and 8-in. diameter. The pipe ends were attached to the top of a vertical column (Figure 6). Each end column could be moved horizontally along the pipe axis to accommodate end connections of each pipe tested. Originally, pinned-end conditions were to be simulated using an 8-in. trunnion. For the 3-in. pipe, a split annular plate was used to fit the pipe to the trunnion (Figure 7).

When testing began it became obvious that the end condition was very critical to the damping in the system. The most consistent pinned-end results for the 3-in. pipe resulted from removing the top half of the split plate so that the pipe was resting on the lower half. For the 8-in. pipe fixed-end condition, the ends were secured by both the end plate and the trunnion (Figure 8). For the 8-in. pipe, the best pinned-end results were obtained by bolting the end of the pipe to the end plate, which was in turn bolted to the vertical column (Figure 9). The arrangement shown in Figure 9, with pipe bolted to the end plate, provided the best fixed-end arrangement for the 3-in. pipe.

Table 2 lists the piping supports used during the tests. Four spring hangers, sized to support the weight of the two pipes (empty and water filled), are shown in Figure 10. Each hanger was connected to the plate attached to the overhead beam, and linked to the pipe via a double-bolt pipe clamp (Figure 11). Each spring hanger was loaded so that the spring was compressed to approximately the midpoint of the working range (Figure 12). Maximum spring travel for each spring hanger was approximately 2-1/4 in.

The rod hanger was simply a solid 5/8-in.-diameter rod connecting the pipe and overhead beam. Figure 13 shows the rod-to-pipe connection.

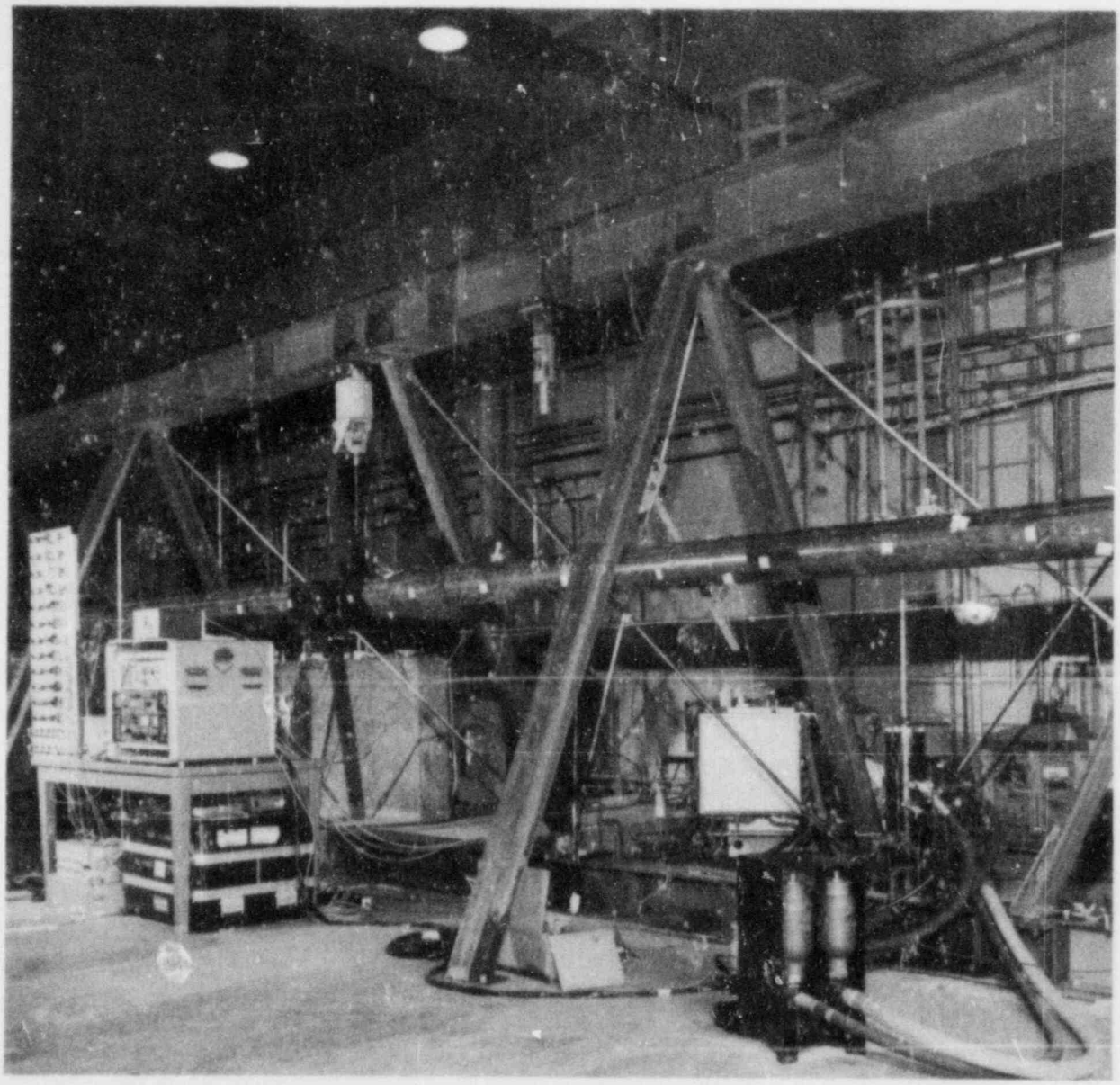

Figure 4. Overall test fixture.

The sway brace (Figure 5) had a 600-lb maximum capacity. It was tested both in the preloaded and unloaded conditions. The constant-force hanger (Figure 14) was rated at 1577 lb with a maximum travel of 2 in. Two identical snubbers were tested (Figure 15). One had been installed for a time in the INEL Loss-of-Fluid Test facility while the other was unused.

Test Excitation

Three basic types of test excitation were used. In the first, an instrumented hammer was used to strike the pipe (Figure 16). This produced an impulse force at low excitation levels. The second method of excitation used a 3.3-kip hydraulic shaker, clamped to a wide-flange beam anchored to the floor (Figure 17). A slender rod (stinger) connected the shaker to a load cell, which in turn was connected to a pipe clamp around the pipe. The shaker was driven by a hydraulic power supply and could be programmed for either a random or sinusoidal output using the signal generator and control unit shown on the right side of Figure 18. The final method, which used the largest loads in the tests, was accomplished with a 50-ton overhead crane. Straps were hung from the crane hook to a load

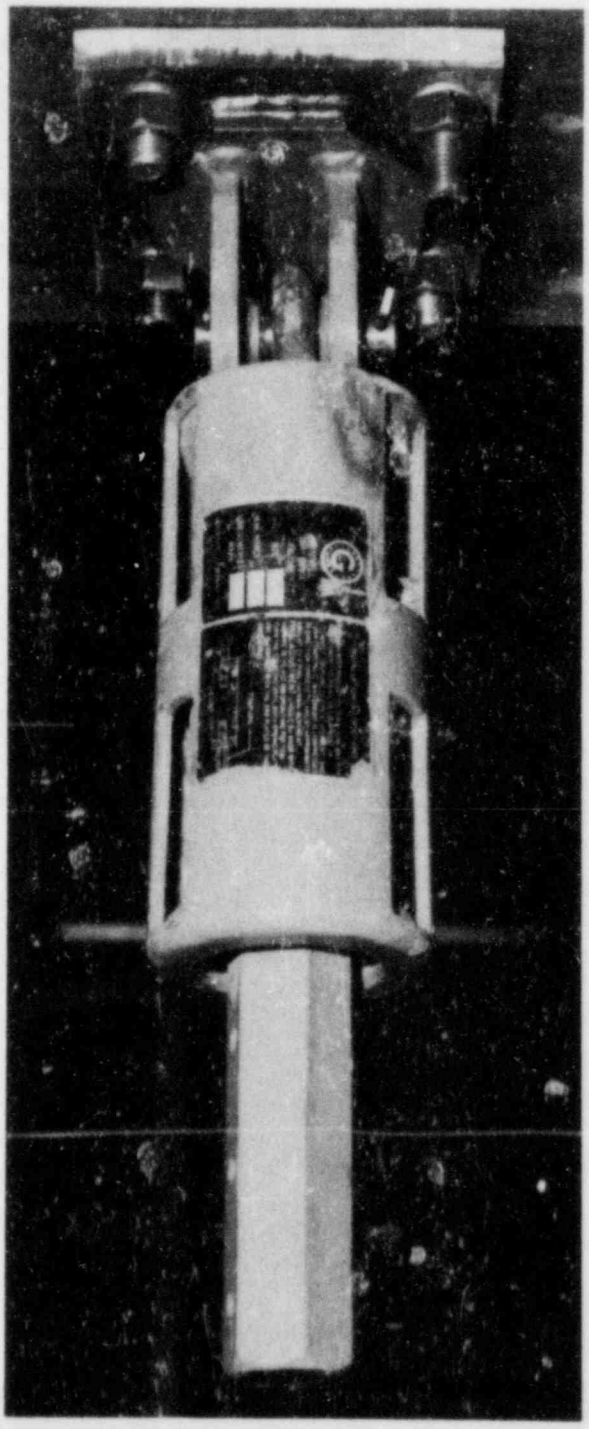

Figure 5. Sway brace showing connection to overhead beam.

gauge, which was in turn connected to a quick-release device (Figure 19). The quick-release device (Figure 20) had a hook, which fit into a rectangular lug on the top of the pipe. When the long actuation bar moved vertically downward, the hook would rotate, releasing the pipe and allowing it to vibrate freely.

Instrumentation

Table 3 summarizes the instrumentation used in these tests. The input forces to the pipe were measured by load cells in the instrumented hammers, via a load cell on the shaker stinger and various sizes of static load gauges on the snapback device, depending on the size of the load (Figure 19). Displacements were measured by a linear variable differential transformer (LVDT) mounted between the floor beam and the pipe. Strain gauges were placed on the tops and bottoms of the pipes at the midpoints, quarter points, and ends (Figure 21). A strain gauge was placed on each side of the 3-in. pipe at the quarter point to measure side motions. Strain conditioning equipment is pictured in the left side of Figure 18. Accelerometers were mounted on the pipe using magnetic blocks (Figure 22).

Data Acquisition

For modal testing, one input channel and seven response channels were digitized, filtered, Fourier transformed, averaged, and converted to frequency response and coherence functions on the data acquisition modal analyzer (Figure 23). The input channel recorded the forcing function for hammer and shaker tests, while the response channels recorded accelerometer, strain gauge, and LVDT data. For snapback data, no input forcing function was recorded. Initial loads, displacements, and strain were recorded before the pipe was released. All channels could be used for output data.

Test Matrix

A summary of the more than 100 tests conducted is presented in Appendix A. The tests were designated PDSXXY, where PD stands for "pipe damping," S is the pipe size in inches, XX is the test sequence number, and Y designates the type of excitation—H for impact and shaker tests, and F for snapback tests. These tests were chosen to vary one parameter at a time and to try to gain knowledge of how these parameters affect piping system damping. The basic test sequence for both the 3-in. and 8-in. pipes was to begin with the pipe empty and the ends pinned. For the 3-in. pipe, the ends were fixed and finally the pipe was filled. The 8-in. pipe test sequence involved filling the pipe and finally fixing the ends.

Data Reduction

Reduction of the data was accomplished on the EG&G modal analyzer. Hammer data and shaker data were reduced using the frequency response function method, and the built-in software suitable for computing frequencies, damping, and mode shapes. In most cases, the mode shapes were easily identifiable because the dynamic properties of a straight beam are already well known. Damping was calculated using the MODAL-PLUS[12] feature of the analyzer, and also using the simple half-power method. All data reduction was carried out in the frequency domain.

For snapback tests, the data were recorded in the time domain. They were subsequently transformed to the frequency domain to check the frequency content and to ensure just one mode was being excited. If only a single mode was present, the time-domain data was used to calculate damping. In the case of the straight pipe, it is impossible to excite higher modes without exciting the fundamental mode. Therefore, to compute damping for higher modes, the data had to be filtered, thereby eliminating the effect of lower modes. In some cases, the effect of the higher modes had to be filtered to compute damping for the lowest mode.

Table 2. Support types used

Type	Manufacturer	Type, Size
Spring hanger	ITT Grinnell	Figure 296,[a] 0
Spring hanger	ITT Grinnell	Figure 296, 3
Spring hanger	ITT Grinnell	Figure 296, 7
Spring hanger	ITT Grinnell	Figure 296, 9
Rod hanger	ITT Grinnell	5/8 in.
Sway brace	ITT Grinnell	Figure 296, 2
Constant-force hanger	ITT Grinnell	80-V
Snubber	Int. Nuclear Safeguards	MSVA-2
Snubber	Int. Nuclear Safeguards	MSVA-2

a. See ITT Grinnell Catalog PH-74-R.

Table 3. Instrumentation

Instrument	Manufacturer	Model
Load cells	PCB Piezotronics	223 B
Accelerometers	PCB Piezotronics	308B02
Strain gauges	Micro-Measurements	Series EA, 1/8 in.
LVDT	Schaevitz	2000 HR
Load gauges	Various[a]	Dial
Hammers	PCB Piezotronics	Various

a. Largest was Dillon 50,000-lb dynamometer.

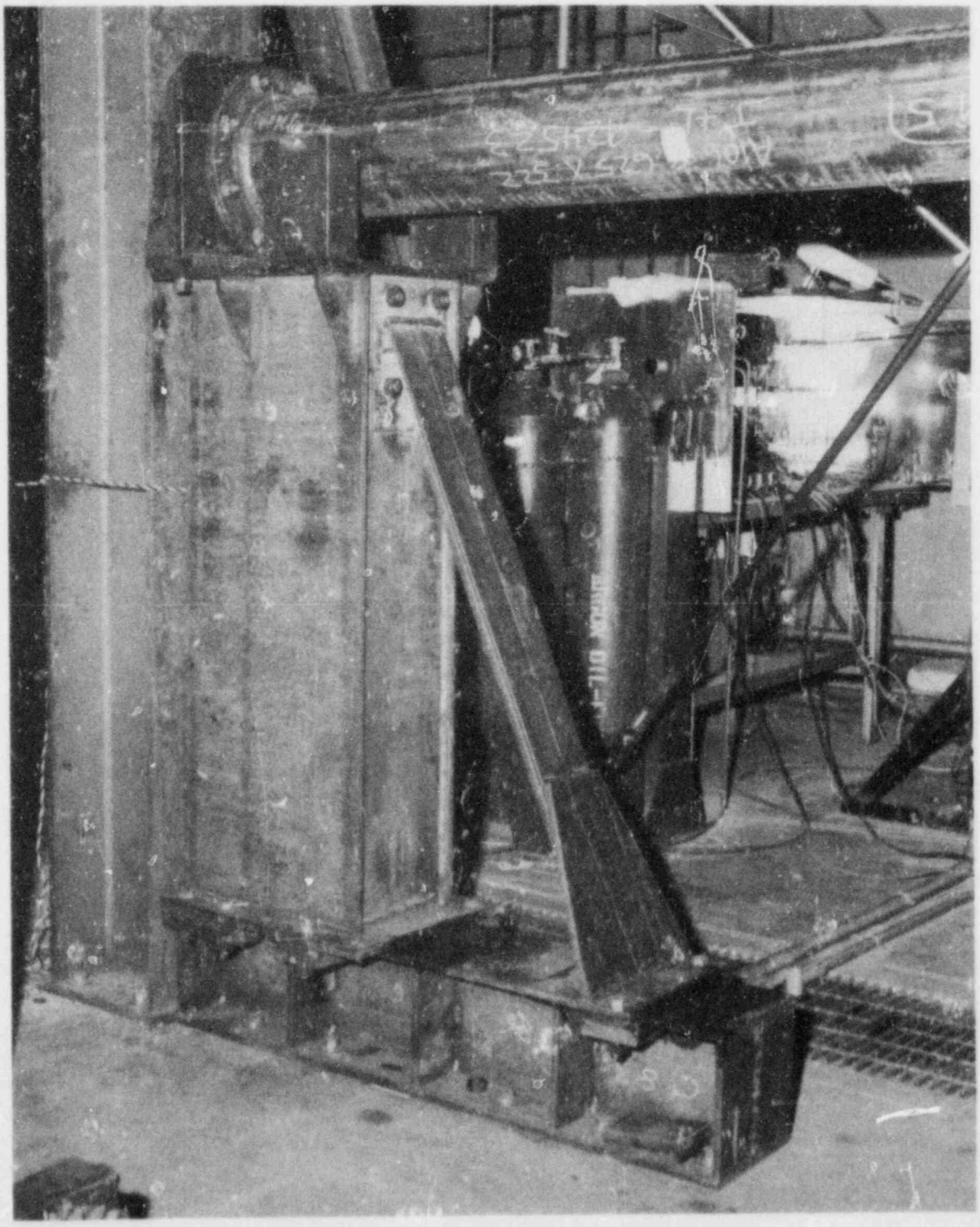

Figure 6. End fixture.

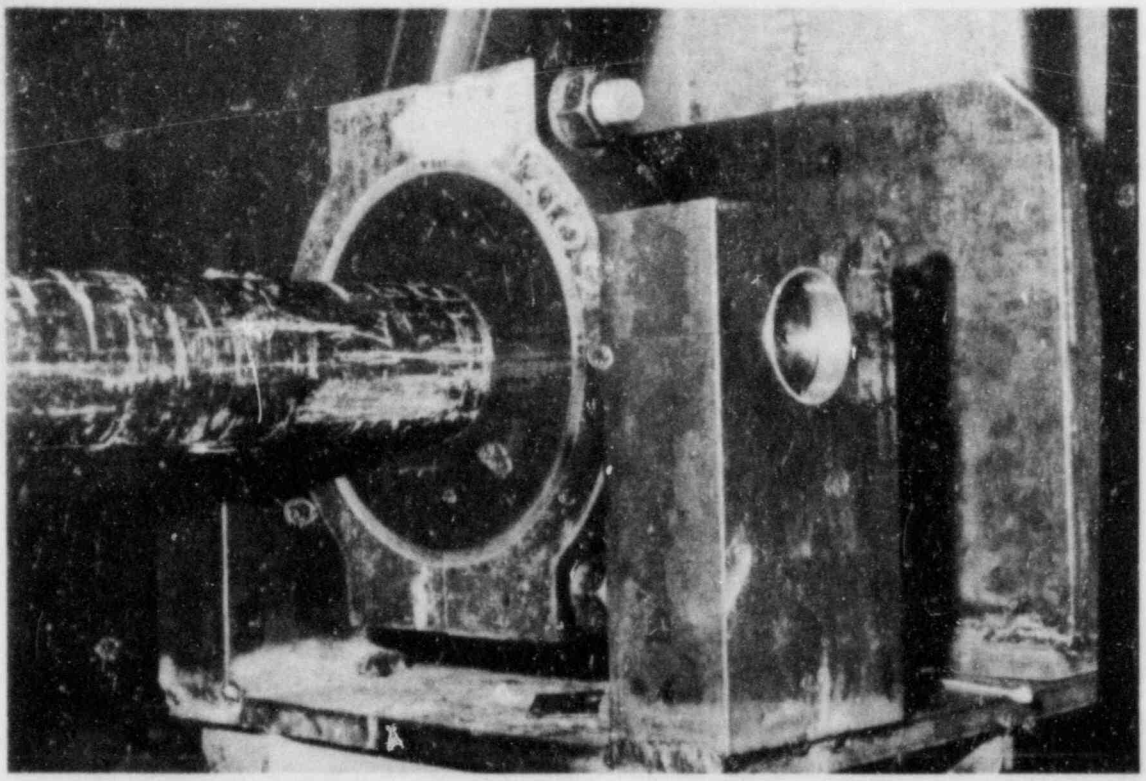

Figure 7. Pinned-end support for 3-in. pipe.

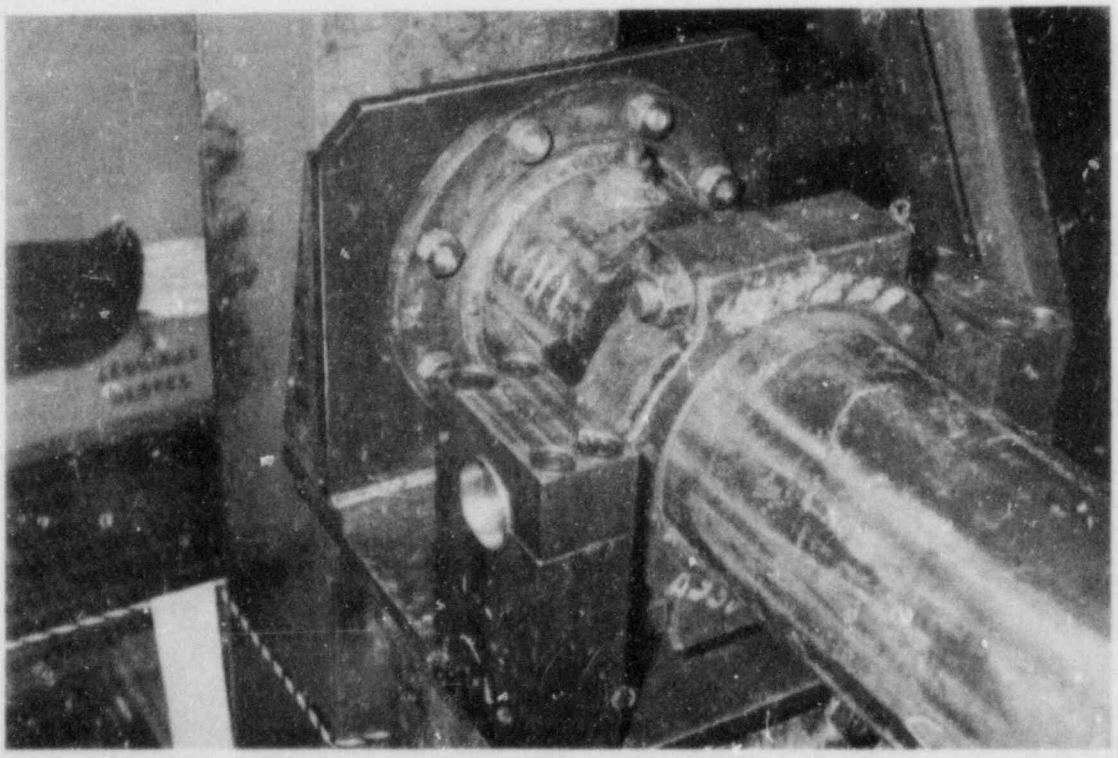

Figure 8. Fixed-end support for 8-in. pipe.

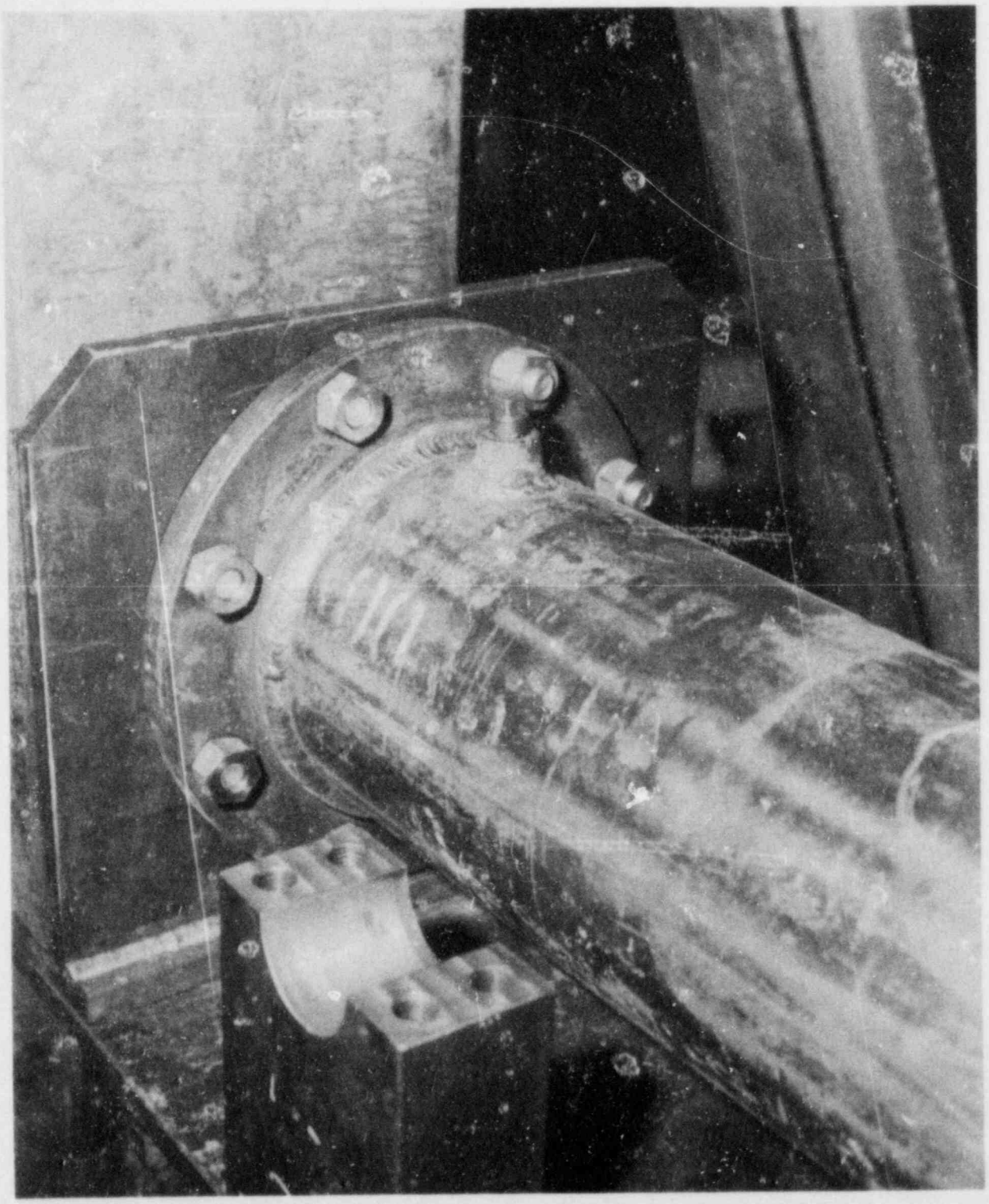

Figure 9. Pinned-end support for 8-in. pipe.

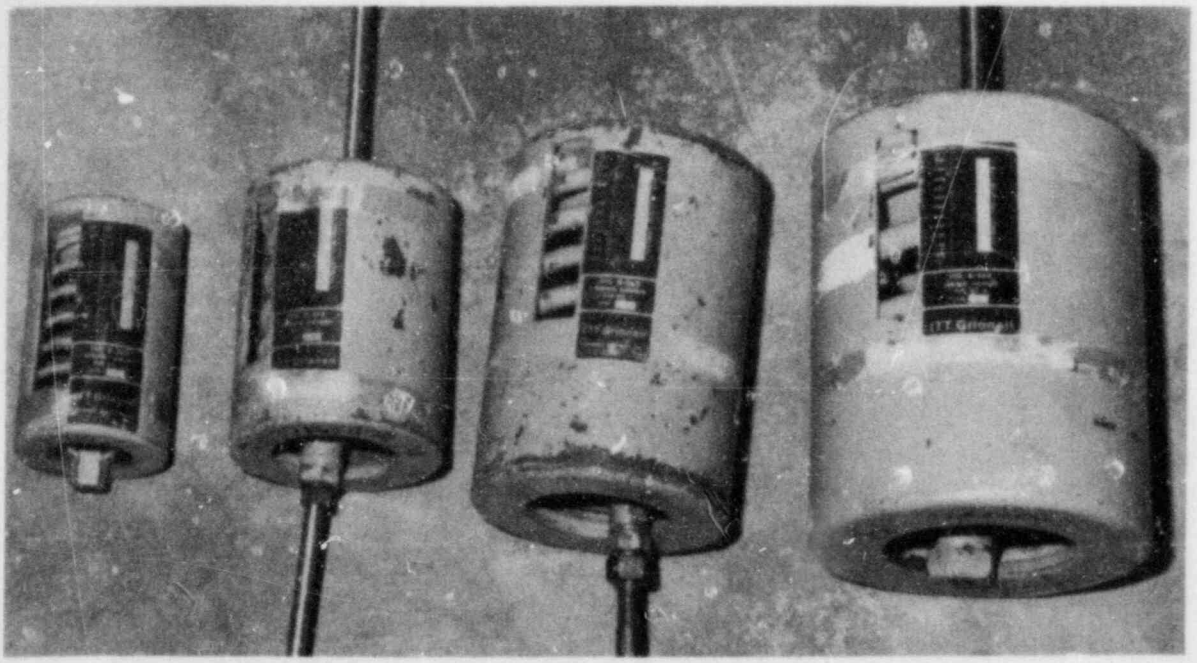

Figure 10. Spring hangers.

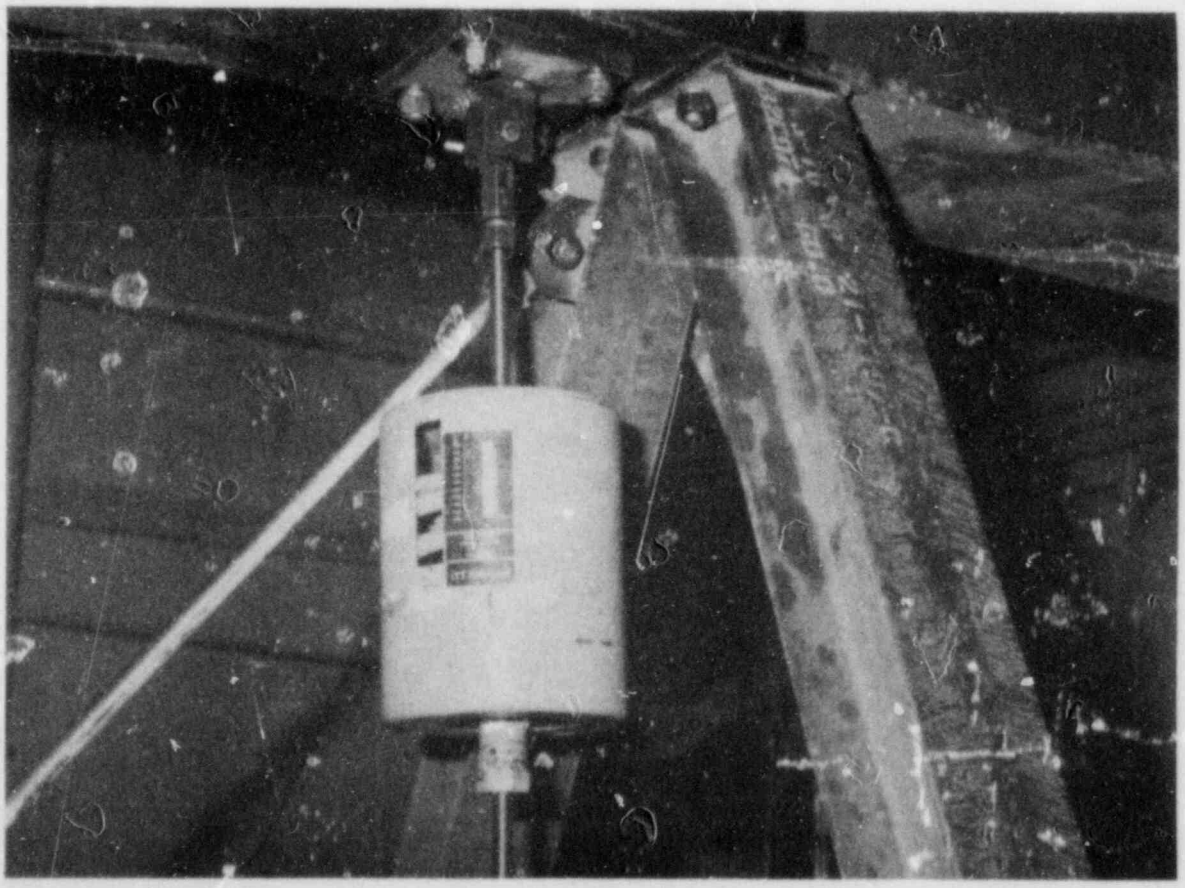

Figure 11. Support connections for spring hanger.

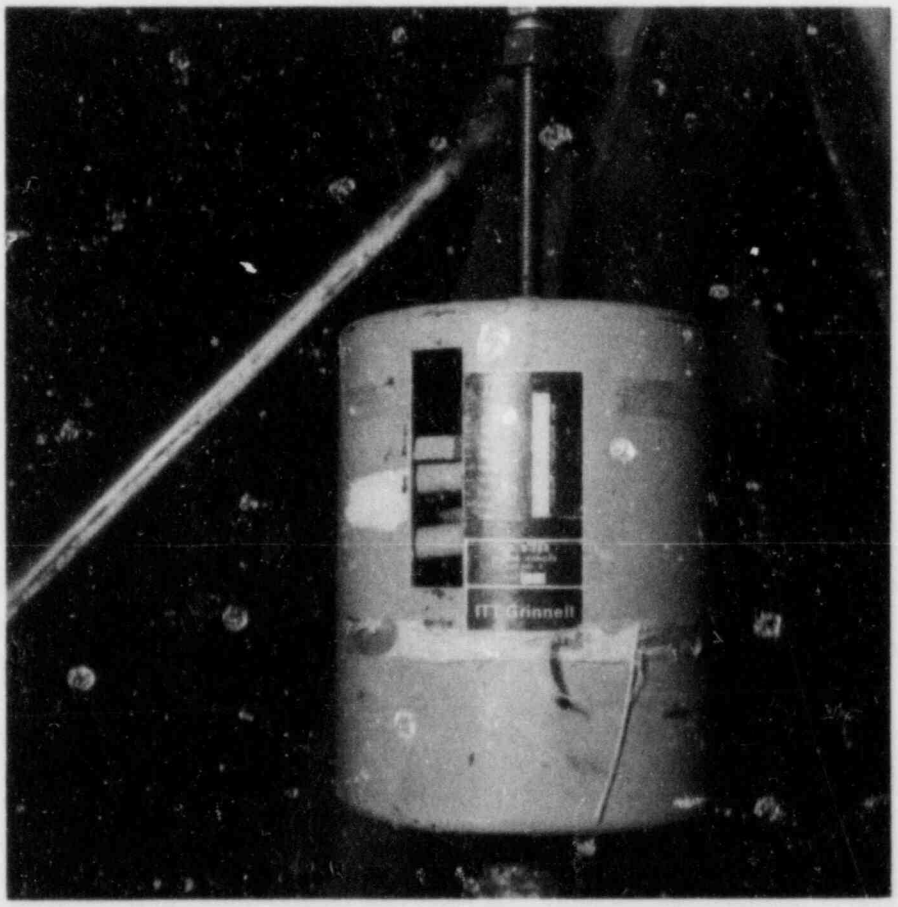

Figure 12. Loaded position of spring hanger.

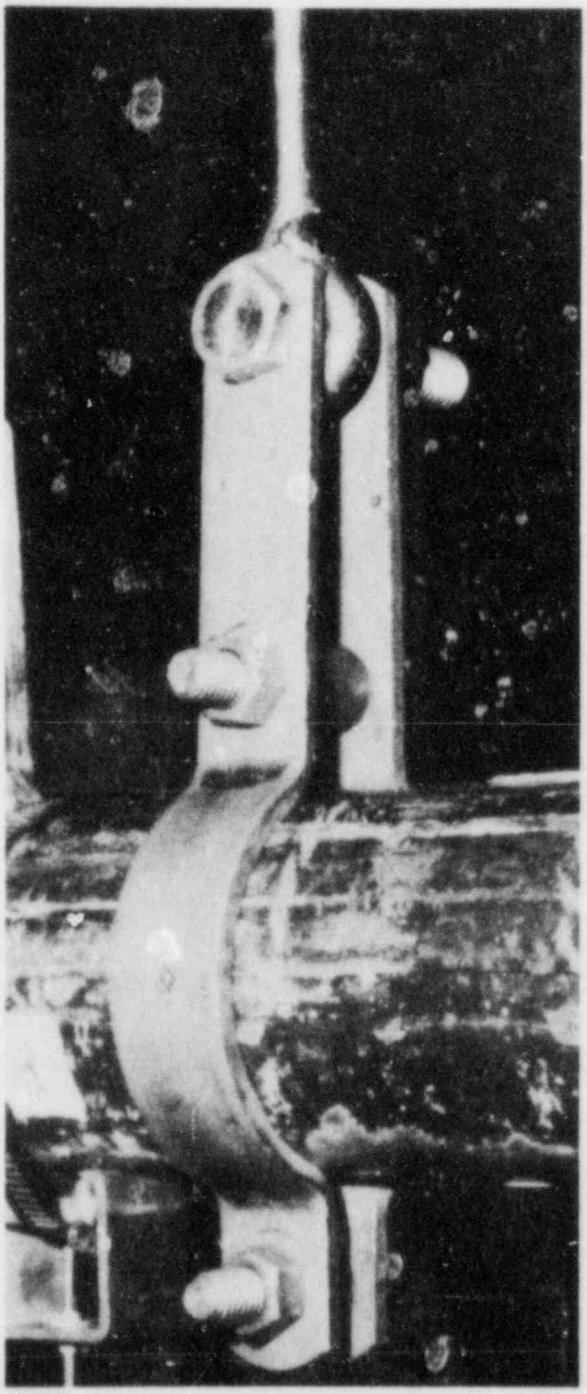

Figure 13. Pipe clamp connection.

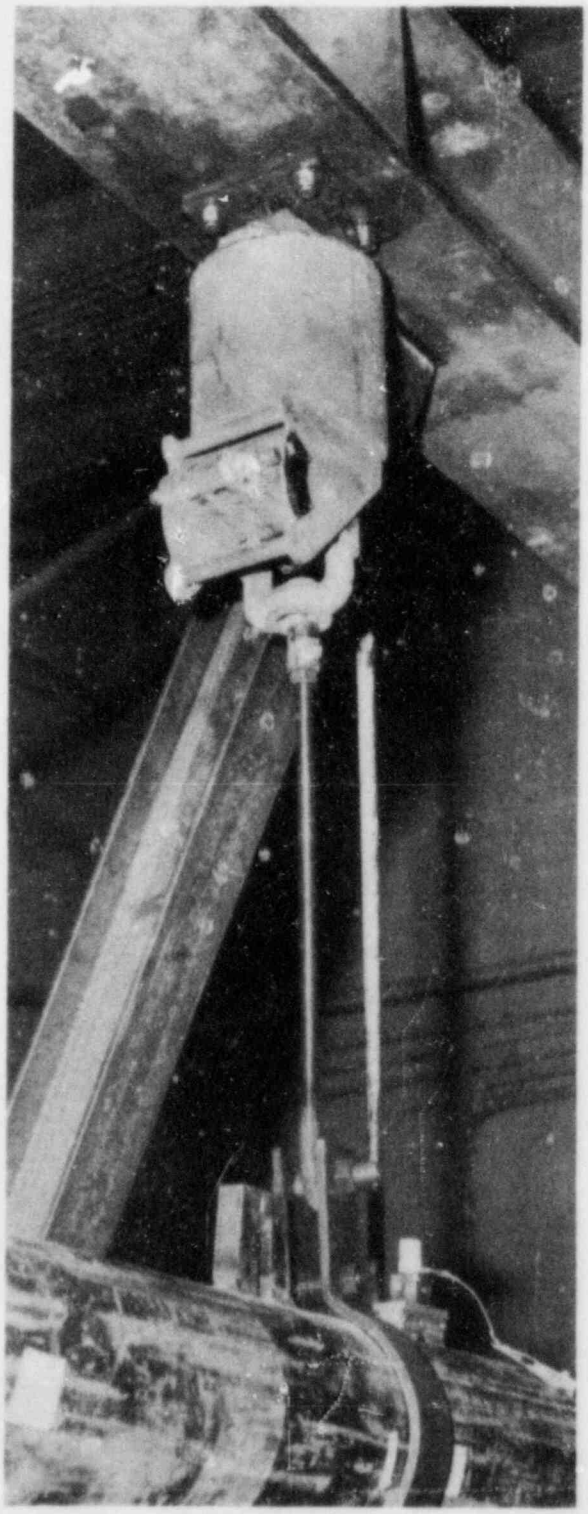

Figure 14. Support connections for constant-force hanger.

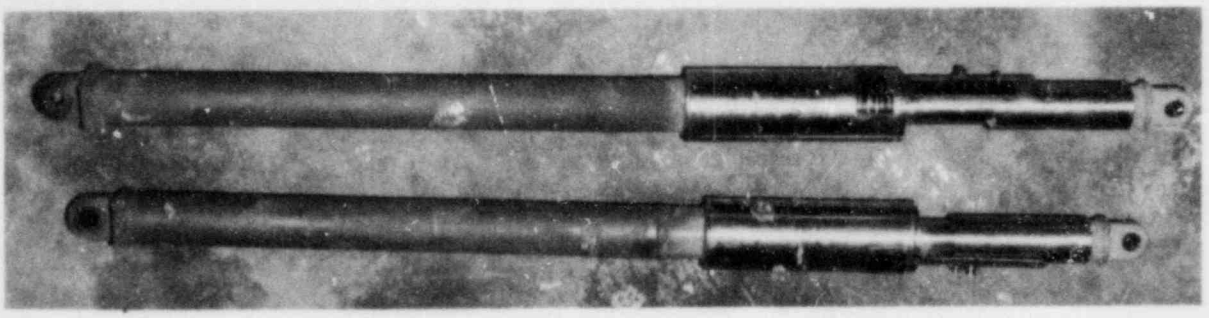

Figure 15. Snubbers.

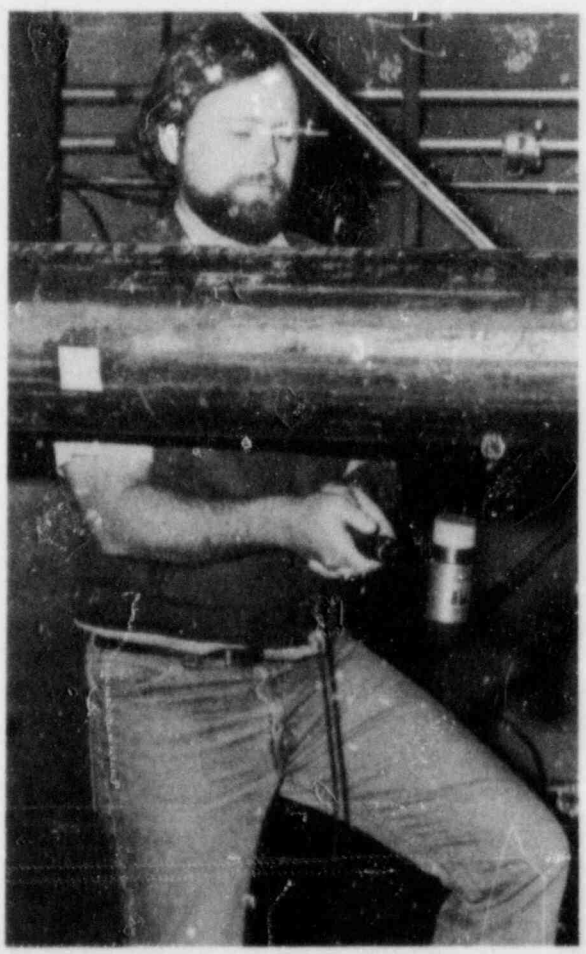

Figure 16. Impact testing of pipe.

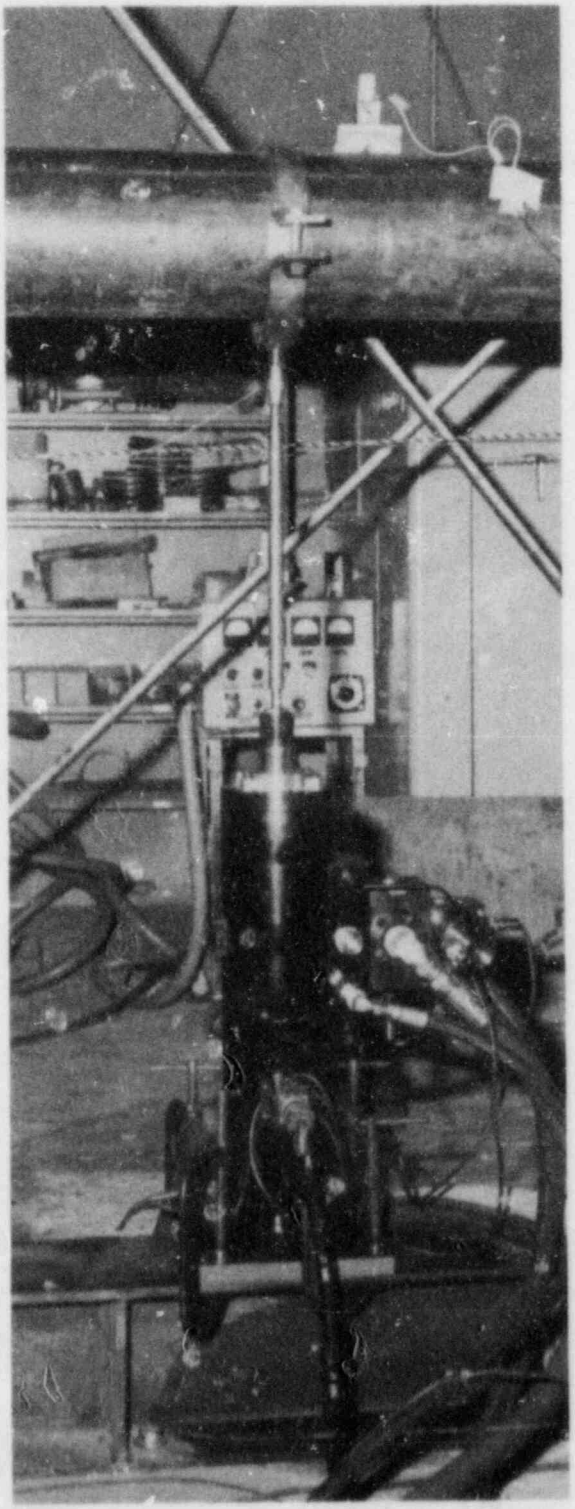

Figure 17. Hydraulic shaker.

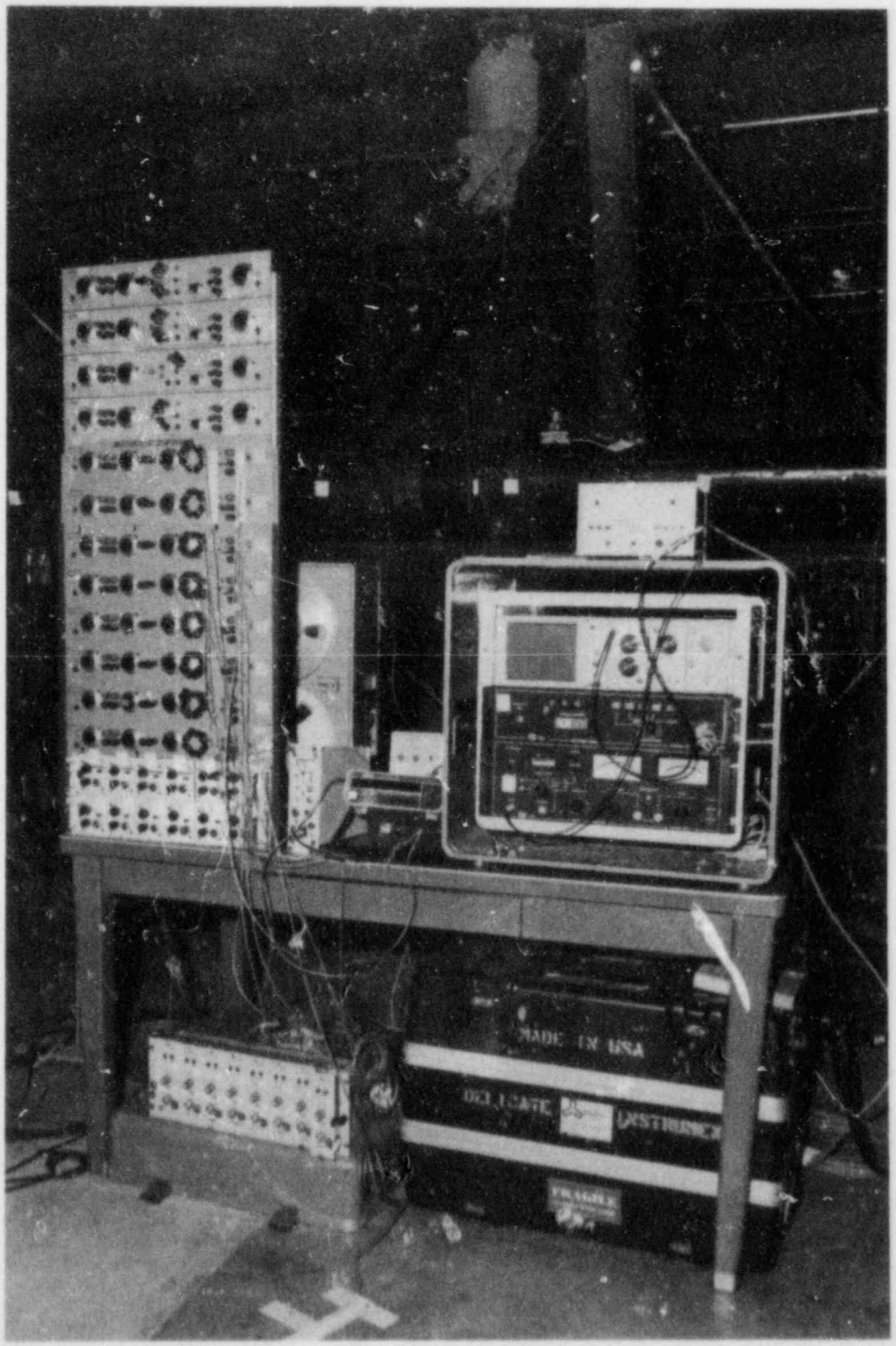

Figure 18. Strain gauge conditioning and hydraulic shaker control panels.

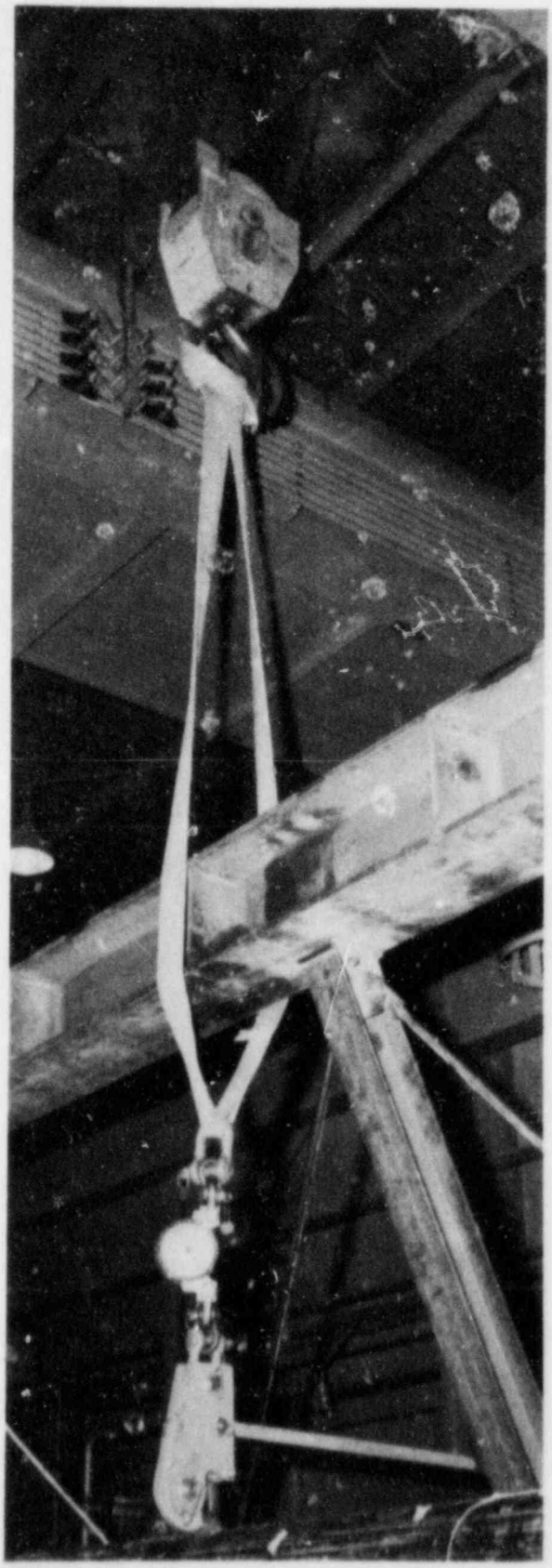

Figure 19. Snapback test setup.

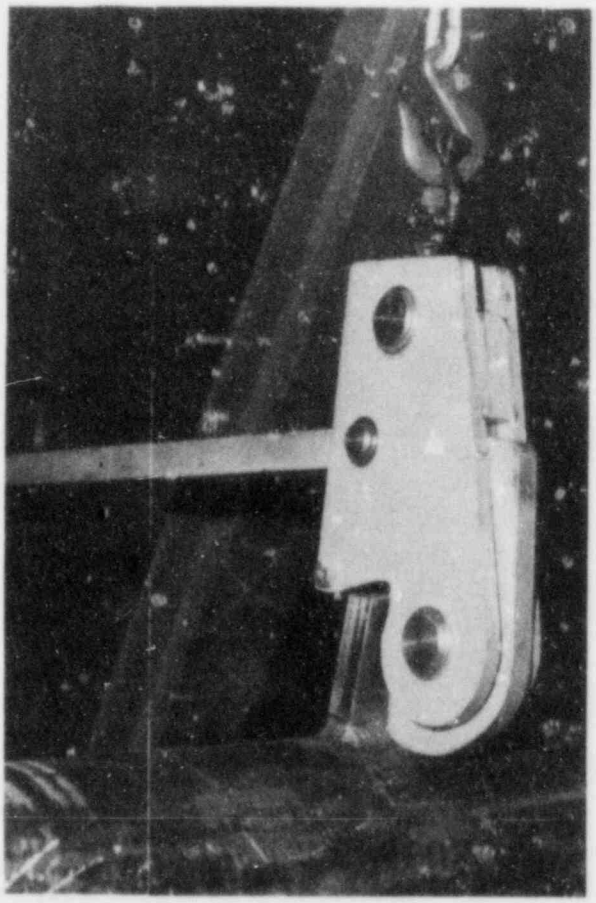

Figure 20. Quick-release device.

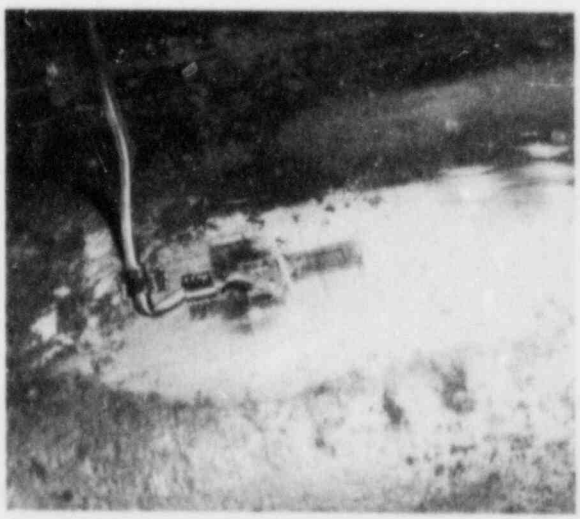

Figure 21. Strain gauge.

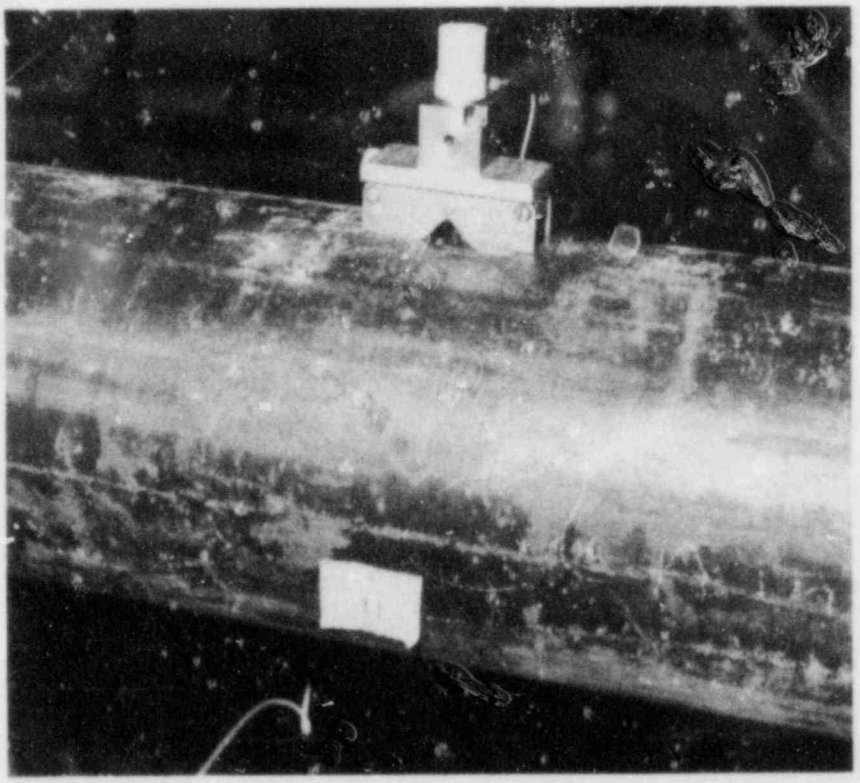

Figure 22. Accelerometer and mount.

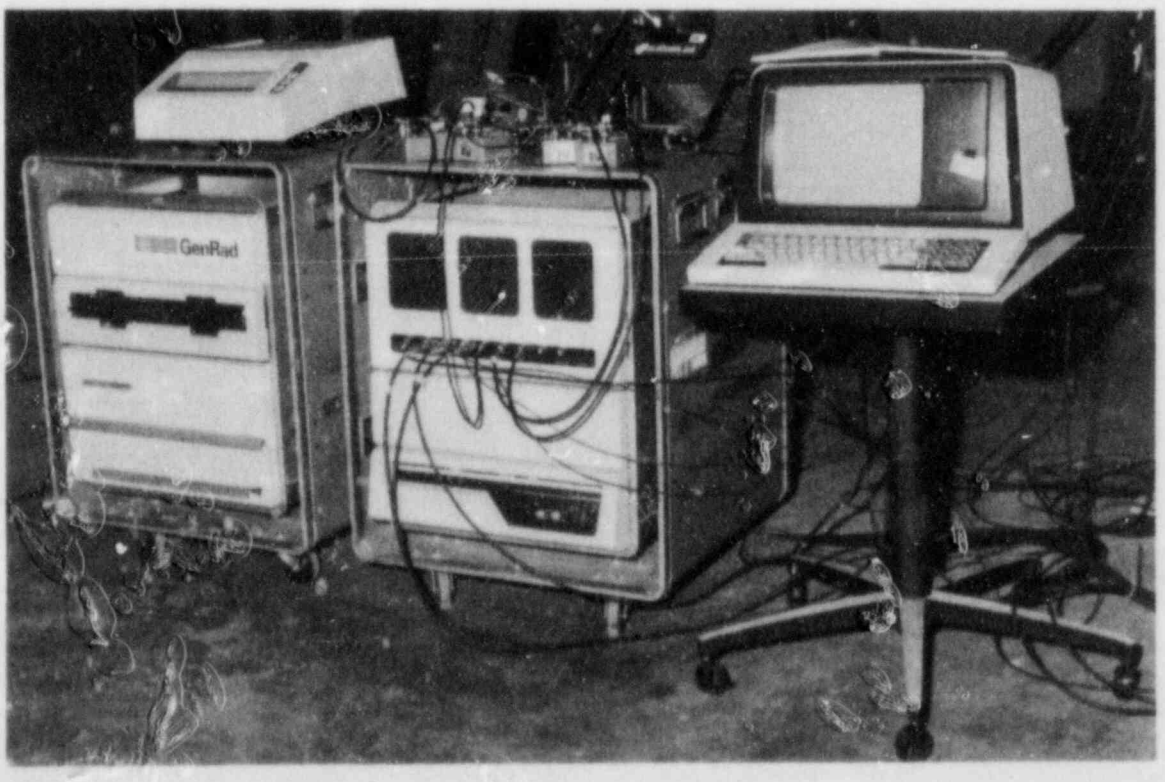

Figure 23. Data acquisition equipment.

TEST RESULTS

This section presents the results of the tests, grouped according to test method. First, a general account of the interaction of the test fixture and piping is discussed, then the details of the pipe tests. In order to give an understanding of the modes and mode shapes in the later discussion, a presentation of the experimental modes and frequencies is compared with theoretical results. The results of snapback, hammer, and shaker tests follow.

The results are reported with respect to the measurement locations chosen for these tests. These are shown in Figure 24, with the distances of each point from location 1, the left end, given in Table 4.

Test Fixture Interaction Study

Several tests were conducted to determine the interaction between the test fixture, the pipe, and the pipe supports. The first test was to determine the frequency of the overhead frame. Hammer tests showed no frequencies below 88 Hz, which was well above the frequency range of interest.

The second condition checked was the effect of the end columns. These were very stiff in the vertical direction, but were relatively flexible in the horizontal direction. Testing revealed several horizontal modes in the frequency range of interest. However, because the tests were essentially one dimensional in the vertical direction, there was no effect on the computed vertical frequencies and damping from the horizontal motion.

Because the shaker was mounted to the floor, there was the possibility that significant energy could have been transmitted from the shaker through the floor beam to the concrete floor, and thence to the end columns, which would shake the pipe. Shaker tests were conducted with the shaker clamped to the floor beam, both attached and unattached to the pipe. In another test, the shaker was suspended from the pipe with a reaction mass attached to the shaker. That is, the pipe supported the shaker entirely. These tests showed that there was no feedback through the floor below about 20 Hz. At frequencies from 20-33 Hz, a slight effect was noticeable. From the results it was judged that the amount of feedback was low enough to be acceptable.

Mode Shapes and Frequencies

Frequencies for the straight pipe were computed based on the nominal dimensions for Schedule 40 piping. The approximate pipe length was varied between 32 and 33-1/2 ft, depending on how the ends were supported. Results for modes below

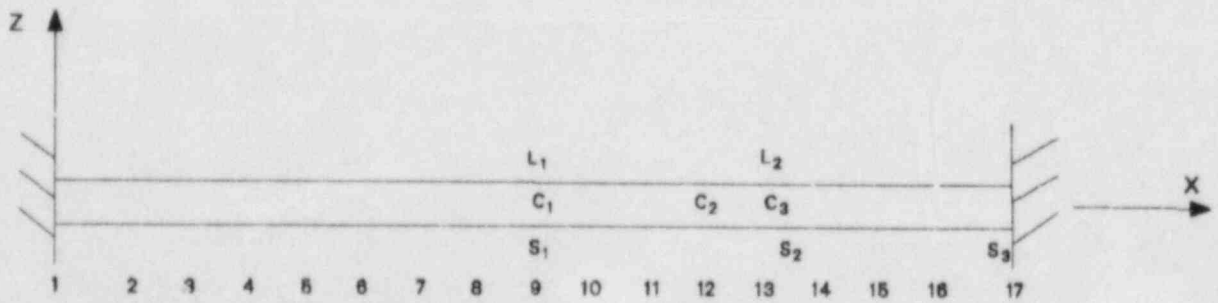

Figure 24. Instrument locations.

Table 4. Measurement locations

Location	Distance from Location 1	
	3-in. pipe	8-in. pipe
1	0 ft	0 ft
2	2 ft 9 in.	3 ft
3	4 ft 9 in.	5 ft
4	6 ft 9 in.	7 ft
5	8 ft 9 in.	9 ft
6	10 ft 9 in.	11 ft
7	12 ft 9 in.	13 ft
8	14 ft 9 in.	15 ft
L_1	16 ft 6 in.	16 ft 5-1/2 in.
C_1	16 ft 8-1/2 in.	16 ft 11 in.
9	16 ft 9 in.	17 ft
S_1	17 ft 2 in.	17 ft 1-1/2 in.
10	18 ft 9 in.	19 ft
11	20 ft 9 in.	21 ft
C_2	22 ft 3 in.	22 ft 3 in.
12	22 ft 9 in.	23 ft
L_2	24 ft 7-1/4 in.	24 ft 5-1/2 in.
C_2	24 ft 9 in.	24 ft 11-1/2 in.
13	24 ft 9 in.	25 ft
S_2	25 ft 3-1/8 in.	25 ft 2-1/2 in.
14	26 ft 9 in.	27 ft
15	28 ft 9 in.	29 ft
16	30 ft 9 in.	31 ft
S_3	32 ft 7-1/4 in.	32 ft 3-1/2 in.
17	33 ft 5-1/2 in.	33 ft 5 in.

33 Hz are listed under the "theoretical" column in Table 5. Adding piping supports changed the frequencies, and all combinations have not been calculated. Because a number of tests were conducted on the 3-in. pipe with a rod support at the midpoint, the frequency corresponding to the mode with both ends as well as the midpoint fixed is included.

Illustrations of mode shapes for the first three modes of the fixed/fixed condition are shown in Figure 25a, b, and c. Figure 25d depicts the mode with a snubber or rod support at the midpoint. In this case, only the modes shown in Figures 25b and d would be present, while those in Figures 25a and c would be eliminated.

Frequencies recorded from the tests are listed under the "experimental" column in Table 5. These do not coincide exactly with the theoretical predictions due to uncertainties in end conditions, dimensions, and material properties. In particular, fixed-end measurements on the 3-in. pipe were consistently below predictions, indicating that there was at least some rotation of the ends. Pinned-end, first-mode measurements on the 8-in. pipe were higher than predicted, indicating that at least some resistance to rotation was present.

Snapback Test Results

Results of the snapback tests are discussed in this section. In general, the procedure followed was to

Table 5. Modes and Frequencies

Pipe Size (in.)	Empty (E) or Filled (F)	Pinned (P) or Fixed (F) Ends	Frequency (Hz)	
			Experimental	Theoretical
3	E	P	2.52	2.48
			9.89	9.95
			22.27	22.39
3	E	F	4.50	5.16
			12.08	14.21
			18.03	18.00[a]
			24.50	27.87
3	F	F	3.83	4.33
			10.14	11.92
			14.50	15.10[a]
			20.81	23.37
8	E	P	7.40	5.75
			23.20	23.03
8	F	P	5.74	4.34
			16.88	17.36
8	F	F	11.02	10.73
			26.10	29.56

a. Rod support at midpoint.

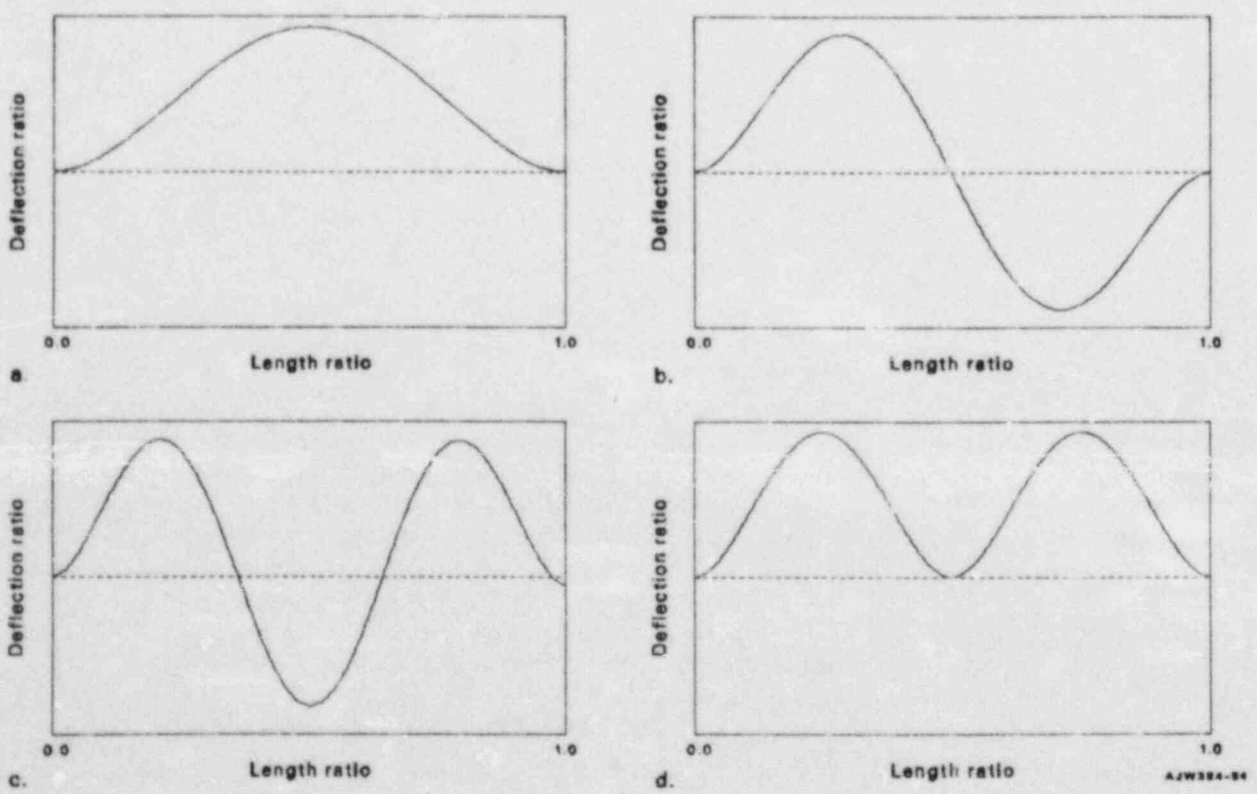

Figure 25. Theoretical mode shapes.

view the time-domain data for each measuring instrument, select the most promising one or ones, view the data transformed to the frequency domain, filter if necessary, and then compute log-decrement damping from the resulting time-domain data. For selected cases, damping was also calculated using the half-power method on the frequency-domain data.

Snapback damping was computed for each mode as the vibrational displacement attenuated, or "rung down." Earlier it was shown that the damping could be computed from the decaying oscillation which involves two or more cycles. Since the vibrational amplitudes are decreasing, we are not dealing with just a single response level. Therefore, for log-decrement damping, estimations were performed on sequential cycles of the ring down. Thus, if damping versus amplitude was plotted, a representation could be made such that a straight horizontal line would be drawn between the amplitudes used to compute damping (see Figure 26). The ends of the horizontal lines represent the magnitudes of the peaks used to compute log-decrement damping. Each successive pair of horizontal lines in Figure 26 has been joined by a vertical line. Alternatively, the average amplitude of the two cycles could be plotted, such as the "x" points in Figure 26. For this report, the latter method was chosen and only the midpoint values are shown.

One important point to note in high-level snapback testing is that the applied load level has to be somewhat greater than the amplitude that appears in the damping versus vibrational amplitude plot. This is a result of at least two factors. The first is that the maximum displacement in Figure 26 was 1.634 in. while the average point plotted is only 1.463 in., over 10% lower. Obviously the higher the damping, the greater this effect. The second factor is that the static deflection shape and the dynamic mode shape are not the same. As the load is released, the pipe deflection changes shape to conform to the vibrational mode shape, and the amplitude may either increase or decrease. This is because in effect the static deflection is made up of the combined effect of all the dynamic modes, while most of the vibrational energy is confined to the lowest mode. Consequently, in general, the initial amplitude cannot be used in the damping calculation. This effect is more pronounced for strain calculated damping than for displacements because the strain involves the second derivative of displacement, or

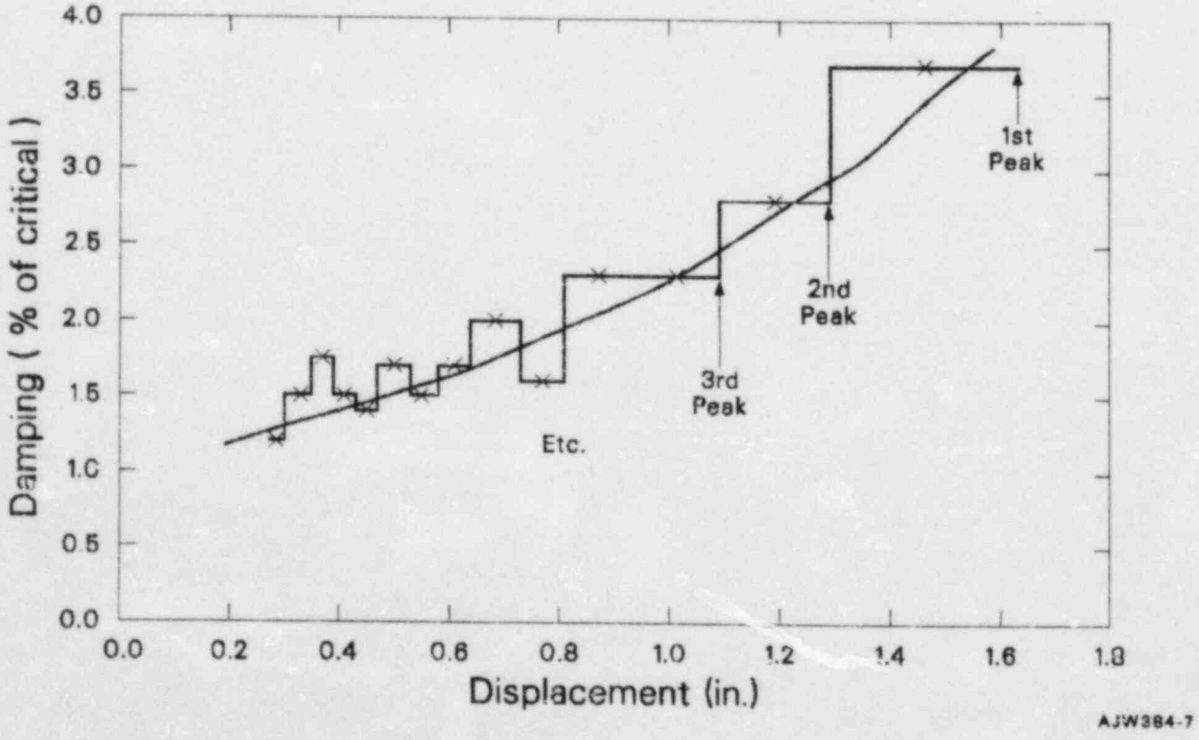

Figure 26. Typical snapback test data.

curvature. For some of the snapback data, the pipe was deflected to a high initial strain, but the cycles available for use in calculating damping have considerably lower magnitude.

For SA-106 Grade B steel, the ASME Code[13] values for stresses are Class 1: S_m = 20 ksi; Class 2: S = 15 ksi; S_y = 35 ksi. Definitions of these stresses can be found in Reference 13. Corresponding elastically computed strain values are listed in Table 6. These can be used as a basis for estimating the vibratory strains at operating basis earthquake (OBE) and safe shutdown earthquake (SSE) allowable levels.

3-in. Pipe—Pinned-End Results. Three snapback tests were performed with the 3-in. pipe empty and in the pinned-end-support condition. In all three cases, the pipe was displaced approximately 1 in., which correlated to about 100 μ in./in. strain at the midpoint of the pipe. Table 7 lists the accelerations used to calculate the log-decrement damping for Test PD301F. The differences in acceleration values, after the first one or two cycles, were 0.035, 0.0247, and 0.0286 g for the three tests.

The difference in g level for successive oscillations is almost constant in each case. In fact, the data plot for Test PD303F in Figure 27 shows that the amplitude decreases almost linearly for successive cycles, which is indicative of Coulomb friction or damping (see the earlier section, Damping). Figure 28 shows the calculated damping values along with the equivalent Coulomb damping curve fitted to the data points.

3-in. Pipe—Fixed-End Results. Three series of tests were performed with the ends of the 3-in. pipe fixed. In the first series of 8 tests the pipe was empty; and in the second series of 13 tests the pipe was filled with water. In the third series at high strain levels, the pipe was again empty.

In Tests PD304F and PD305F, the spring hanger was located at the one-third position and the pipe was plucked at the midpoint with a low force (less than 50 lb) and a 500-lb force, respectively. Data for this transient, which rang down from about 50 μ in./in., are shown in Table 8. In this case, the damping started at less than 1% of critical damping, then increased as the vibrations damped out.

Table 6. Allowable strains for SA-106B piping

Class	Level	ASME Code[a] Allowable (lesser of)	Stress (ksi)	Strain[b] (10^{-6} in./in.)
1	OBE	1.5 S_y	52.5	1220
		1.8 S_m	36.0	
1	SSE	2.4 S_y	84.0	2033
		3.0 S_m	60.0	
2	OBE	1.5 S_y	52.5	915
		1.8 S_h	27.0	
2	SSE	2.0 S_y	70.0	1525
		3.0 S_h	45.0	
		S_y	35.0	1186

a. Class 2 allowable limits were revised in 1981 to values stated here. Before 1981 there were lower allowable values.

b. E = 29.5 x 10^6 psi. Strain is computed as the lesser of the two values in the stress column divided by E.

Table 7. Snapback Test PD301F data[a]

Acceleration (g)	Difference (g)	Damping (% of critical)	Frequency (Hz)
0.59			
0.5355	0.0545	1.54	2.63
0.5073	0.0282	0.86	2.66
0.4718	0.0355	1.15	2.59
0.435	0.0368	1.34	2.66
0.3968	0.0388	1.46	2.64
0.3634	0.0334	1.40	2.58
0.3252	.0382	1.77	2.67
0.29	0.0352	1.87	2.61
0.255	0.035	2.04	2.61
0.22	0.035	2.35	2.64
0.1864	0.0336	2.64	2.67
0.1539	0.0325	3.17	2.61
0.1198	0.0341	4.0	2.64
0.08655	0.0333	5.17	2.73
0.05091	0.0356	8.45	2.83
0.0177	0.0332	16.82	—

a. These data correspond to Figure 28 that shows damping decreasing with increasing acceleration, which is indicative of Coulomb friction.

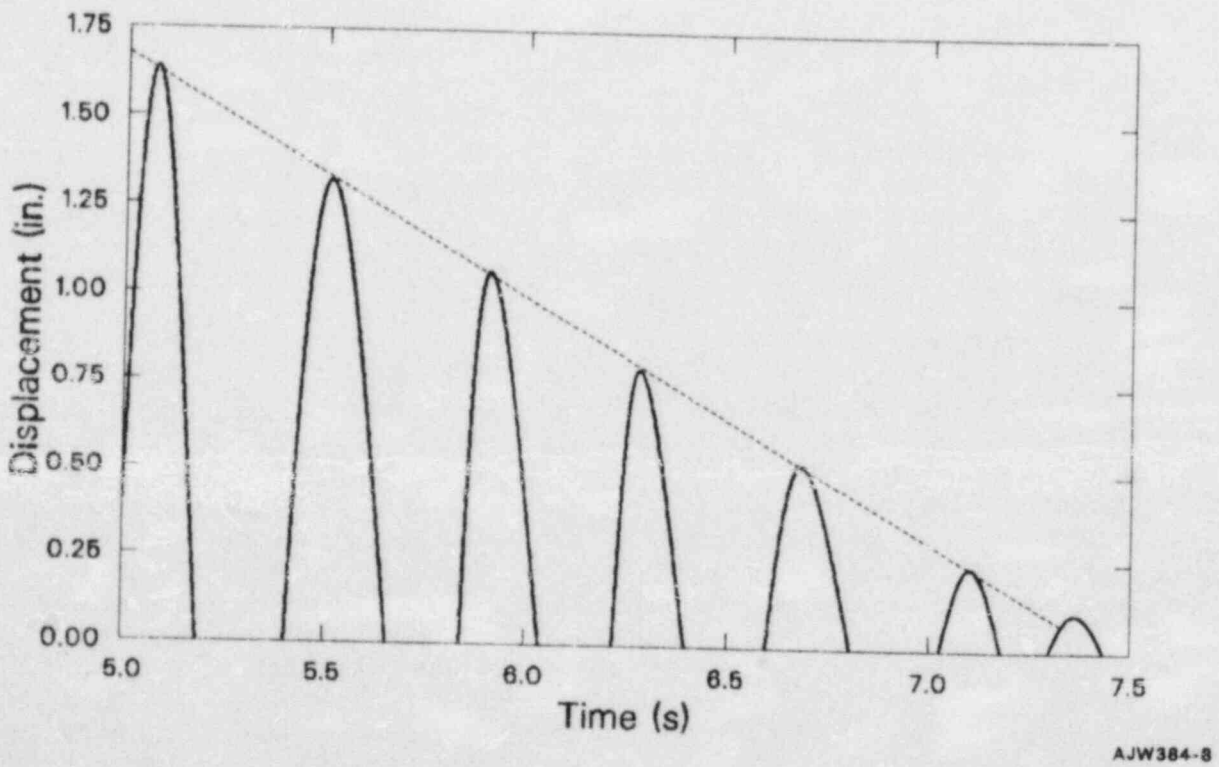

Figure 27. Coulomb damping effect.

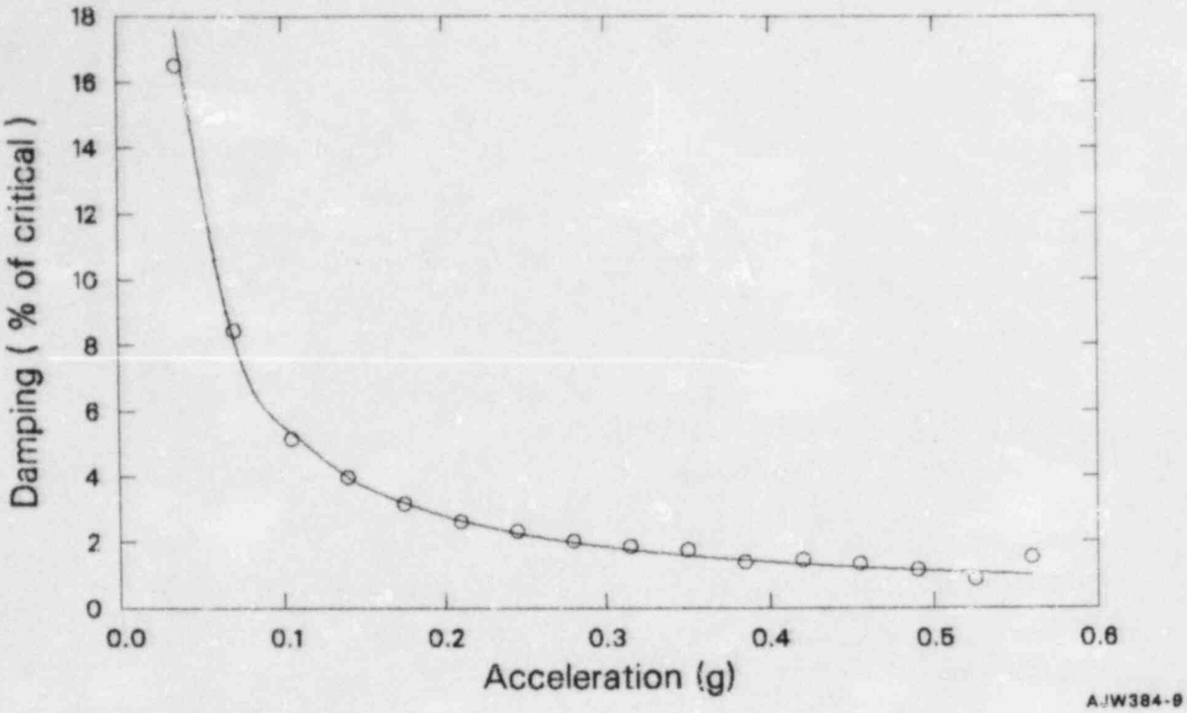

Figure 28. Snapback data for Test PD301F, 3-in. pipe, empty, pinned ends, spring hanger at midpoint.

The data are plotted in Figure 29. As with the low-vibration, pinned-end data, there is evidence of Coulomb damping.

In Test PD305F, the displacement was slightly greater than 1 in. (1.188) with a peak strain of 409 μ in./in. The ring down occurred from about 310 μ in./in. and the damping was calculated as 0.4%. Thus, it appears that the curve in Figure 29 would approach 0.4% of critical damping at higher displacements.

Tests PD306F and PD307F were for 250 and 500 lb plucks with the spring hanger at the midpoint. In Test PD307F, the initial strain was 200 μ in./in. and the main vibration took place at 100 μ in./in. and lower strains. Damping was calculated to be 0.6 to 0.7%.

In Test PD307F, the initial strain was 421 μ in./in. and the primary vibrations took place at 210 μ in./in. and lower strains. For the accelerometer located at 5Z, the damping was 0.3%.

In Tests PD308F through PD311F, the pipe was empty with the rod hanger at the midpoint. The pipe was plucked at the quarter point with forces of 500, 1000, 1500, and 1800 lb. Because the rod hanger was essentially rigid, except for the gaps between the eye rod and the connection bolts, the former first mode at 4.5 Hz was no longer present. The two modes of interest are a mode at about 12 Hz, in which the pipe vibrates antisymmetrically about the center as shown in Figure 25b; and a mode at about 18 Hz in which the pipe vibrates symmetrically about the center as shown in Figure 25d. The rod support was located nearly at the nodal point for the 12-Hz mode. Consequently, there was no noticeable effect on damping from the support. Data from the LVDT at location 12Z showed first-mode damping was only 0.4% of critical in Test PD308F. Data from the accelerometer at location 5Z indicated critical damping was only 0.2% in Test PD309F. Strain gauge data for Test PD311F indicated 0.3% from 247.4 μ in./in. to 207.2 μ in./in. For the 12-Hz mode, the pipe rotated at the rod support. In the 18-Hz mode, the pipe moved vertically at the rod support. At lower levels of vibration where the pipe weight was greater than the vibrational force so that the pipe rested on the rod support, the damping was only 0.4% of critical as measured by the LVDT located at 12Z. At higher vibration levels the pipe would "lift off" and vibrate audibly as the clamp bolts clattered in the eye of the rod. In Test PD309F, the damping was 2.2% of critical.

Table 8. Snapback Test PD304F data (11Z)[a]

Acceleration (g)	Difference (g)	Damping (% of critical)	Frequency (Hz)
0.5333			
0.495	0.0383	1.187	4.525
0.4717	0.0233	0.7685	4.525
0.445	0.0267	0.9262	4.525
0.4287	0.0163	0.638	4.459
	0.0160	0.605	4.444
0.4127			
0.3933	0.0194	0.763	4.444
0.3700	0.0233	0.973	4.494
0.3565	0.0135	0.613	4.494
0.3386	0.0179	0.822	4.444
	0.0174	0.838	4.444
0.3212			
0.302	0.0192	0.981	4.444
0.2823	0.0197	1.075	4.444
0.2658	0.0165	0.955	4.444
0.2475	0.0183	1.136	4.52
	0.0199	1.322	4.598
0.2276			
0.2095	0.0181	1.325	4.598
0.1931	0.0164	1.295	4.444
0.1764	0.0167	1.442	4.598
0.1602	0.0162	1.586	4.440
	0.0180	1.900	4.614
0.1422			
0.1242	0.0180	2.158	4.357
0.1087	0.0155	2.116	4.614
0.09353	0.0152	2.441	4.525
0.07825	0.01528	2.838	4.459
	0.01338	2.985	4.592
0.06487			
0.05062	0.01425	3.949	4.334
0.03645	0.01417	5.264	4.494
0.02148	0.01497	8.417	4.762
0.006909	0.01457	18.05	—

a. These data correspond to Figure 29 that shows decreasing damping with increasing acceleration, which is indicative of Coulomb friction.

Beginning with Test PD315F, the pipe was filled with water. In Tests PD315F and PD318F, the size 3 spring hanger was placed at the support location one-third of the distance from the end of the pipe, and the pipe was plucked with 500-lb forces at the quarter point and midpoint, respectively. Data from the strain gauge located at 13X are plotted in Figure 30 and from the LVDT located at 12Z are plotted in Figure 31. Both show a damping of 1 to 1.5% of critical except at low levels where the Coulomb friction effect seen in earlier tests is evident.

In Test PD319F, the pipe was snapped with a 750-lb load at the quarter point, and was supported with the rod hanger at the midpoint, as well as the spring hanger at the one-third location. The lowest mode of 3.8 Hz was no longer present. The mode at 10 Hz had 0.6% of critical damping, calculated using the accelerometer at location 15Z.

The spring hanger was removed and Tests PD323F through PD329F were conducted with increasing snapback loads up to a maximum of 3500 lb. The maximum strain for the highest level test, PD329F, was 1794 μ in./in., or about 1.5 times yield strain, at the midpoint of the pipe. After the release, the vibration divided into the first two modes, each with about one-half the initial strain. The damping for the lower antisymmetrical mode was low, less than 1%. For the higher 14.5-Hz mode, the damping was higher and exhibited a Coulomb friction effect (see Figures 2 and 32).

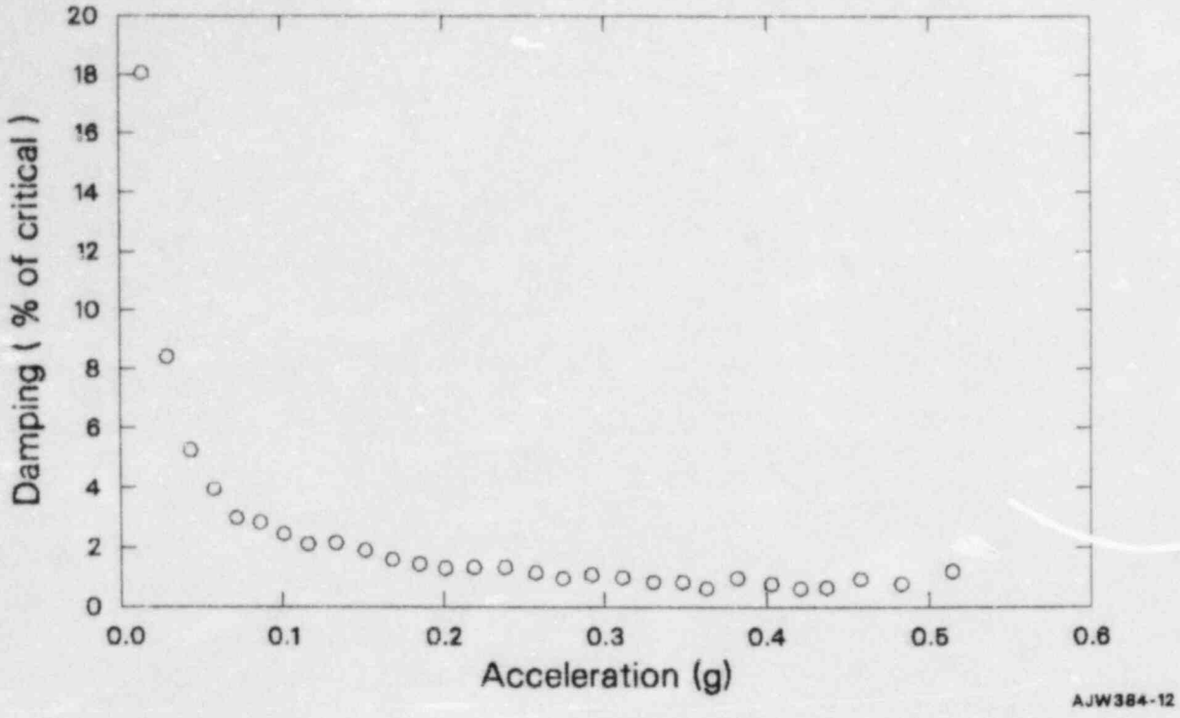

Figure 29. Snapback data for Test PD304F, 3-in. pipe, empty, fixed ends, spring hanger at third point.

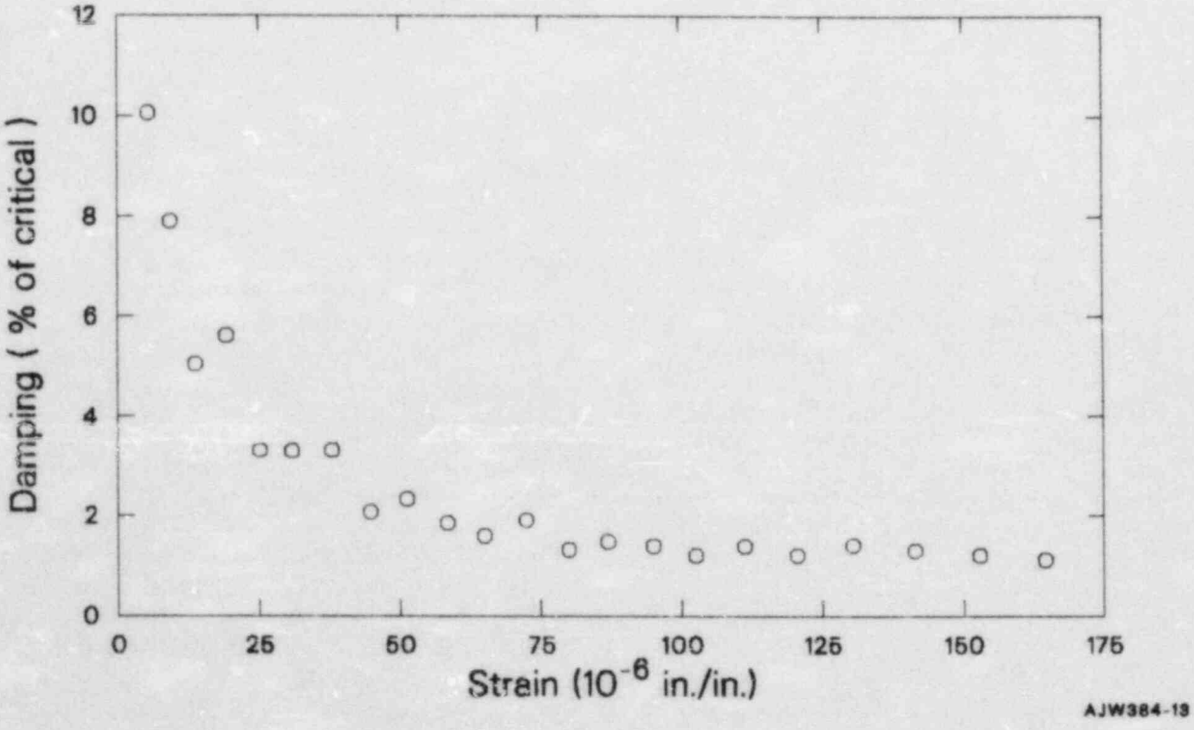

Figure 30. Snapback data for Test PD315F, 3-in. pipe, filled, fixed ends, spring hanger at third point.

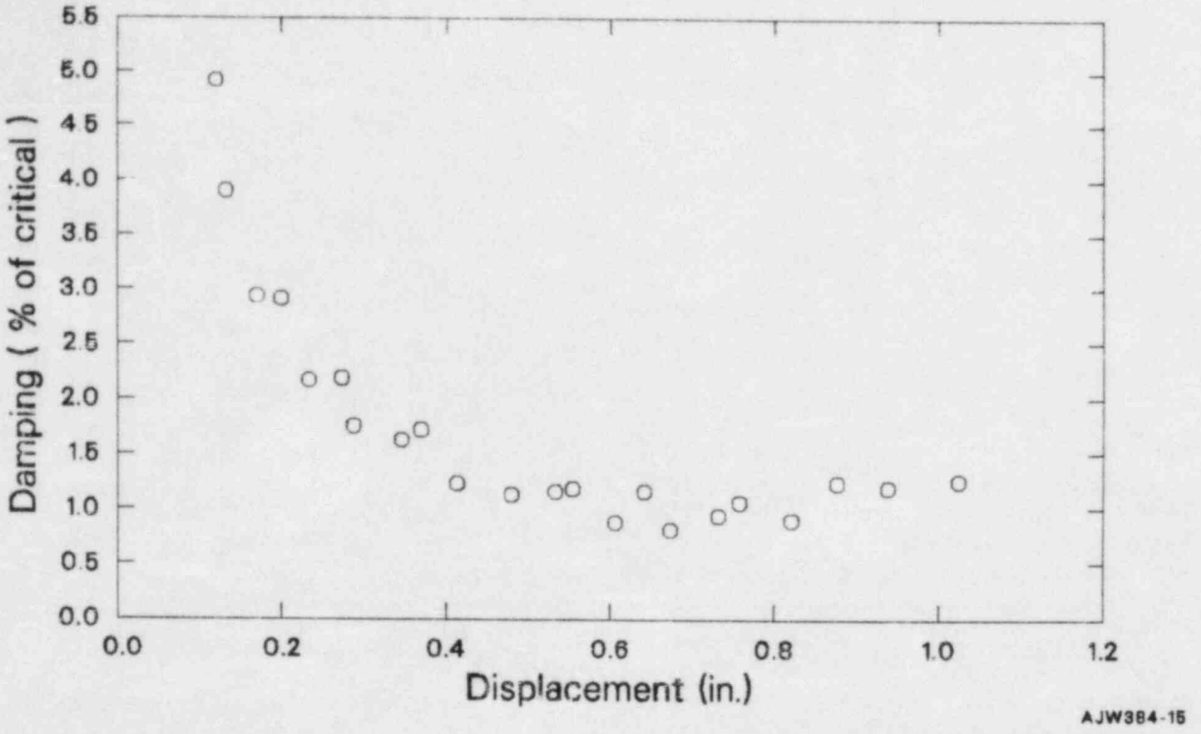

Figure 31. Snapback data for Test PD318F, 3-in. pipe, filled, fixed ends, spring hanger at third point.

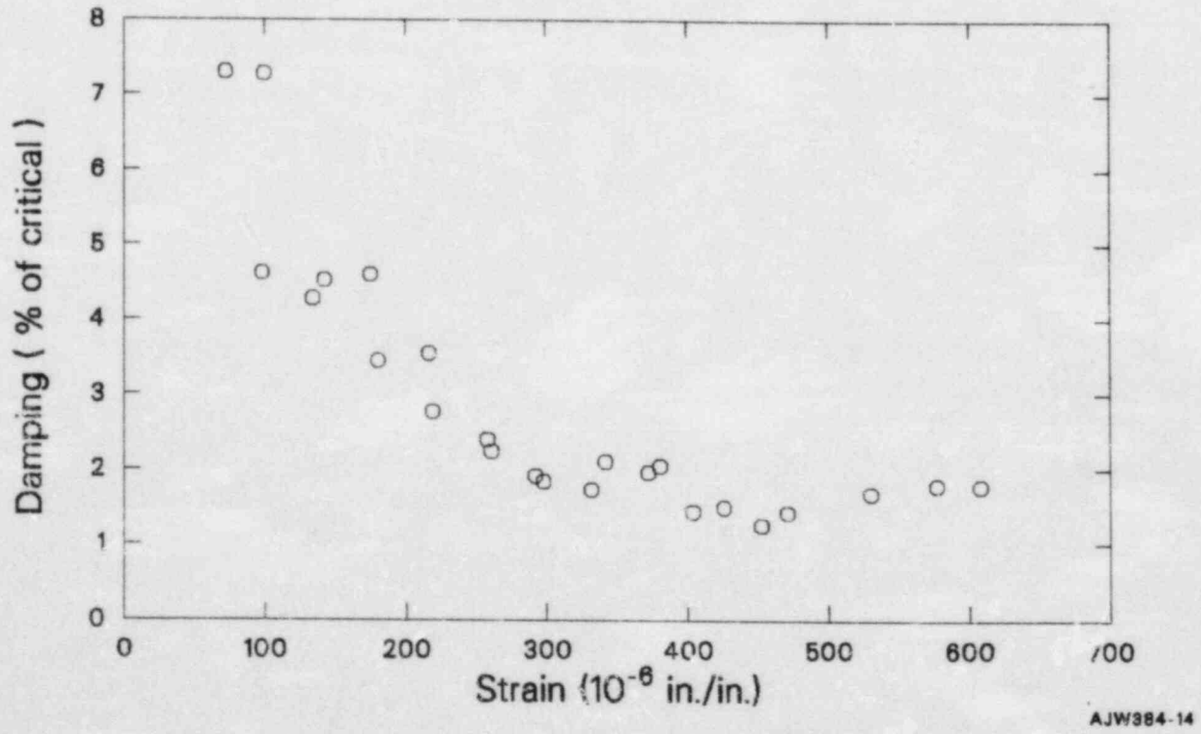

Figure 32. Snapback data for Test PD329F, 3-in. pipe, filled, fixed ends, rod hanger at center.

The final series of tests on the 3-in. pipe was conducted with the pipe empty, supported at the ends only, and plucked at the midpoint. The snapback loads in Tests PD330F through PD333F were 2000, 3000, 4000, and 5000 lb, respectively. The maximum strain for Test PD333F was 2829 μ in./in., well above the 2016 μ in./in. strain level at which a plastic hinge would be predicted. In fact, after testing the pipe did show evidence of plastic deformation. Figure 33 plots damping as a function of strain. At about 1500 μ in./in. strain, the damping reaches 5% of critical.

8-in. Pipe—Empty, Pinned-End Results. Three snapback tests were conducted with the ITT Grinnell size 7 spring hanger at a location one-third of the length from one end. The first, Test PD801F, was at a low level (less than 50 lb), while the second and third tests were at 1000 lb and 2000 lb (PD803F and PD804F, respectively). Data are listed in Table 9 and plotted in Figure 34. The damping decreases with amplitude, but the interval is not as regular as pure Coulomb damping. The second mode damping was very low and was determined as 0.5% of critical. For Test PD801F, the maximum strain was less than 5 μ in./in. In Tests PD803F and PD804F, the damping was also very low. For the 1000-lb snap, the strain gauge located at 9X measured damping of 0.3% and the accelerometer located at 11Z measured 0.3%. For the 2000-lb snap, damping was 0.5% measured by the LVDT and 0.4% measured by the strain gauge located at 9X.

Four tests (PD806F, PD807F, PD808F, and PD809F) were performed with the constant-force hanger at the midpoint, and the pipe plucked at the quarter point. The snap forces were 1000, 2000, 3000, and 4000 lb, respectively. Of these, the 1000-lb snap barely overcame the hanger friction force and the pipe did not oscillate enough that damping could be computed. In Tests PD807F and PD808F, the maximum strain gauge (from location 9X) readings were 200 μ in./in. and 262.6 μ in./in. Plots of the data are shown in Figures 35, 36, and 37. As with the low level 3-in. pipe spring hanger data, there is definite evidence of Coulomb friction, although the difference in amplitude between successive cycles is not linear. The damping is probably a combination of Coulumb damping and some other type. Damping values determined using this large constant-force hanger and the 8-in. empty pipe were the largest damping values obtained for any tests reported herein with comparable displacements.

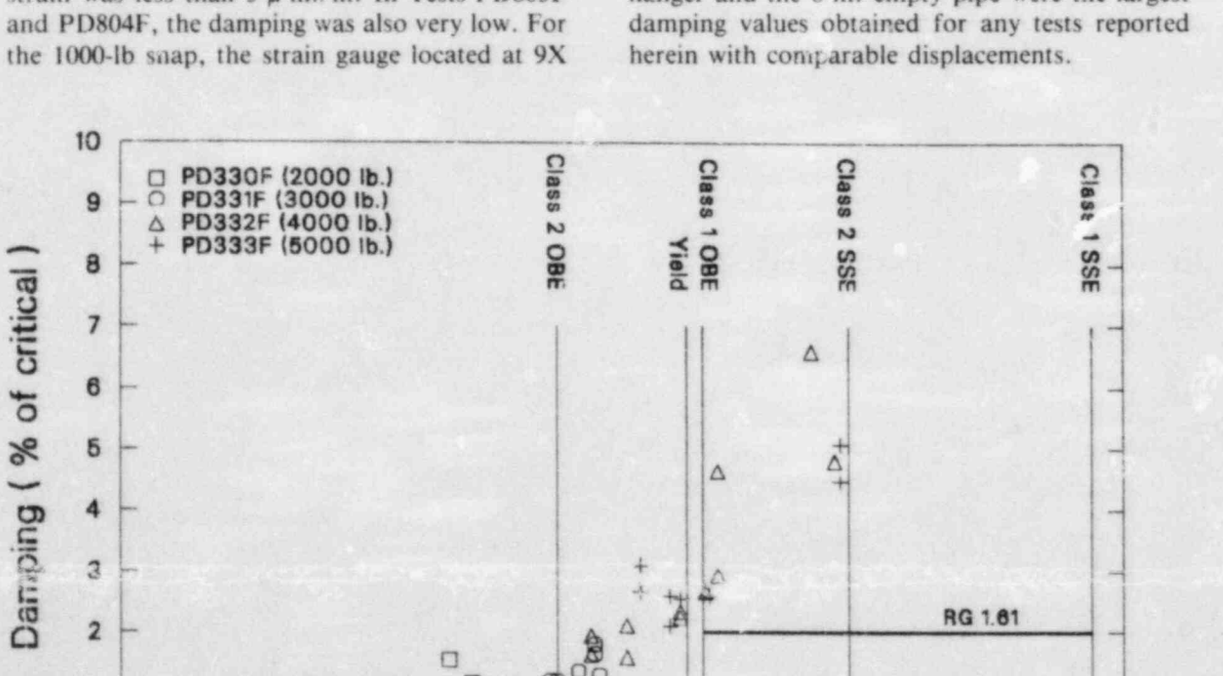

Figure 33. High strain level snapback data, 3-in. pipe, empty, fixed ends, no intermediate supports.

Table 9. Snapback Test PD801F data[a]

Deflection (mils)	Difference (mils)	Damping (% of Critical)
Upper Peaks		
10.58		
9.891	0.599	1.07
9.309	0.582	0.965
8.418	0.891	1.60
7.612	0.806	1.66
6.715	0.897	2.00
5.952	0.763	1.92
5.224	0.728	2.07
4.492	0.732	2.38
3.848	0.644	2.46
3.212	0.636	2.87
2.652	0.560	3.05
2.047	0.605	4.13
1.497	0.550	4.98
1.227	0.270	3.16
0.887	0.340	5.16
Lower Peaks		
9.95		
9.317	0.633	1.04
8.5	0.817	1.46
7.683	0.817	1.60
6.820	0.863	1.94
5.855	0.965	2.43
5.07	0.785	2.29
4.40	0.67	2.25
3.79	0.61	2.31
3.15	0.64	2.95
2.36	0.69	4.57
1.85	0.51	3.86
1.26	0.59	6.14
0.698	0.562	9.39

a. These data correspond to Figure 34 that shows decreasing damping with increasing deflection, which is indicative of Coulomb friction.

For Tests PD809F and PD810F, the sway brace was placed at the one-third location and loaded to approximately 300 lb. Two snapback force levels were used, 1000 and 4000 lb. For Test PD809F, the damping was very low and was computed as 0.6% (30 to 60 μ in./in.). Data for low-amplitude-level displacements are plotted in Figure 38. At this low level, the Coulomb damping previously encountered is seen again. Data for Test PD810F are plotted in Figure 39.

8-in. Pipe—Water Filled, Pinned Ends. Only two tests with pinned ends were conducted after the pipe was filled with water. The purpose of these tests was to determine how the natural frequency of the pipe changed when water was added. The first (Test PD811F) was excited by a hammer blow in the vertical direction, and the second (Test PD812F) was excited in the horizontal direction. Measured natural frequencies (in Hz) were:

PD811F	PD812F
5.74	5.14
16.88	11.04
18.38	13.09
38.99	24.59
	45.10

As shown in Table 5, the frequencies decreased for the first two vertical modes as predicted by theory. Measured damping was very low ($<<1\%$) for all modes.

8-in. Pipe—Water Filled, Fixed Ends. Four tests were run with the sway brace installed initially at zero load at the one-third location, and the pipe plucked at the quarter point with 1000-, 4000-, 6000-, and 8000-lb forces. In Tests PD814F and PD815F, damping was computed as 0.3% and 0.8%. Data for the two higher-level tests are plotted in Figures 40 and 41.

Four tests were run with the constant-force hanger at the one-third position and plucked at the quarter point. Pluck forces for Tests PD819F through PD822F were 1500, 3500, 5500, and 7500 lb. For Test PD819F, the maximum measured strains were 50 μ in./in. at location 9X and 120 μ in./in. at location 17X. Based on the limited data it appears Coulomb damping is present. For Tests PD820F and PD821F, the maximum strains were 220 μ in./in. at location 9X and 470 μ in./in. at location 17X. Data for the LVDT at location 12Z and the accelerometer located at 8Z for the first and second modes respectively are plotted in Figures 42 and 43.

In Tests PD823F through PD826F, the constant-force hanger remained at the one-third location, while the pipe was snapped at the midpoint with 1200-, 2200-, 5200-, and 7200-lb plucks. Since the pipe snapback location was the midpoint instead of the quarter point, the pipe had greater imposed displacements than in Tests PD819F through PD822F. Thus, the pipe would have more energy

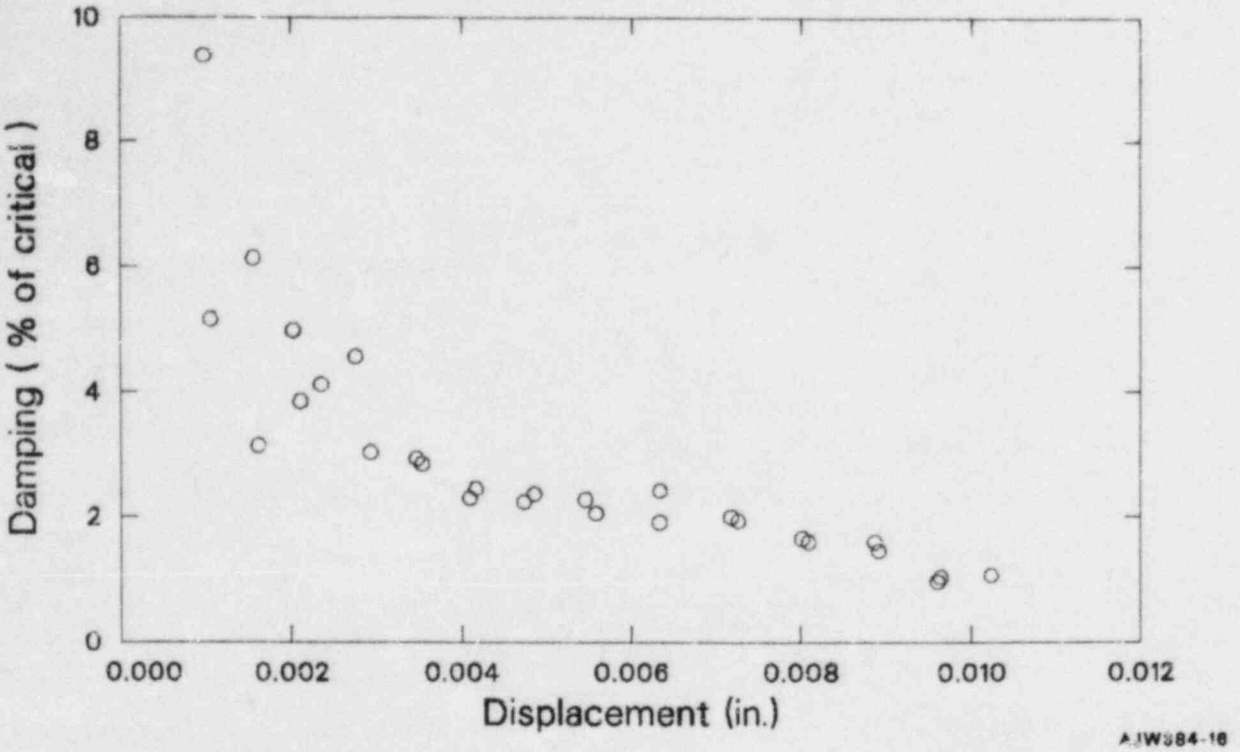

Figure 34. Snapback data for Test PD801F, 8-in. pipe, empty, pinned ends, spring hanger at third point.

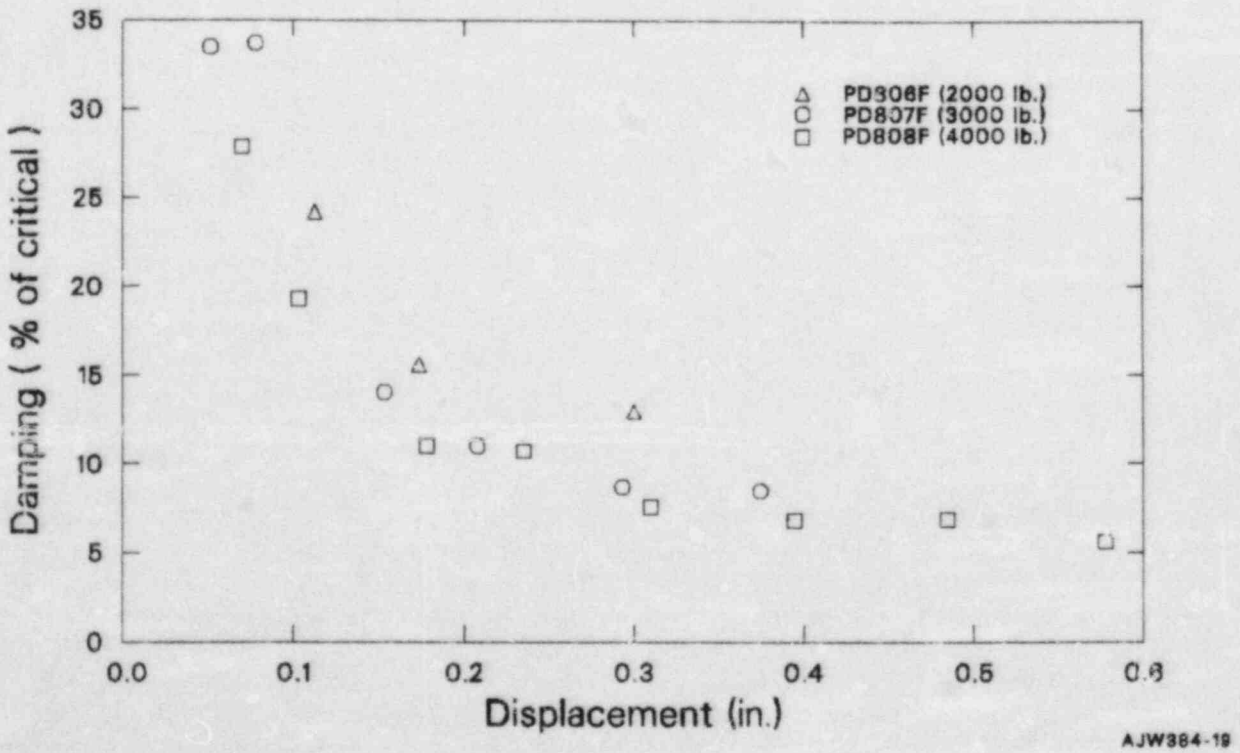

Figure 35. LVDT snapback data for 8-in. pipe, empty, pinned ends, constant-force hanger at midpoint.

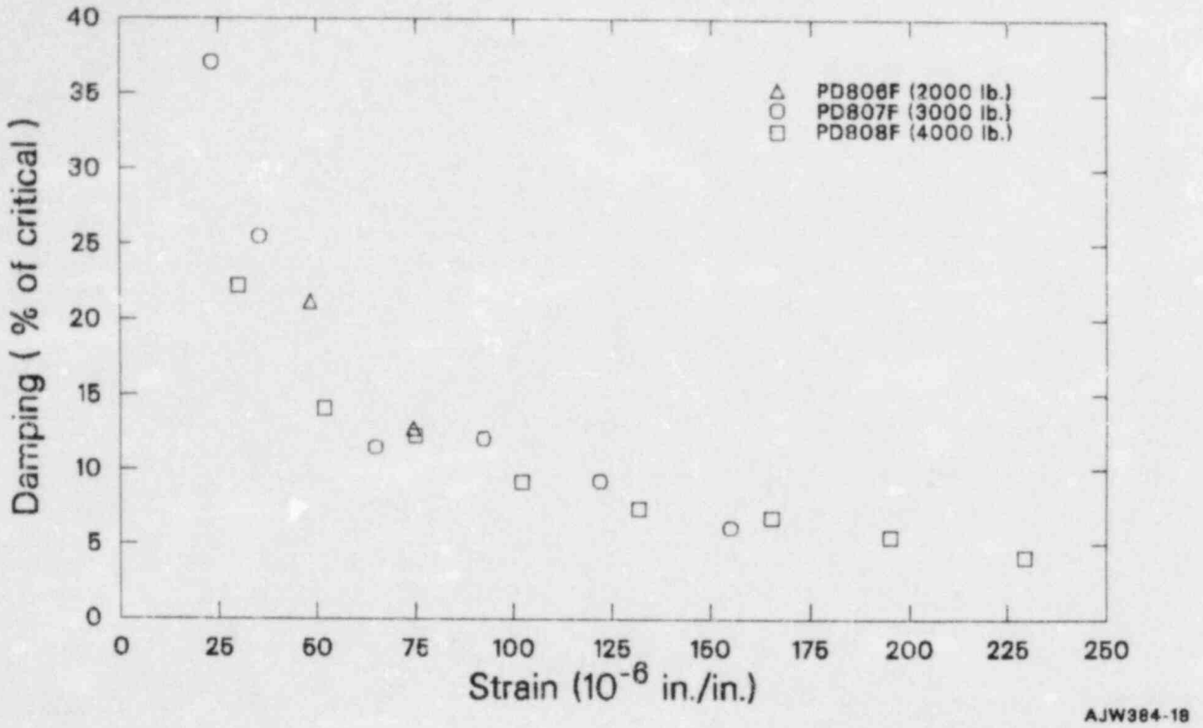

Figure 36. Strain gauge snapback data for 8-in. pipe, empty, pinned ends, constant-force hanger at midpoint.

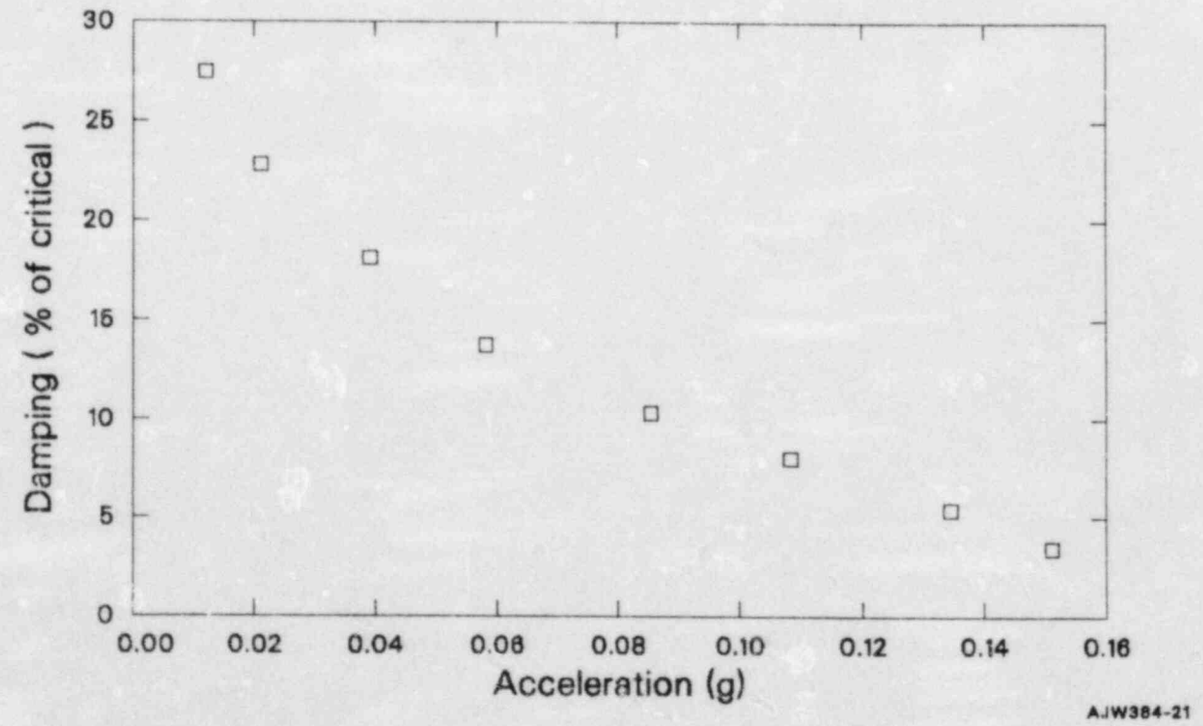

Figure 37. Accelerometer snapback data for Test PD808F, 8-in. pipe, empty, pinned ends, constant-force hanger at midpoint.

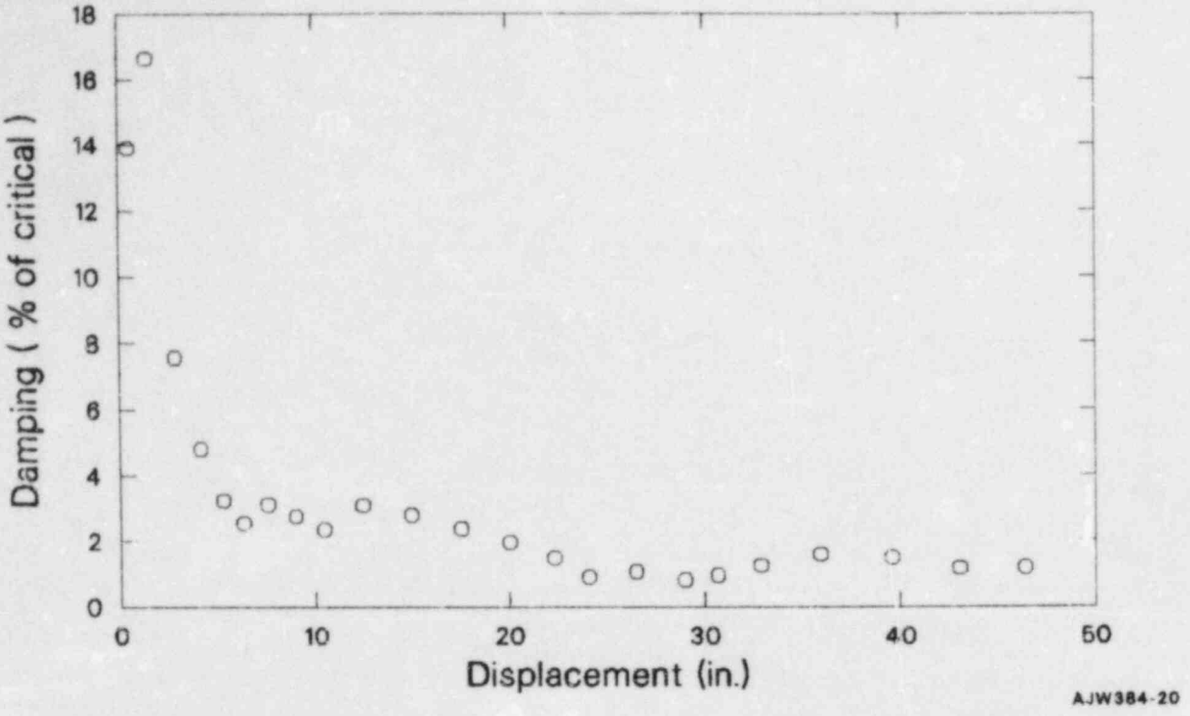

Figure 38. LVDT snapback data for Test PD809F, 8-in. pipe, empty, pinned ends, sway brace at third point.

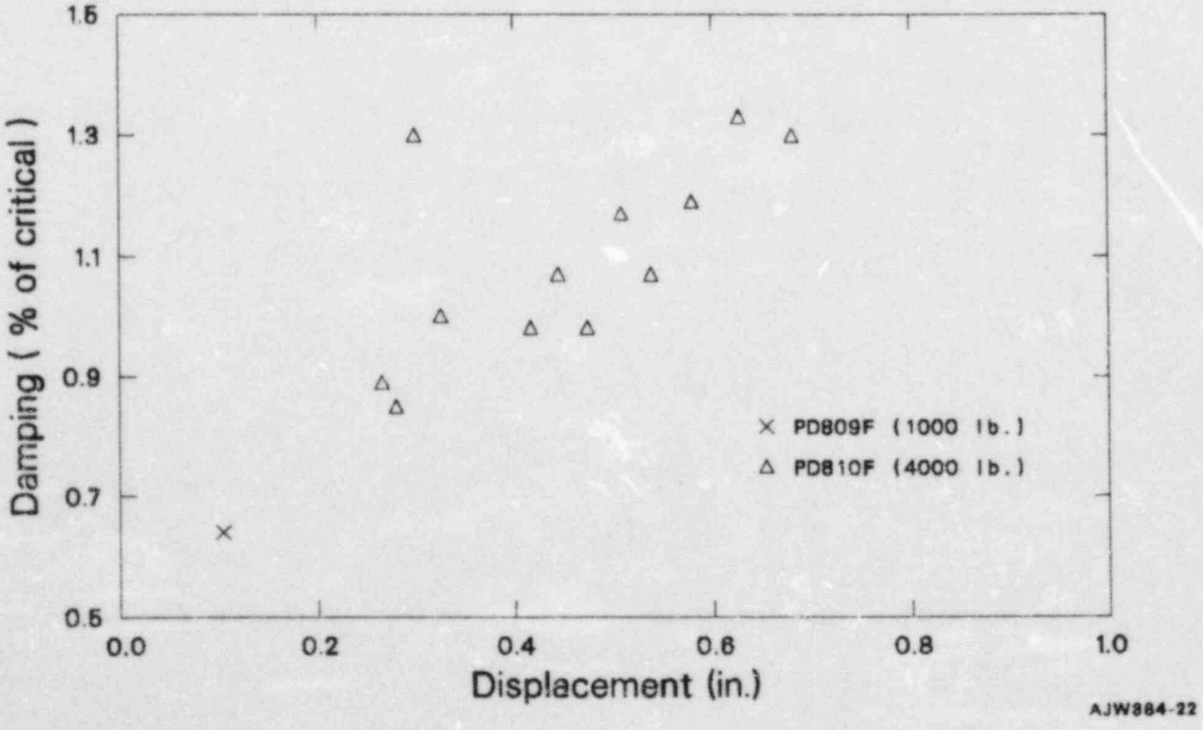

Figure 39. LVDT snapback data for 8-in. pipe, empty, pinned ends, sway brace at third point.

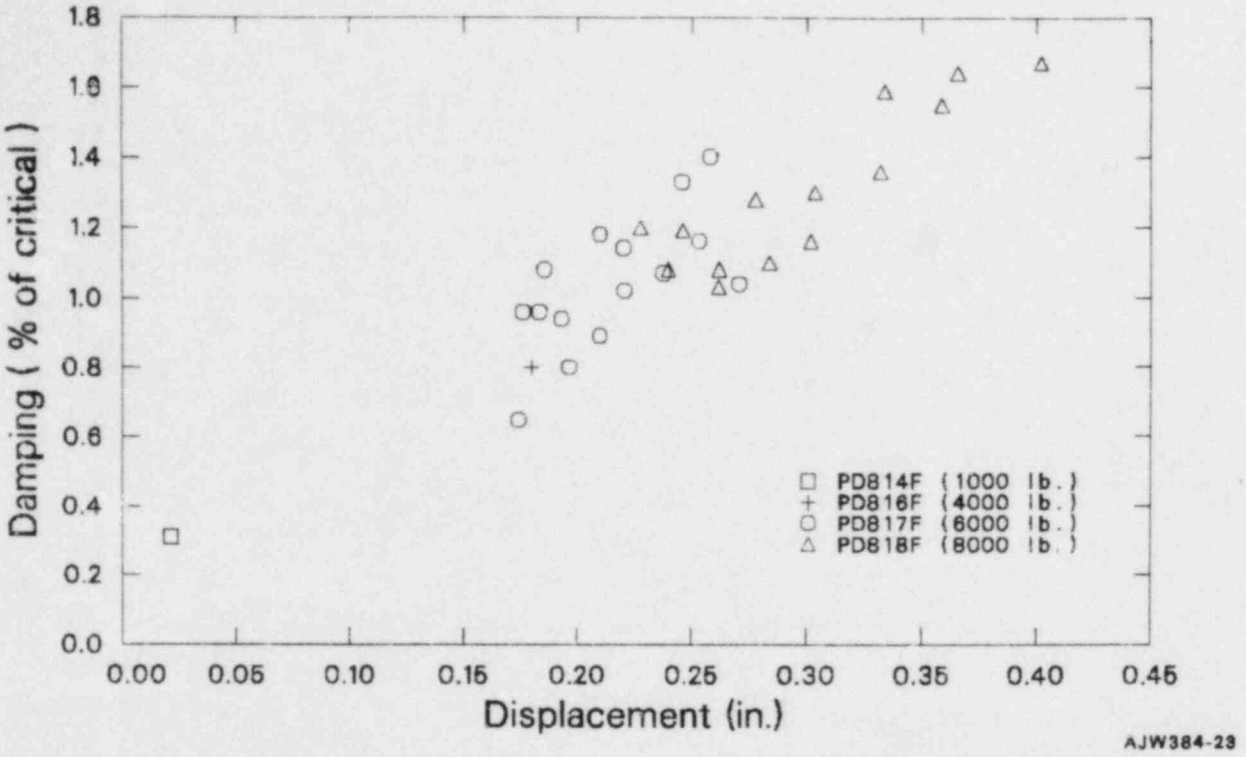

Figure 40. LVDT snapback data for 8-in. pipe, filled, fixed ends, sway brace at third point.

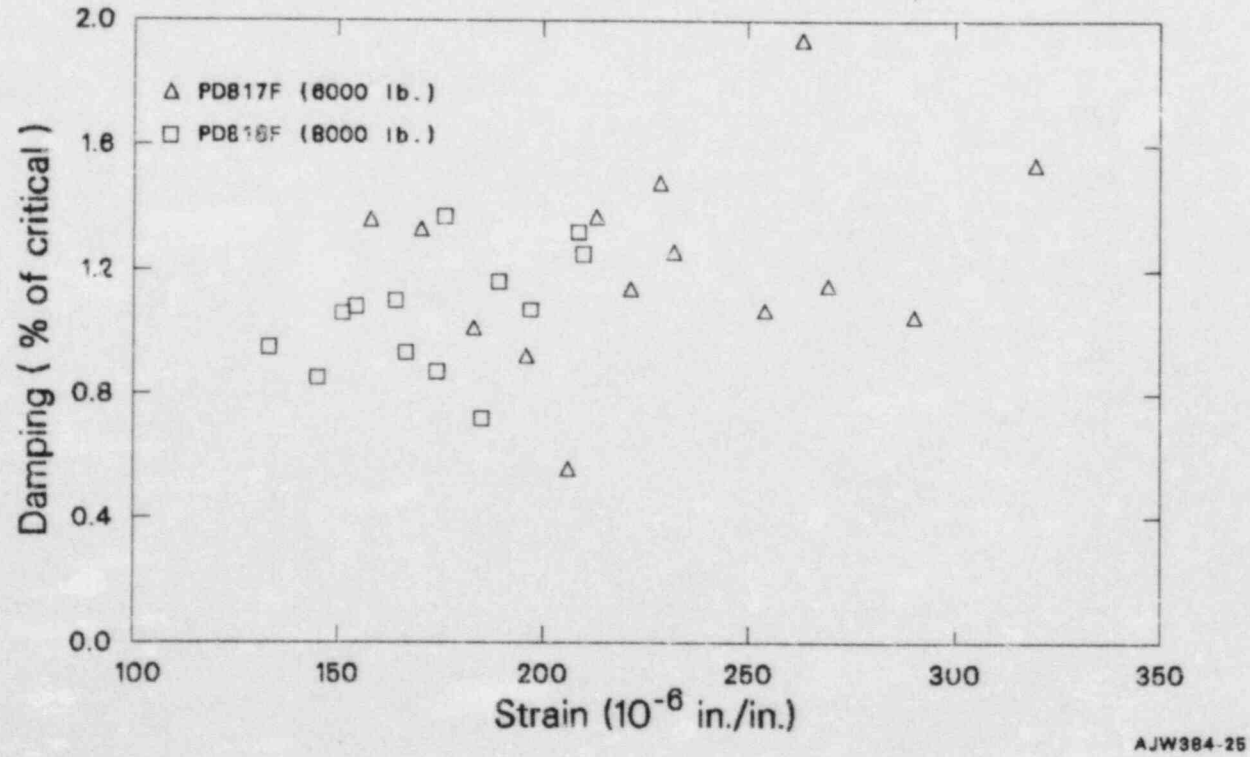

Figure 41. Strain gauge snapback data for 8-in. pipe, filled, fixed ends, sway brace at third point.

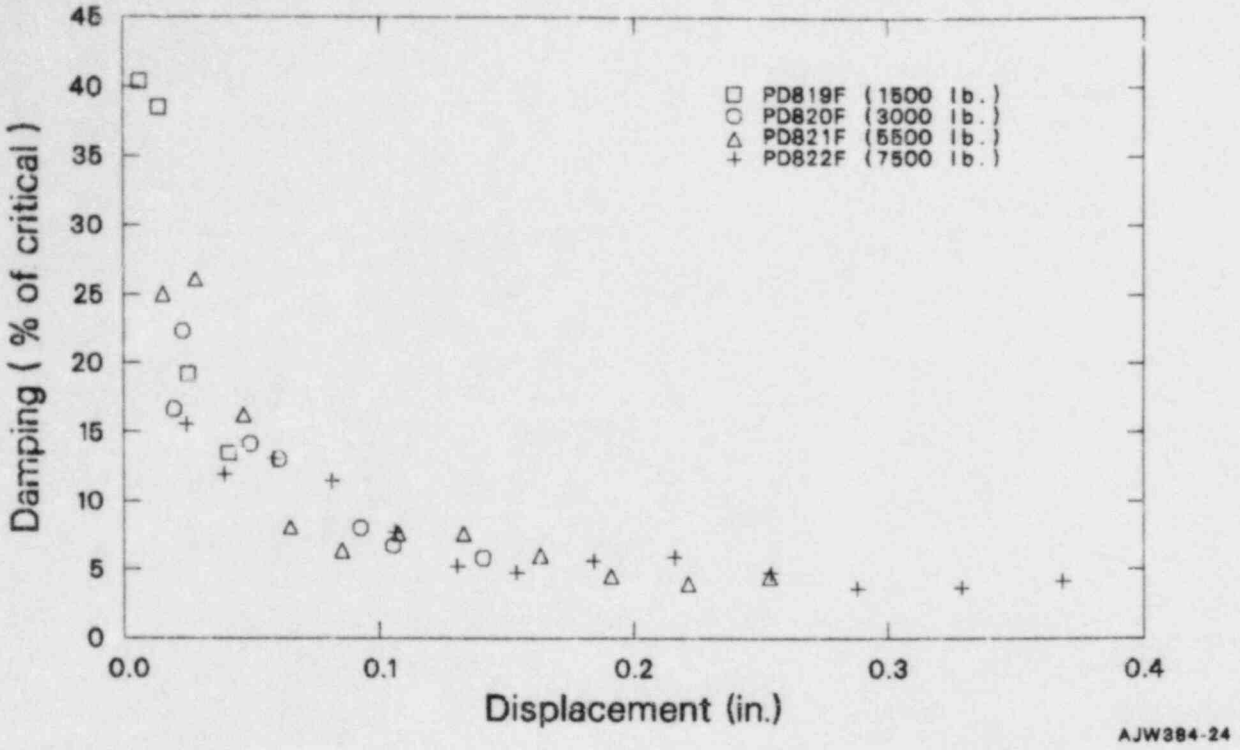

Figure 42. Snapback data for 8-in. pipe, filled, fixed ends, constant-force hanger at third point.

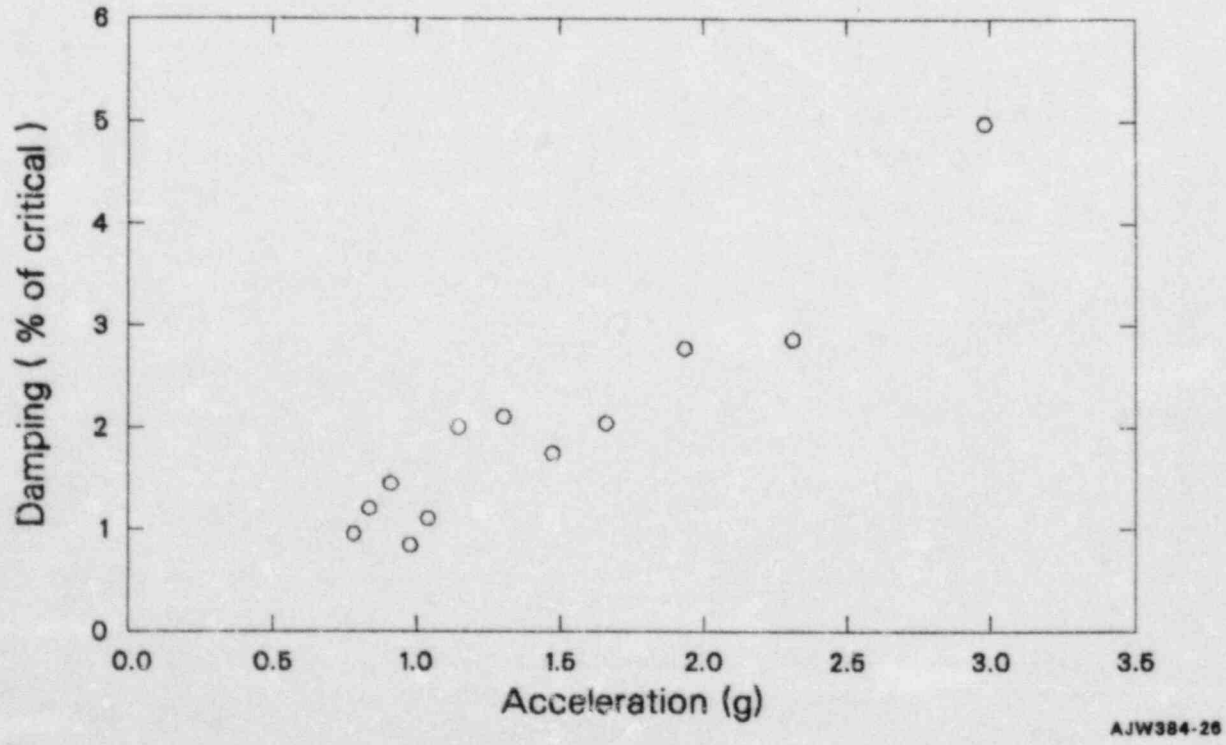

Figure 43. Accelerometer data for second mode of snapback Test PD822F, 8-in. pipe, filled, fixed ends, constant-force hanger at third point.

per cycle compared to the energy dissipation of the constant-force hanger. First mode damping is plotted in Figure 44. Increases in damping indicative of Coulomb damping occurred below 0.2 in. Accelerometer data for Tests PD823F and PD824F are plotted in Figure 45.

Loads of 2000, 4000, 6000, and 8000 lb applied at the midpoint were used for Tests PD827F through PD830F, which measured damping with the unloaded sway brace at the one-third location. The results, plotted in Figure 46, show the same trend as for sway brace Tests PD814F through PD818F that damping increases with displacement.

The large size 9 spring hanger (Figure 12) was positioned at the one-third location, and the pipe was plucked at the midpoint for Tests PD831F through PD834F respectively. Snapback loads were 2000, 4000, 6000, and 8000 lb. Sufficient points were obtained from Tests PD831F and PD834F to determine the trend of the data. Maximum strain for Test PD834F was 672 μ in./in. (from the strain gauge located at 9X). Unfiltered data for these two tests are plotted in Figure 47. The damping is fairly constant in the 1.5 to 2.0% range at amplitudes above about 0.1 in. The mean damping above 0.1 in. is 1.75% of critical damping. Below 0.1 in., the effect of Coulomb damping becomes apparent as the pipe vibration amplitude diminishes.

Log-decrement calculations for snapback tests using snubbers presented more difficulty than for other supports because the pipe would not vibrate about its midposition, but instead ratcheted from its statically deflected shape to the unloaded position. A displacement history for a snubber is shown in Figure 48. No meaningful log-decrement-damping calculation can be made with this trace. The acceleration traces do not show this same type of ramp function about which the oscillation takes place. Therefore, damping was calculated from acceleration traces. The rating on the snubber was 2000 lb. For tests at 3000, 4000, and 6000 lb, the snubber locked and served as a rigid restraint. In Tests PD840F (1000-lb snap force) and PD837F (2000-lb snap force), the characteristic ratcheting action took place. Results are plotted in Figure 49.

The final series of tests were conducted using only the end supports, with the pipe loaded to higher load levels. In Tests PD842F through PD844F, the load levels were 10, 12, and 15 kips respectively. Damping versus strain and displacement are plotted

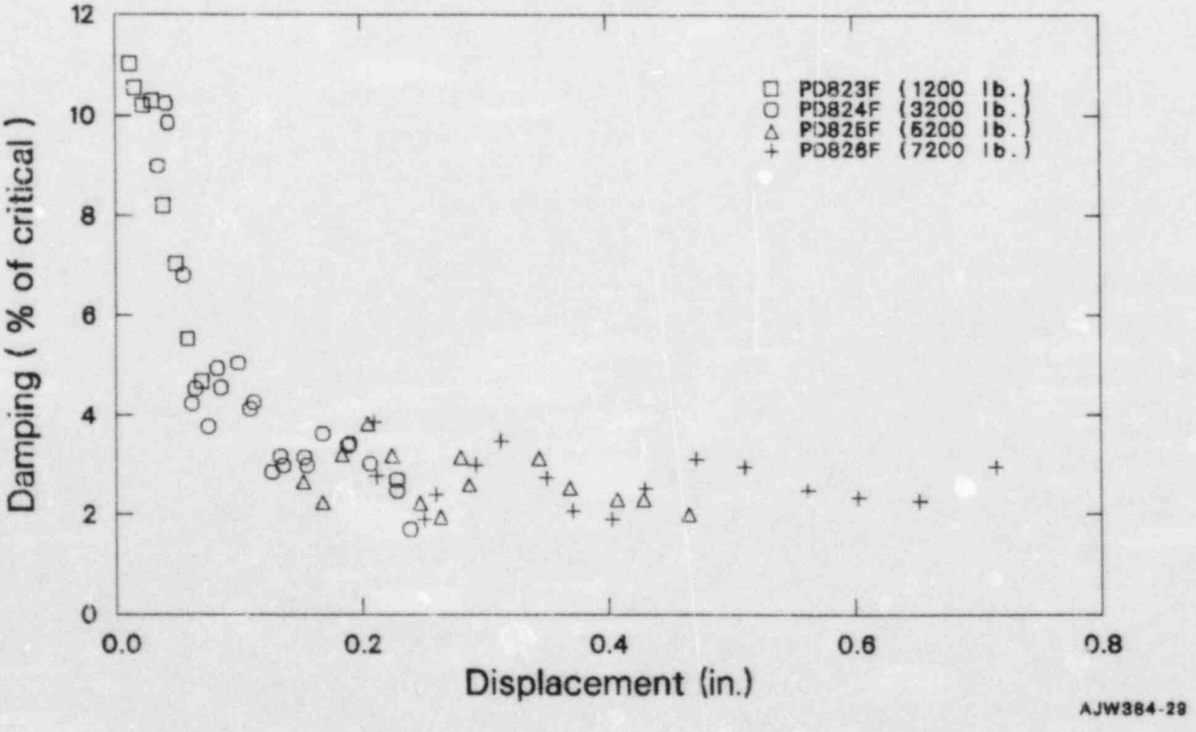

Figure 44. LVDT snapback data for 8-in. pipe, filled, fixed ends, constant-force hanger at third point.

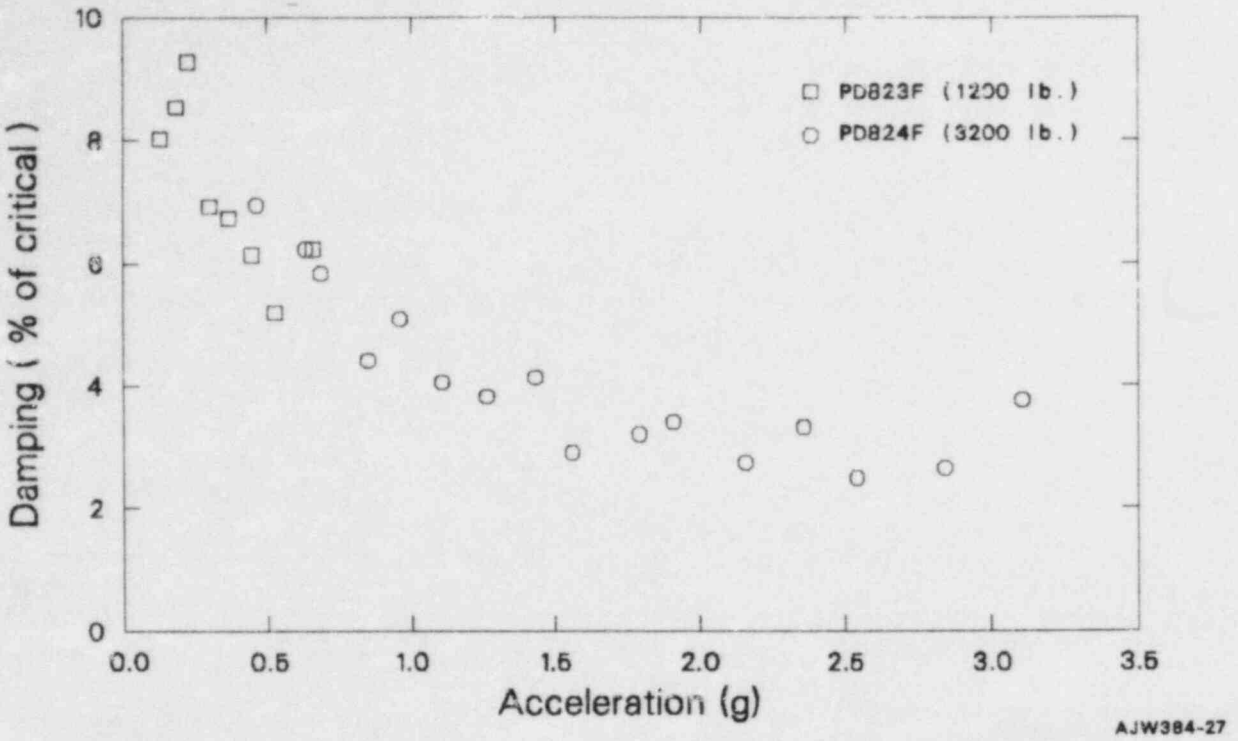

Figure 45. Accelerometer snapback data for 8-in. pipe, filled, fixed ends, constant-force hanger at third point.

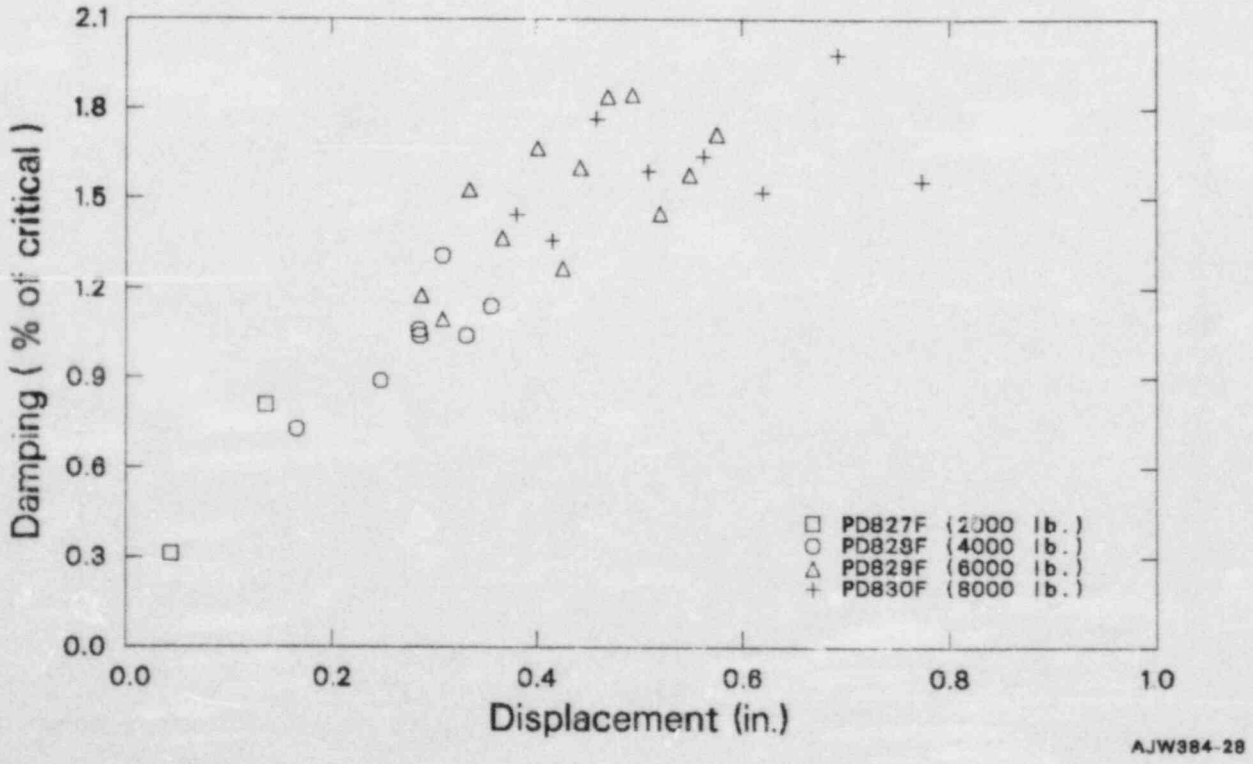

Figure 46. Snapback data for 8-in. pipe, filled, fixed ends, sway brace at third point.

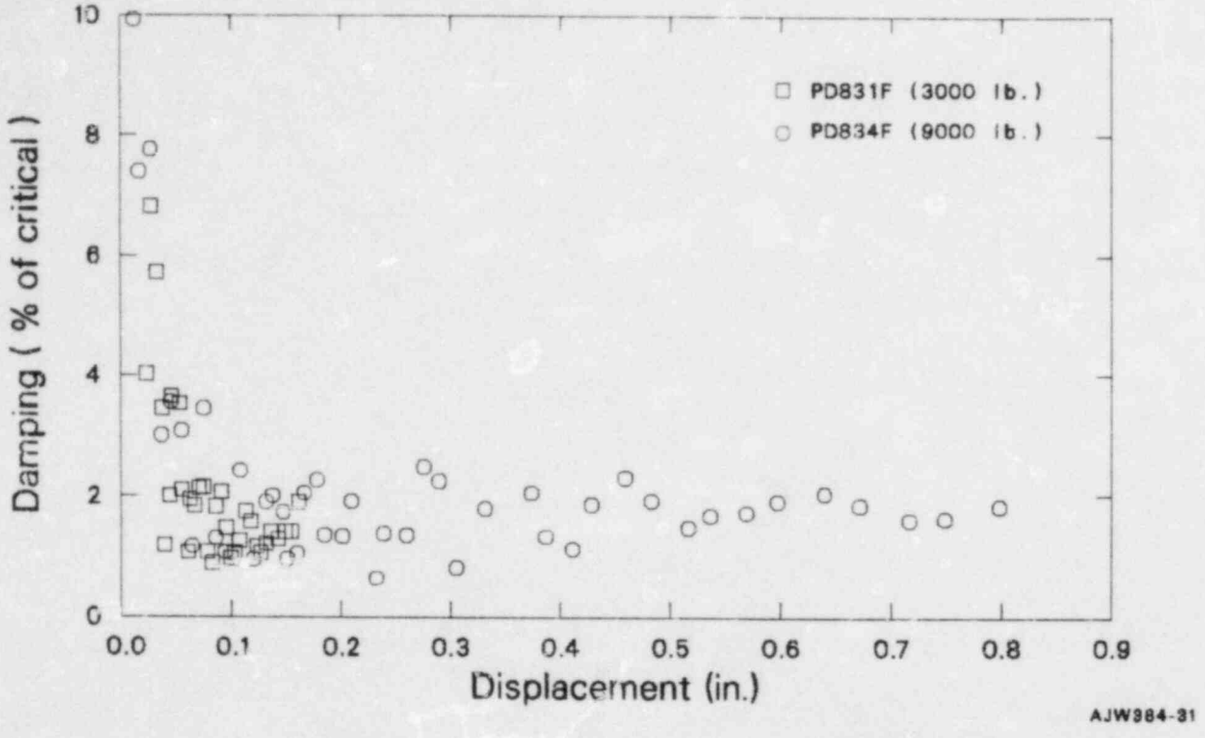

Figure 47. Snapback data for 8-in. pipe, filled, fixed ends, spring hanger at third point.

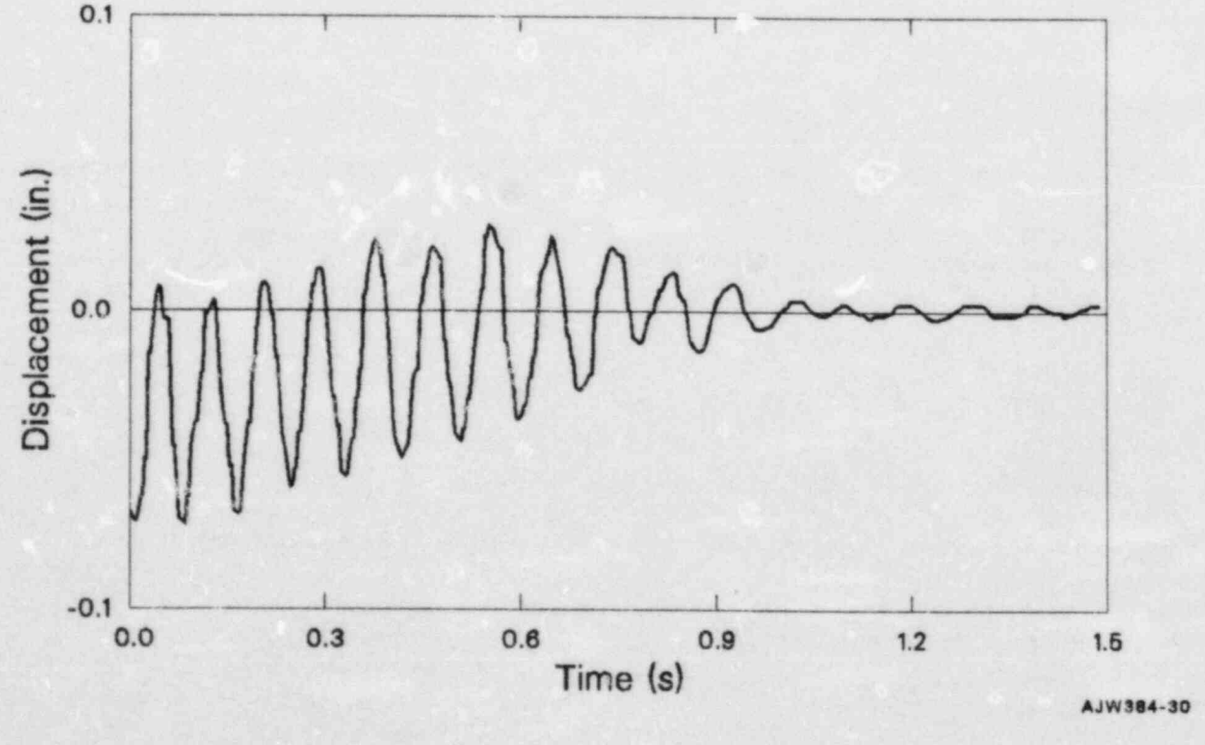

Figure 48. Snubber displacement trace.

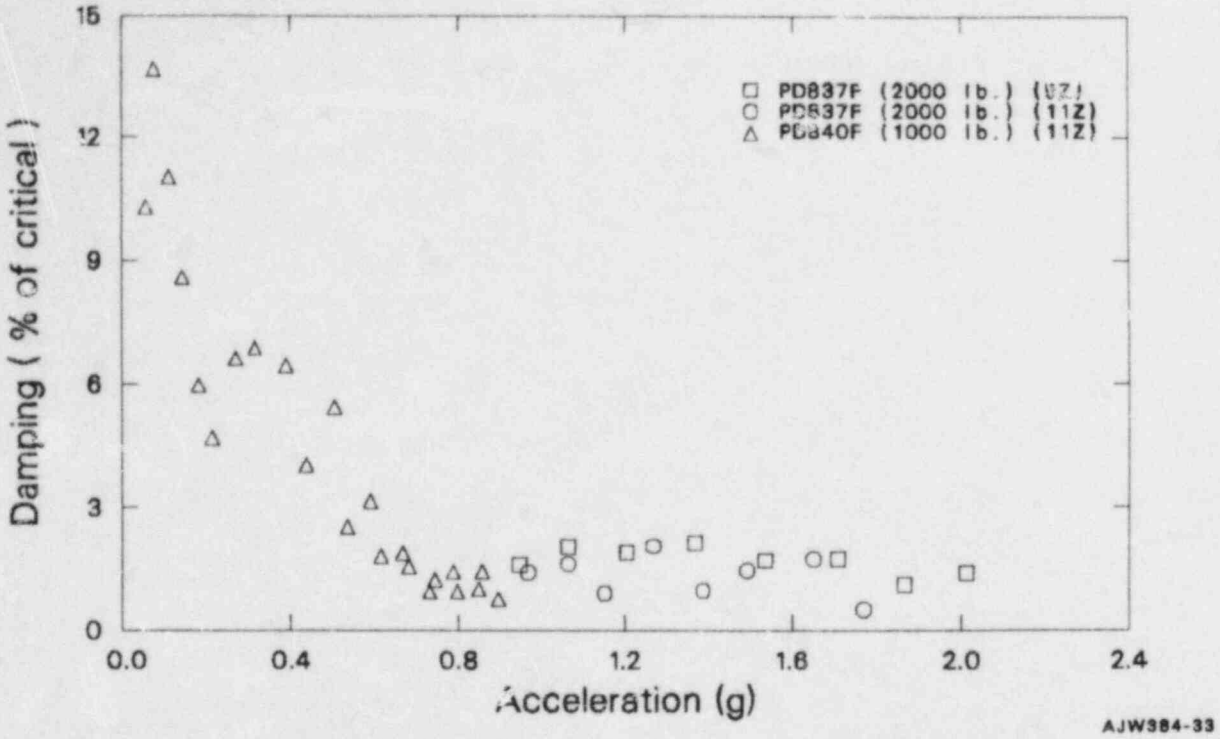

Figure 49. Snapback data for 8-in. pipe, filled, fixed ends, snubber at third point.

in Figures 50 and 51. They show increasing damping with increasing vibration amplitude levels.

In Tests PD845F through PD849F, the snapback force levels were 14, 17, 20, 22, and 25 kips. These tests were in the OBE and SSE level ranges. The maximum strain was 1892 μ in./in. for Test PD849F. The data are plotted in Figure 52. Each test followed a different path from about 2.5% of critical damping at 400 μ in./in. to about 12% of critical damping at yield strain. All data are greater than 5% of critical damping for levels above OBE, and are considerably higher than the 3-in. pipe data.

Shaker and Impact Test Results

Damping data for the 3-in. and 8-in. pipes were also determined by use of frequency response functions (FRF). These results are discussed and observations are outlined in this section.

Excitations for these tests consisted of random and swept-sine forced vibrations using a hydraulic shaker and force impulse transients using an instrumented hammer. The damping estimations were determined using the complex-exponential-curve-fitting technique and the half-power method. The half-power method was employed by, first, squaring the FRF and then applying the half-power technique to resonant peaks of interest. In general, both methods agreed well in damping and frequency estimation as long as the resolution of the FRF was sufficiently high for the given mode.

3-in. Pipe Test Results. Table 10 summarizes the results of the damping studies on the 3-in. pipe determined from experimental FRFs. The damping of the first mode for all pinned-ended-condition tests with no intermediate pipe supports is consistently less than 1% of critical damping. The higher damping of the corresponding fixed-ended tests shows that the end supports or their connections offer a damping increase of about 1% of critical.

In general, it is observed in these tests that single pipe supports tend to selectively impart characteristic damping to specific modes of the piping response rather than all modes equally, or in some proportion to mode frequency such as mass or stiffness proportional damping. As one example, the snubbers tended to increase the damping of the second and third modes much more significantly than the first and fourth modes. Damping in the

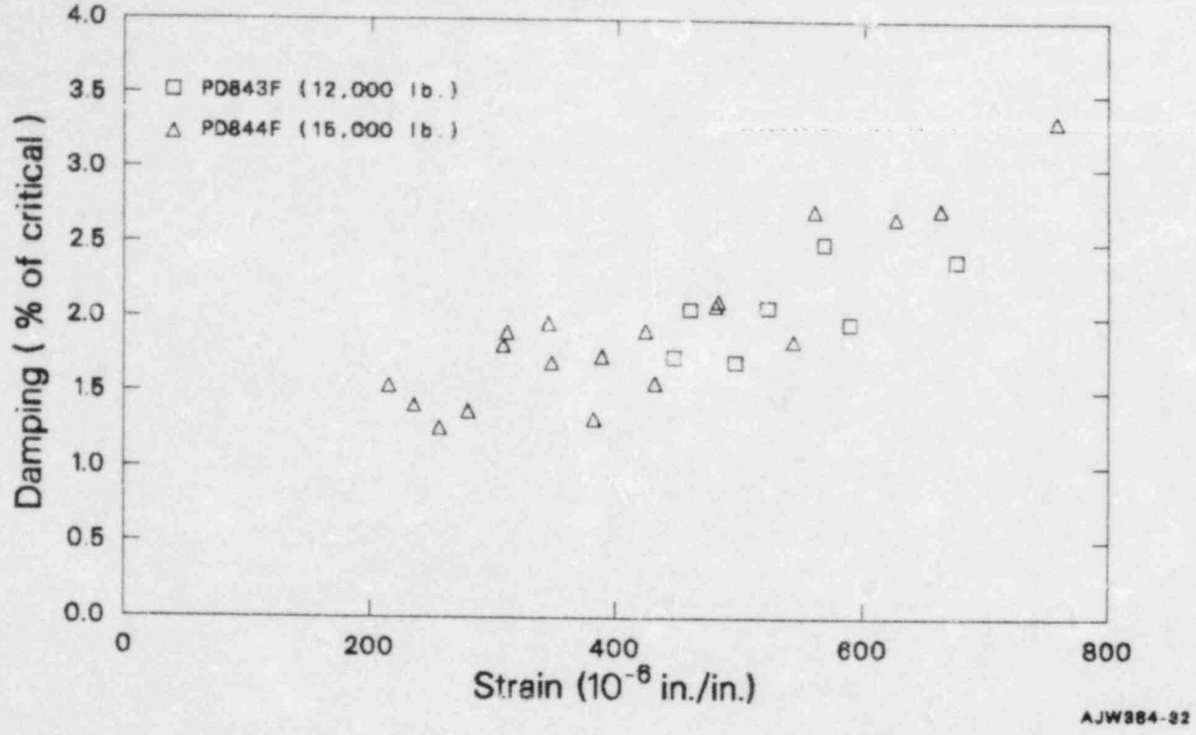

Figure 50. Strain gauge snapback data for 8-in. pipe, filled, fixed ends, no intermediate supports.

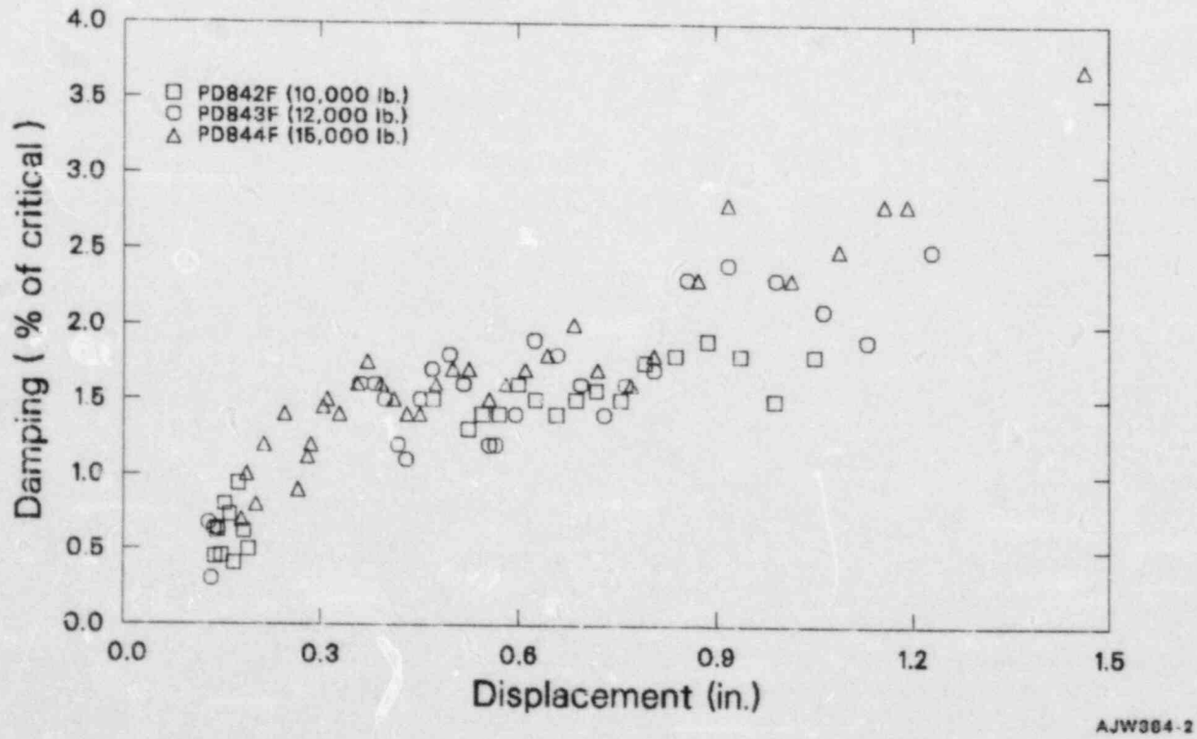

Figure 51. LVDT snapback data for 8-in. pipe, filled, fixed ends, no intermediate supports.

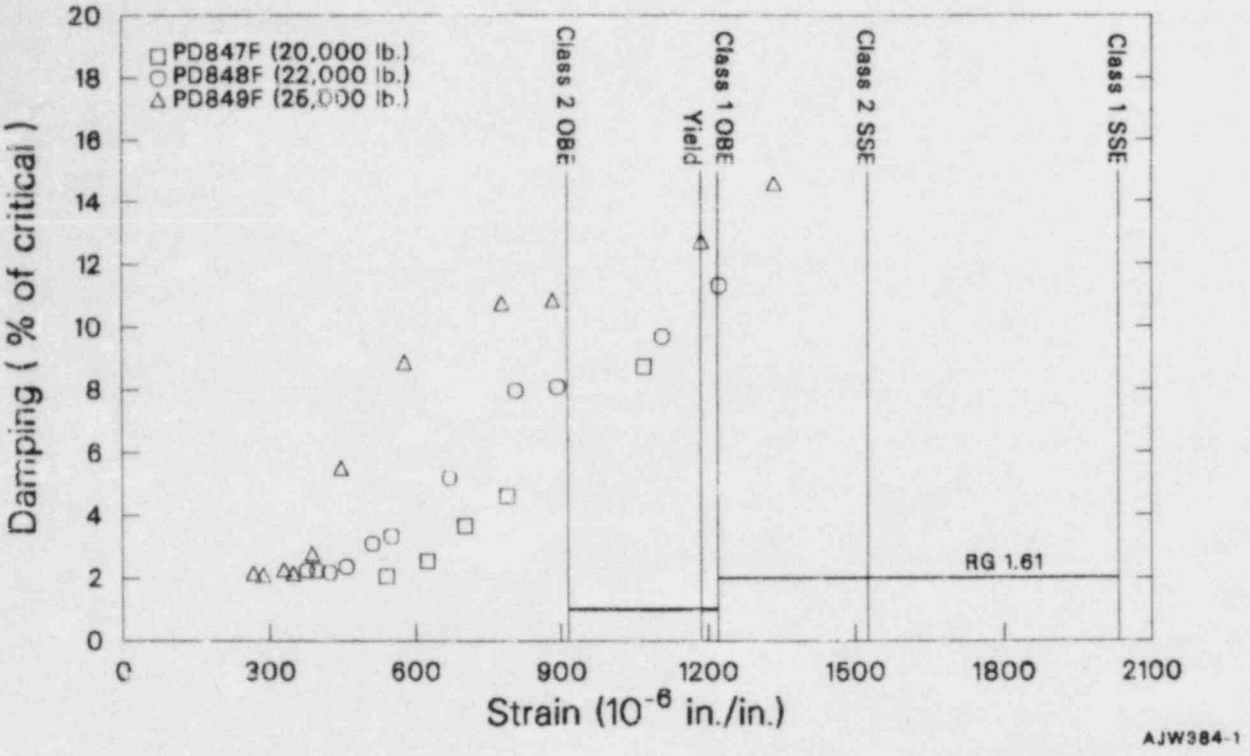

Figure 52. High-strain-level data 8-in. pipe, filled, fixed ends, no intermediate supports.

second mode generally ranged from 5.5 to 11% and in the third mode from 2 to 5.7%. The second mode was also affected by higher damping (5 to 12%) from the rod hanger when the bolted connection at the pipe clamp was loose (as it is normally installed). Tightening of this connection on the rod hanger correspondingly dropped the second mode damping to less than 1%. Similarly, tightening the connection when a snubber was the support did not change the damping from the normal condition. The spring hanger generally did not increase damping in any modes if the level of strain was above 100 μ in./in. Below this strain level in the pipe, damping of the order of 5% was imparted to the first piping mode. This could be due to Coulomb friction in the spring hanger at those low levels.

Good comparisons are achieved when damping calculations from the frequency response functions are plotted against strain levels in the pipe and are compared with damping versus strain curves from snapback tests. One example is shown by plotting damping data for the first mode of Tests PD309H, PD358H, PD354H, PD353H, PD355H, PD356H, and PD357H on the damping versus strain graph of snapback data for Test PD315F (see Figure 53). These tests represent data from the same type of pipe support and location. This tends to reinforce the credibility of the technique of determining damping as a function of strain for a given mode and support configuration from a single snapback test.

8-in. Pipe Test Results. The damping test data are summarized in Table 11. As discussed earlier, the resolution of the experimental FRF affects the accuracy of the damping calculations, especially when the half-power method is used.

Evaluation of single-support effects indicates that the sway brace and spring hanger both offer very little damping increase over the unsupported condition. The damping at very low strain levels was not significantly increased, in contrast to the 3-in. pipe tests where damping increased at low strain levels. The lack of high damping here is due to the considerably more potential strain energy existing in this pipe, compared to that of the 3-in. pipe. The constant-force hanger, on the other hand, shows

Table 10. 3-in. pipe damping calculations with shaker excitation

Test	Damping (% of Critical)	Frequency (Hz)	Type of Pipe Support	End Condition	Strain Level (μ in./in.)	Type of Excitation	Water Condition	Notes
PD352H	1.1	4.38	None	Fixed	260	Shaker	Empty	
	1.1	11.94						
	0.4	24.46						
	0.5	38.84						
	2.0	45.00						
PD312H	2.6	4.53	None	Fixed	—	Impact	Empty	
	0.6	12.47						
	0.4	25.31						
	0.6	39.81						
	2.8	45.62						
PD301H	0.9	2.52	None	Pinned	—	Impact	Empty	
	0.4	9.89						
	0.5	22.27						
	0.3	38.93						
PD351H	1.0	11.99	New snubber	Fixed	100	Shaker	Empty	Snubber at midpoint of span
	5.5	16.05						
	2.0	39.27						
	2.3	44.77						
PD311H	0.6	9.91	New snubber	Pinned	—	Impact	Empty	Snubber at midpoint
	10.5	15.70						
	0.4	38.93						
PD305H	0.8	9.66	Old snubber	Pinned	—	Impact	Empty	Snubber at midpoint
	11.5	13.49						
	5.1	25.99						
	0.5	38.92						
PD306H	0.5	9.89	Old snubber	Pinned	—	Impact	Empty	Snubber at midpoint, tight connection
	9.3	13.70						
	5.7	25.77						
	0.5	39.15						
PD307H	0.7	9.85	Old snubber	Pinned	—	Impact	Empty	Snubber at midpoint undersized pin
	16.6	14.29						
	3.5	25.27						
	0.4	38.90						
PD353H	1.5	4.44	Spring hanger	Fixed	120	Shaker	Empty	Standard pin, hanger at 1/3 point
	1.7	11.69						
	0.4	24.41						
	0.4	38.30						
	2.7	44.58						
PD354H	1.6	4.52	Spring hanger	Fixed	120	Shaker	Empty	Standard pin, hanger at 1/3 point
	0.6	11.98						
	0.4	24.54						
	0.6	37.96						
	2.3	44.25						
PD356H	1.4	4.53	Spring hanger	Fixed	200	Shaker	Empty	Loose connection, hanger at 1/3 point
	1.1	11.97						
	0.5	24.54						
	0.5	37.82						
	2.1	44.24						

Table 10. (continued)

Test	Damping (% of Critical)	Frequency (Hz)	Type of Pipe Support	End Condition	Strain Level (μ in./in.)	Type of Excitation	Water Condition	Notes
PD357H	1.4	4.52	Spring hanger	Fixed	200	Shaker	Empty	Undersized pin, hanger at 1/3 point
	1.1	11.95						
	0.4	24.55						
	0.5	37.83						
	1.9	44.23						
PD358H	1.6	4.50	Spring hanger	Fixed	100	Shaker	Empty	Undersized pin, hanger at 1/3 point
	0.7	11.93						
	0.3	24.53						
	0.5	37.88						
	1.9	44.50						
PD355H	1.6	4.54	Spring hanger	Fixed	200	Shaker	Empty	Standard pin, hanger at 1/3 point
	1.2	11.96						
	0.4	24.58						
	0.5	37.86						
	2.0	44.13						
PD302H	5.5	2.66	Spring hanger	Pinned	—	Impact	Empty	Hanger at midpoint
	0.3	9.78						
	0.5	21.56						
	0.1	28.97						
	2.9	38.76						
PD309H	3.5	2.61	Spring hanger	Pinned	—	Impact	Empty	Hanger at 1/4 point
	0.8	9.61						
	0.7	21.80						
	0.4	38.61						
PD364H	0.5	11.90	Rod hanger	Fixed	50	Shaker	Empty	Hanger at midpoint
	5.4	16.66						
	1.6	39.12						
PD363H	1.0	12.02	Rod hanger	Pinned	100	Shaker	Empty	Hanger at midpoint
	12.0	16.21						
	1.4	39.36						
	2.0	46.82						
PD304H	0.7	9.79	Rod hanger	Pinned	—	Impact	Empty	Hanger at midpoint, tight connection
	0.8	15.34						
	0.4	38.64						
	2.1	48.24						
PD303H	0.4	9.72	Rod hanger	Pinned	—	Impact	Empty	Hanger at midpoint, loose connection
	4.8	14.09						
	0.7	38.84						
PD314H	0.7	12.10	Rod hanger	Fixed	—	Impact	Empty	Hanger at midpoint, loose connection
	0.5	18.15						
	0.9	39.08						
	1.0	48.72						
PD365H	—	11.89	Rod hanger	Fixed	150	Shaker	Empty	Hanger at midpoint, tight bolt
	0.4	17.85						
	0.5	37.69						
	2.3	40.92						
	2.1	46.43						
	1.7	48.62						

Table 10. (continued)

Test	Damping (% of Critical)	Frequency (Hz)	Type of Pipe Support	End Condition	Strain Level (μ in./in.)	Type of Excitation	Water Condition	Notes
PD366H	0.5 2.0 3.7 6.1	11.94 17.22 37.37 44.92	Rod hanger	Fixed	400	Shaker	Empty	Hanger at midpoint, tight bolt
PD367H	0.5 3.2 0.8	10.17 14.57 33.43	Rod hanger	Fixed	100	Shaker	Full	Hanger at midpoint, filled with water
PD359H	1.2 7.8 2.7 2.2	11.90 16.11 37.98 44.24	Old snubber, spring hanger	Fixed	100	Shaker	Empty	Snubber at midpoint, hanger at 1/3 point
PD361H	3.6 7.9 1.9 2.5	11.96 24.06 37.84 44.45	Old snubber, spring hanger	Fixed	100	Shaker	Empty	Snubber at midpoint, hanger at 1/3 point, undersized pin
PD362H	1.0 6.9 1.9 2.5	11.89 15.96 37.99 44.40	New snubber, spring hanger	Fixed	100	Shaker	Empty	Snubber at midpoint, hanger at 1/3 point
PD360H	0.2(-) 3.9 1.7 2.0	11.86 16.27 37.51 44.45	Old snubber, spring hanger	Fixed	200	Shaker	Empty	Snubber at midpoint, hanger at 1/3 point

quite high damping (16 to 47%) in the first mode for low strain levels (< 30 μ in./in.). In the 100 to 400 μ in./in. strain level, it shows damping around 2 to 3%.

An interesting nonlinearity seems to be occurring in Tests 869, 870, 871, and 872. As the strain level in the pipe increases from 100 to 400 μ in./in., the damping level of the first mode decreases from 3 to 1.7% and the resonant frequency decreases from 11.64 to 9.61 Hz. The damping level decreased because of Coulomb friction. Further studies are needed to determine the cause of resonant frequency decreases.

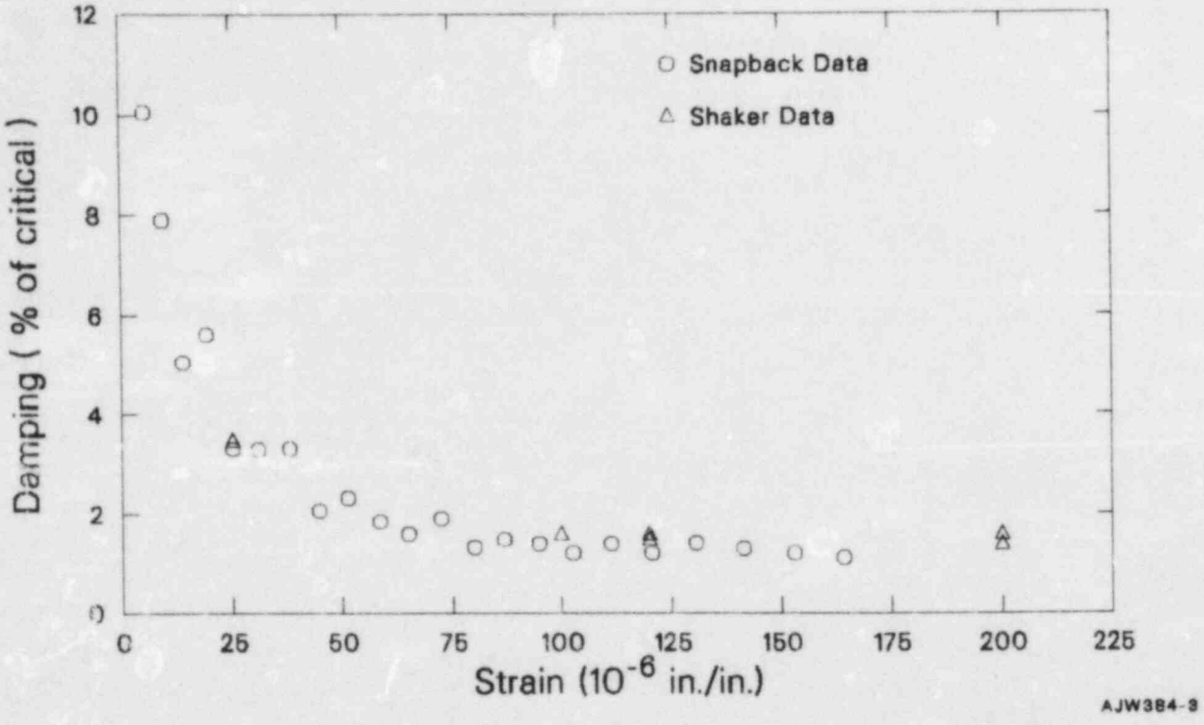

Figure 53. Comparison of snapback- and shaker-induced damping results.

Table 11. 8-in. pipe damping calculations with shaker excitation

Test	Half-Power Damping		Complex Exp. Damping		Type of Pipe Support	End Condition	Strain Level (μ in./in.)	Type of Excitation	Water Condition	Notes
	Critical (%)	Frequency (Hz)	Critical (%)	Frequency (Hz)						
PD851H	0.8 0.6	7.50 23.31	0.9 0.5	7.51 23.22	None	Simple	—	Random	Empty	
PD862H	0.5	7.32	0.3	7.33	None	Simple	—	Random	Empty	
PD852H	1.3 0.8	7.43 22.82	1.0 0.5	7.44 22.90	Spring hanger	Simple	—	Random	Empty	Hanger at midpoint
PD854H	1.9 2.1	7.50 23.29	1.2 1.6	7.51 23.26	Spring hanger	Simple	30	Swept sine	Empty	Hanger at midpoint
PD855H	1.8 1.0	7.48 23.52	1.0 1.0	7.48 23.34	Spring hanger	Simple	60	Random	Empty	Hanger at midpoint
PD856H	0.7 0.2	7.48 7.44	0.6 0.7	7.48 7.44	Spring hanger	Simple	60 100	Random	Empty	Hanger at midpoint
PD857H	0.7	7.33	0.8	7.52	Spring hanger	Simple	80	Swept sine	Empty	Hanger at midpoint
PD858H	1.3	7.52	1.2	7.53	Spring hanger	Simple	15	Swept sine	Empty	Hanger at midpoint
PD802H	2.2	7.58	0.9	7.59	Spring hanger	Simple		Impact	Empty	Hanger at midpoint
PD860H	2.1 0.9	7.47 23.06	1.0 0.6	7.47 23.02	Sway brace	Simple	50	Random	Empty	Brace at midpoint
PD861H	0.7	7.48	0.7	7.47	Sway brace	Simple	20	Random	Empty	Brace at midpoint
PD859H	27-37 4.1	8.0-10.3 23.38	16-47 2.1	8.3-9.7 23.41	Constant-force hanger	Simple	—	Random	Empty	Hanger at midpoint
PD803H	20-32 0.6	8.3-10.1 23.44	13-47 0.3	8.2-10.2 23.40	Constant-force hanger	Simple	—	Impact	Empty	Hanger at midpoint
PD863H	2.4 1.2 0.6	5.58 17.82 38.71	1.1 0.6 0.7	5.54 17.80 38.79	None	Simple	—	Random	Full	
PD867H	1.0 0.8	9.68 25.62	0.7 0.6	9.81 25.63	None	Fixed	—	Random	Full	
PD868H	0.4	9.75	0.4	9.76	None	Fixed	200	Swept sine	Full	
PD869H	3.6 2.6	11.43 26.08	3.0 2.2	11.64 26.15	Constant-force hanger	Fixed	100	Random	Full	Hanger at 1/3 point
PD870H	3.3	10.62	3.6	10.56	Constant-force hanger	Fixed	150	Random	Full	Hanger at 1/3 point
PD871H	2.2 3.0	9.70 25.62	2.1 3.2	9.73 25.57	Constant-force hanger	Fixed	200	Swept sine	Full	Hanger at 1/3 point
PD872H	1.7	9.60	1.7	9.61	Constant-force hanger	Fixed	400	Swept sine	Full	Hanger at 1/3 point
PD873H	2.1	25.00	2.3	25.07	Constant-force hanger	Fixed	200	Swept sine	Full	Hanger at 1/3 point

CONCLUSIONS AND RECOMMENDATIONS

A number of inferences can be drawn from the test results reported herein. These are summarized below. These results, as well as similar research efforts now being conducted, will serve as the bases for future tests to determine effective damping in piping systems.

Effect of Type of Supports

1. At very low amplitudes, the spring hangers produced apparent high damping due to Coulomb friction between the spring and its casing. With significant amplitudes, the spring hanger contributions to damping became small. (Figures 28, 29, 31, 34, 47)

2. The constant-force hanger dissipated a great deal of energy, resulting in higher damping than for the spring hangers. A Coulomb friction effect with higher damping at lower magnitudes was observed. (Figures 35, 36, 37, 42, 44, 45)

3. With tight connections, the rod hanger did not introduce additional damping. However, with loose connections causing impact between the bolt and the eye of the rod hanger, higher damping levels were calculated.

4. The sway brace contribution to damping was similar to that of the spring hangers. The frequency response functions did not exhibit significant nonlinear behavior as did the snubbers and rod hanger with a loose connection.

5. In general, the snubbers produced higher damping than spring hangers and sway braces, except for the mode where the snubber was located at the nodal point. In these tests, they were loaded only to low design-operating levels.

Effect of Test Methods

1. For linear systems, the logarithmic decrement and frequency-domain calculations gave similar damping results. For nonlinear systems, the logarithmic decrement could prove more reliable. However, using several test methods on a given configuration would give an analyst more confidence in the results.

2. The LVDT, strain gauges, and accelerometers gave similar damping values. However, the accelerometers measured all modes well while the LVDT generally responded only to the lower modes. Thus, the LVDT was particularly valuable for log-decrement testing because often only the trace of one mode was recorded. Much more trouble, associated with 60-Hz electrical noise, was evident with the strain gauges than with the other instruments.

3. Sine-sweep testing gave much better resolution and coherence than did random testing, resulting in more accurate damping calculations. A method that worked well in these tests was to first use a random excitation to quickly identify the modal frequencies. Then the hydraulic shaker frequency was set near to that of the mode to be tested. The amplitude was raised to the desired level, then the frequency was slowly swept through an interval around the central frequency. The sine-sweep testing also gave better resolution than the transformed snapback data. However, the sine-sweep testing was considerably more time consuming.

4. Because the deflected shape changes from the static deflection (essentially containing many modes) to the dynamic-mode shape (dominated by the lowest mode) in snapback testing, the first cycle of data is difficult to use to determine damping. This is unfortunate because this first cycle contains the highest level of excitation, levels that are of most interest for OBE and SSE.

General Effects

1. At low excitation levels, especially with spring hangers present, damping decreased as response amplitude increased, giving evidence of Coulomb friction.

2. At higher levels of excitation, as for example in the SSE and OBE stress level range, damping increased with amplitude.

3. The high-stress-level damping was considerably greater for the water-filled 8-in. pipe than for the empty 3-in. pipe. At SSE levels, damping for both pipes was above 5% of critical. Damping for the 8-in. pipe was also above 5% of critical at OBE levels, while OBE data for the 3-in. pipe were in the 1 to 3% of critical damping range.

4. The relative energy of the pipe to the energy dissipated by the supports is important. For example, in Figures 35 and 42 for the constant-force hanger, the case with water in the pipe had significantly less damping than for the pipe without water at the same amplitudes, because the mass of the pipe was greater and the ratio of dissipated energy to vibrational energy was lower.

5. Damping is dependent on the positions of the support with respect to the mode shape. For example, when a support is located near a nodal point such as the midpoint of the span in Figure 25b, there is minimal motion of the support, and low damping results. An exception occurs when there can be impact energy losses due to a loose connection, such as in the midpoint of the span shown in Figure 25d.

6. In general, damping was higher in configurations with loose fittings resulting in vibrational clatter. An exception occurred when spring hangers were present. These hangers kept a tension on the loose connection and essentially eliminated clatter.

7. From shaker and hammer data in Table 10, there is no apparent trend to indicate that damping in the 33 to 50-Hz range is different from that in the 20 to 33-Hz range.

8. In general, single pipe supports tend to selectively impart characteristic damping to selected modes of the piping response.

Future Work

1. EG&G Idaho plans to conduct additional tests in 1984. A two- or three-dimensional simple piping segment will be tested at the ARA-III high bay area under conditions similar to the one-dimensional test described in this report. Tests at high strain levels will be emphasized. Data at frequencies above 33 Hz will also be recorded to assess the effect of damping at higher frequencies. In addition in 1984, EG&G Idaho plans to use a piping system at the ANCO Engineers laboratory in Culver City, California, to perform additional vibration testing to determine damping.

2. Results of this study point out the need for additional testing, especially in the OBE to SSE stress range. Much of the data gathered to date have been at low excitation levels and extrapolated to OBE and SSE levels. The results of this testing show that damping is amplitude dependent and that use of low-level excitation could produce too high a damping estimate due to Coulomb friction effects, while intermediate-level results could produce too low an estimate. Thus data obtained from low level in situ testing should be used with caution.

3. Most of the damping data assessed to date has been focused on application to the seismic range—from 1 to 33 Hz. More test results are needed in the higher frequency range above 33 Hz to provide a best-estimate damping for fluid transient problems. At present, RG 1.61 does not even address damping for transients other than seismic events.

4. From an analytical point of view, uniform viscous damping is the easiest type of damping to apply and therefore is being used extensively in piping dynamic analyses. It assumes damping is linear—with frequency, with amplitude, with support configuration. However, tests may show that the nature of damping is just too complex to be represented by uniform damping alone. Based on both test data and existing analytical capabilities, an assessment should be made as to the most effective, realistic, and practical methods of applying damping to the piping system analysis process.

REFERENCES

1. U.S. Atomic Energy Commission, *Damping Values for Seismic Design of Nuclear Power Plants*, Regulatory Guide 1.61, October 1973.

2. U.S. Nuclear Regulatory Commission, *Standard Review Plan for the Review of Safety Analysis Reports for Nuclear Power Plants*, NUREG-0800, July 1981.

3. A. G. Ware, *A Survey of Experimentally Determined Damping Values in Nuclear Power Plant Piping Systems*, NUREG/CR-2406, EGG-2143, EG&G Idaho, Inc., November 1981.

4. A. G. Ware, "Experimental Damping Data for Dynamic Analysis of Nuclear Power Plant Piping Systems," *1983 ASME Pressure Vessel and Piping Conference, Portland, Oregon, June 1983, ASME PVP, 73, pp. 133-150.*

5. A. G. Ware, *Parameters that Influence Damping in Nuclear Power Plant Piping Systems*, NUREG/CR-3022, EGG-2232, EG&G Idaho, Inc., November 1982.

6. A. G. Ware, "Nuclear Power Plant Damping Parametric Effects," ASME 83-PVP-67, *1983 ASME Pressure Vessel and Piping Conference, Portland, Oregon, June 1983.*

7. S. L. Busch, *A Comparison of Piping System Stresses Reflecting Support Optimization Based Upon Varying Response Spectra Damping Values*, EG&G Report RE-A-83-008, February 1983.

8. N. M. Newmark, J. A. Blume, and K. K. Kapur, "Design Response Spectra for Nuclear Power Plants," *ASCE Structural Engineering Meeting, San Francisco, April 1973.*

9. C. M. Harris, and C. E. Crede, *Shock and Vibration Handbook*, Second Edition, McGraw-Hill Book Co. Inc., 1976.

10. W. T. Thomson, *Theory of Vibration with Applications*, 2nd Edition, Prentice-Hall, 1981.

11. M. H. Richardson, *Detection of Damage in Structures from Changes in their Dynamic (Modal) Properties—A Survey*, NUREG/CR-1431, UCRL-15103, Lawrence Livermore Laboratory, Livermore, California, 94550, April 1980.

12. Structural Dynamics Research Corporation, *Modal-Plus User Manual*, Version 6.0, August 1981.

13. American Society of Mechanical Engineering *ASME Boiler and Pressure Vessel Code*, Section III, Nuclear Power Plant Components, 1980 Edition, through Winter 1983 Addenda.

APPENDIX A
TEST MATRIX

APPENDIX A
TEST MATRIX

This appendix presents, in Tables A-1 through A-5, a summary of the more than 100 tests conducted. The tests were designated PDSXXY, where PD stands for "pipe damping," S is the pipe size in inches, XX is the test sequence number, and Y designates the type of excitation—H for impact and shaker tests and F for snapback tests.

Table A-1. Hammer (impact) test matrix

Test Number[a]	End Condition[b]	Filled or Empty[c]	Description[d]
PD301H	P	E	End supports only
PD302H	P	E	SH 0 at midpoint
PD303H	P	E	RH at midpoint, loose connection
PD304H	P	E	RH at midpoint, tight connection
PD305H	P	E	Used snubber at midpoint
PD306H	P	E	Used snubber at midpoint, tight connection
PD307H	P	E	Used snubber at midpoint, loose connection
PD308H	P	E	Used snubber at midpoint, SH 0 at quarter point
PD309H	P	E	SH 0 at 1/4 location
PD310H	P	E	SH 0 at 1/4 location, horizontal excitation
PD311H	P	E	New snubber at midpoint
PD312H	F	E	End supports only
PD313H	F	E	End supports, modal survey
PD314H	F	E	RH at midpoint, loose connection
PD801H	P	E	End supports only
PD802H	P	E	SH 7 at 1/3 location
PD803H	P	E	CFH at midpoint

a. See page A-3 for test designation nomenclature description.

b. P = Pinned
F = Fixed

c. E = Empty
F = Filled with water

d. SH = Spring hanger
RH = Rod hanger
CFH = Constant-force hanger

Table A-2. Shaker test matrix for 3-in. pipe

Test Number[a]	End Condition[b]	Filled or Empty[c]	Description[d]
PD351H	F	E	New snubber at midpoint
PD352H	F	E	End supports only
PD353H	F	E	SH 0 at 1/3 location
PD354H	F	E	SH 0 at 1/3 location
PD355H	F	E	SH 0 at 1/3 location, higher strain
PD356H	F	E	SH 0 at 1/3 location (loose connection), higher strain
PD357H	F	E	SH 0 at 1/3 location (small pin), higher strain
PD358H	F	E	SH 0 at 1/3 location (small pin), lower strain
PD359H	F	E	Old snubber at center, SH 0 at midpoint
PD360H	F	E	Old snubber at center, SH 0 at midpoint
PD361H	F	E	Old snubber at center, SH 0 at midpoint
PD362H	F	E	New snubber at center, SH 0 at midpoint
PD363H	F	E	RH at midpoint
PD364H	F	E	RH at midpoint, lower strain
PD365H	F	E	RH at midpoint, tight pin connection
PD366H	F	E	RH at midpoint, tight pin connection, higher strain
PD367H	F	F	RH at midpoint

a. See page A-3 for test designation nomenclature description.

b. P = Pinned
F = Fixed

c. E = Empty
F = Filled with water

d. SH = Spring hanger
RH = Rod hanger
CFH = Constant-force hanger

Table A-3. Shaker test matrix for 8-in. pipe

Test Number[a]	End Condition[b]	Filled or Empty[c]	Type of Excitation	Description[d]
PD851H	P	E	Random	End supports only
PD852H	P	E	Random	SH 7 at 1/3 location
PD853H	P	E	Random	SH 7 at 1/3 location, floor shake
PD854H	P	E	Sine sweep	SH 7 at 1/3 location
PD855H	P	E	Sine sweep	SH 7 at 1/3 location
PD856H	P	E	Sine sweep	SH 7 at 1/3 location, zoom
PD857H	P	E	Sine sweep	SH 7 at 1/3 location, zoom
PD858H	P	E	Sine sweep	SH 7 at 1/3 location, zoom
PD859H	P	E	Random	CFH at 1/2 location
PD860H	P	E	Random	SB at 1/3 location
PD861H	P	E	Random	SB at 1/3 location, zoom
PD862H	P	E	Random	End supports only, zoom
PD863H	P	F	Random	End supports only
PD864H	P	F	Random	End supports only, zoom
PD865H	P	F	Random	End supports only, suspended shaker
PD866H	P	F	Random	End supports only, horizontal
PD867H	F	F	Random	End supports only
PD868H	F	F	Random	End supports only, zoom
PD869H	F	F	Random	CFH at 1/3 location
PD870H	F	F	Random	CFH at 1/3 location
PD871H	F	F	Sine sweep	CFH at 1/3 location
PD872H	F	F	Sine sweep	CFH at 1/3 location, first mode
PD873H	F	F	Sine sweep	CFH at 1/3 location, second mode
PD874H	F	F	Random	Snubber at 1/3 location

a. See page A-3 for test designation nomenclature description.

b. P = Pinned
F = Fixed

c. E = Empty
F = Filled with water

d. SH = Spring hanger
RH = Rod hanger
CFH = Constant-force hanger

Table A-4. Snapback test matrix for 3-in. pipe

Test Number[a]	End Condition[b]	Filled or Empty[c]	Description[d]
PD301F	P	E	SH 0 at midpoint
PD302F	P	E	SH 0 at 1/4 location, snap at midpoint
PD303F	P	E	SH 0 at 1/4 location, snap at 1/4
PD304F	F	E	SH 0 at 1/3 location (low excitation)
PD305F	F	E	SH 0 at 1/3 location (500-lb snap)
PD306F	F	E	SH 0 at midpoint, (250-lb snap)
PD307F	F	E	SH 0 at midpoint, (500-lb snap)
PD308F	F	E	RH at midpoint (500-lb snap at 1/4)
PD309F	F	E	RH at midpoint (1000-lb snap at 1/4)
PD310F	F	E	RH at midpoint (1500-lb snap at 1/4)
PD311F	F	E	RH at midpoint (1800-lb snap at 1/4)
PD315F	F	F	SH 3 at 1/3 (500-lb snap at 1/4)
PD318F	F	F	SH 3 at 1/3 (500-lb snap at center)
PD319F	F	F	RH at midpoint, SH 3 at 1/3, (750-lb snap at 1/4)
PD320F	F	F	RH at midpoint, (750-lb snap at 1/4)
PD321F	F	F	RH at midpoint, (1500-lb snap at 1/4)
PD322F	F	F	RH at midpoint, (1500-lb snap at 1/4)
PD323F	F	F	RH at midpoint (750-lb snap)
PD324F	F	F	RH at midpoint (1500-lb snap)
PD325F	F	F	RH at midpoint (2000-lb snap)
PD326F	F	F	RH at midpoint (2000-lb snap)
PD327F	F	F	RH at midpoint (2500-lb snap)
PD328F	F	F	RH at midpoint (3000-lb snap)
PD329F	F	F	RH at midpoint (3500-lb snap)

Table A-4. (continued)

Test Number[a]	End Condition[b]	Filled or Empty[c]	Description[d]
PD330F	F	E	End supports only (2000-lb snap)
PD331F	F	E	End supports only (3000-lb snap)
PD332F	F	E	End supports only (4000-lb snap)
PD333F	F	E	End supports only (5000-lb snap)

a. See page A-3 for test designation nomenclature description.

b. P = Pinned
F = Fixed

c. E = Empty
F = Filled with water

d. SH = Spring hanger
RH = Rod hanger
CFH = Constant-force hanger

Table A-5. Snapback test matrix for 8-in. pipe

Test Number[a]	End Condition[b]	Filled or Empty[c]	Description[d]
PD801F	P	E	SH 7 at 1/3 location, hammer
PD802F	P	E	SH 7 at 1/3 location, hammer
PD803F	P	E	SH 7 at 1/3 location, 1000 lb
PD804F	P	E	SH 7 at 1/3 location, 2000 lb
PD805F	P	E	CFH at midpoint, 1000 lb
PD806F	P	E	CFH at midpoint, 2000 lb
PD807F	P	E	CFH at midpoint, 3000 lb
PD808F	P	E	CFH at midpoint, 4000 lb
PD809F	P	E	SB at 1/3 location, 1000 lb
PD810F	P	E	SB at 1/3 location, 4000 lb

Table A-5. (continued)

Test Number[a]	End Condition[b]	Filled or Empty[c]	Description[d]
PD811F	P	F	End supports only, hammer vertical
PD812F	P	F	End supports only, hammer horizontal
PD814F	F	F	SB at 1/3 location, snap at 1/4, 1000 lb
PD816F	F	F	SB at 1/3 location, snap at 1/4, 4000 lb
PD817F	F	F	SB at 1/3 location, snap at 1/4, 6000 lb
PD818F	F	F	SB at 1/3 location, snap at 1/4, 8000 lb
PD819F	F	F	CFH at 1/3 location, snap at midpoint, 1500 lb
PD820F	F	F	CFH at 1/3 location, snap at midpoint, 3500 lb
PD821F	F	F	CFH at 1/3 location, snap at midpoint, 5500 lb
PD822F	F	F	CFH at 1/3 location, snap at midpoint, 7500 lb
PD823F	F	F	SB at 1/3 location, snap at midpoint, 1200 lb
PD824F	F	F	SB at 1/3 location, snap at midpoint, 3200 lb
PD825F	F	F	SB at 1/3 location, snap at midpoint, 5200 lb
PD826F	F	F	SB at 1/3 location, snap at midpoint, 7200 lb
PD827F	F	F	SB at 1/3 location, snap at at 1/4, 2000 lb
PD828F	F	F	SB at 1/3 location, snap at at 1/4, 4000 lb
PD829F	F	F	SB at 1/3 location, snap at at 1/4, 6000 lb
PD830F	F	F	SB at 1/3 location, snap at at 1/4, 8000 lb
PD831F	F	F	SH 9 at 1/3, snap at midpoint 3000 lb
PD832F	F	F	SH 9 at 1/3, snap at midpoint 5000 lb
PD833F	F	F	SH 9 at 1/3, snap at midpoint 7000 lb
PD834F	F	F	SH 9 at 1/3, snap at midpoint 9000 lb
PD835F	F	F	Snubber at 1/3, snap at midpoint, hammer
PD836F	F	F	Snubber at 1/3, snap at midpoint, 2000 lb

Table A-5. (continued)

Test Number[a]	End Condition[b]	Filled or Empty[c]	Description[d]
PD837F	F	F	Snubber at 1/3, snap at midpoint, 2000 lb
PD840F	F	F	Snubber at 1/3, snap at midpoint, 1000 lb
PD842F	F	F	End supports only, snap at midpoint, 10000 lb
PD843F	F	F	End supports only, snap at midpoint, 12000 lb
PD844F	F	F	End supports only, snap at midpoint, 15000 lb
PD845F	F	F	End supports only, snap at midpoint, 14000 lb
PD846F	F	F	End supports only, snap at midpoint, 17000 lb
PD847F	F	F	End supports only, snap at midpoint, 20000 lb
PD848F	F	F	End supports only, snap at midpoint, 22000 lb
PD849F	F	F	End supports only, snap at midpoint, 25000 lb

a. See page A-3 for test designation nomenclature description.

b. P = Pinned
F = Fixed

c. E = Empty
F = Filled with water

d. SH = Spring hanger
RH = Rod hanger
CFH = Constant-force hanger

EG&G Idaho, Inc.
P.O. Box 1625
Idaho Falls, Idaho 83415